Investigation of ASPPs as regulators of pancreatic inflammation & tumorigenesis

Paul Miller

A thesis submitted in fulfilment of the requirements for the degree of

Doctor of Philosophy

New College

Ludwig Institute for Cancer Research

Nuffield Department of Medicine

University of Oxford

Declaration

I confirm that the thesis I am submitting is wholly my own work unless otherwise stated. No part of this thesis has been accepted or is currently submitted for any degree, diploma or certificate in this University or elsewhere. The work described here was carried out during my time as a graduate student at the Ludwig Institute for Cancer Research under the supervision of Professor Xin Lu, Professor Adrian Harris and Dr Sarah De Val.

Word count: 30,824

Investigation of ASPPs as regulators of pancreatic inflammation & tumorigenesis

Abstract

Pancreatic ductal adenocarcinoma (PDAC) is a cancer of unmet need with a 5-year survival following diagnosis of 3% with limited surgical, radiotherapy and chemotherapy treatment options. Central to PDAC tumorigenesis is acquisition of an oncogenic Kras mutation to drive acinar-to-ductal metaplasia and progression to PDAC that is potentiated by NF-κB deregulation. However, PDAC requires the additional loss of tumour suppressors such as p53, SMAD4 or p16. ASPP family members ASPP2 and iASPP regulate both p53 and NF-κB, and are classified as a tumour suppressor and oncogene respectively. However, the precise roles of ASPP2 and iASPP in pancreatic cancer are unknown. In this thesis I demonstrate that ASPP2 suppresses metastasis and iASPP suppresses the pro-inflammatory tumour microenvironment. In a mouse model of PDAC development, ASPP2-deficiency does not alter metaplasia, PanIN progression or primary PDAC onset. However, median survival due to metastasis is significantly reduced in an ASPP2-deficient PDAC model. I demonstrate ASPP2-deficient PDAC can result in increased squamous differentiation defined histologically or via increased p63 expression. I propose ASPP2 is a key suppressor ΔNp63 and the squamous PDAC subtype *in vivo*. Conversely, iASPP is a putative oncogene and high expression in cancer associates with poor prognosis. However, in a mouse model of PDAC, loss of iASPP accelerates PDAC onset and metastasis. I demonstrate that iASPP is a functional tumour suppressor of a pro-inflammatory phenotype in

response to oncogenic Kras and pancreatitis. I propose ASPP2- and iASPP-deficient mouse models of PDAC represent *in vivo* the squamous and immunogenic subtypes of PDAC respectively; and are relevant tools to study mechanisms of metastasis and inflammation-driven carcinogenesis.

Acknowledgements

This thesis is dedicated to my mother Gillian who sadly died whilst writing during my time as a graduate student. She has continually supported me and made numerous sacrifices throughout her life with my father Colin to support my extended education. Her death is a reminder that cancer will affect us all and will motivate me to continue in the field of cancer treatment and research.

I wish to acknowledge Professor Xin Lu who gave me an opportunity as a junior doctor with little laboratory experience when looking for a research project as an academic clinical fellow in 2011. Xin has provided invaluable support and guidance during my time at the Ludwig. Most importantly she gave me the freedom to ask questions and develop my own route to answering them. Supervision has also been provided by Adrian Harris and Sarah De Val who despite the change in direction that my DPhil project took, have provided helpful academic guidance and support throughout my research.

The Ludwig Institute for Cancer Research (LICR) Oxford has grown considerably over the years but remains a supportive family. Lu lab members past and present have each played a part in making my time in the laboratory a stimulating and exciting experience and includes, but is not limited to, Mario, Min, Luca, Gopi, Kathryn, Sofia, Chris, Elliot, Ludo, James, Richard, Shuo and Zinaida. Core LICR members Veronica, Alex, Stan, David, James and Jan have supported administratively and with any laboratory problems.

Indi has been vital to my histology heavy research in providing high quality tissue sections and advice in optimising my tissue work. Indi has also always been available to listen to my difficulties and concerns and I am extremely grateful that she has been a constant presence in the laboratory. Liz and Shan have provided a huge amount of advice and support in managing the large number of mice required for my research. Both are always happy to answer my questions, no matter how basic. Microscopy support has been expertly provided by Mark Shipman who gives high quality advice on image acquisition and optimisation and the slide scanner he helped purchase in 2017 has been crucial to the success of my work.

Professor Robert Goldin provided the human pancreatic disease samples and expert guidance in the pathological interpretation of both human and mouse tissue. He has been both encouraging and insightful in our discussions. Emmanouil Fokas kindly provided KPC mouse tumours samples and KPC mice for breeding that started my colonies of mice that formed the basis of my thesis.

Further thanks go to my family and friends who have provided useful distractions during my DPhil and I look forward to spending more time with them after completion. My close friend Chris Snaith died of a brain tumour 10 years ago whilst I was a medical student. His struggle and the amazing care he received in the UK and USA prompted me to pursue a career in cancer treatment and research. I would not have come to Oxford or the LICR without being inspired by him.

Finally, my wife Hajira has been endlessly supportive and encouraging despite spending longer in the lab than I should on evenings and weekends. Her patience and help has been crucial in getting through my DPhil and she inspires me every day. I look forward to many more holidays together.

Funding

This DPhil was funded by a CRUK clinical research training fellowship and the Ludwig Institute for Cancer Research.

Table of Contents

Declaration **2**

Abstract **3**

Acknowledgements **5**

List of Figures **11**

Abbreviations **13**

Chapter 1: Introduction **15**

1.1 Inflammation in cancer aetiology **15**

1.1.1 The p53 family as regulators of inflammation 15

1.1.2 NF-κB as regulator of inflammation 17

1.1.3 Crosstalk between p53 & NF-κB 18

1.2 Pancreatic ductal adenocarcinoma **19**

1.2.1 Incidence and prognosis 20

1.2.2 Mutational and protein expression landscape of PDAC 21

1.2.3 Inflammation in PDAC aetiology 23

1.2.4 Mouse models of PDAC development 24

1.2.5 Mouse models to study inflammation in PDAC development 26

1.2.6 Role of the immune response in PDAC 30

1.2.7 Mechanisms of metastases 33

1.3 NF-κB and p53 in pancreatic inflammation and PDAC **34**

1.3.1 NF-κB in pancreatic inflammation 34

1.3.2 NF-κB in pancreatic ductal adenocarcinoma 35

1.3.3 p53-family in pancreatic ductal adenocarcinoma 36

1.4 ASPP2 ..... **38**

1.4.1 ASPP2 as a regulator of apoptosis and inflammation 40

1.4.2 ASPP2 in development 41

1.4.3 ASPP2 in tumorigenesis and cancer 42

1.4.4 Hypothesized role of ASPP2 in pancreatic ductal adenocarcinoma 44

1.5 iASPP **45**

1.5.1 iASPP as a regulator of apoptosis and inflammation 47

1.5.2 iASPP in development and tissue homeostasis 47

1.5.3 iASPP in tumorigenesis and cancer 49

1.5.4 Hypothesized role of iASPP in pancreatic ductal adenocarcinoma 50

1.6 Aim of the study **52**

Chapter 2: Materials and methods **53**

2.1 Materials **53**

2.1.1 Reagents 53

2.1.2 *Ex vivo* ADM assay materials 58

2.1.3 SDS-Polyacrylamide Gels 59

2.1.4 Antibodies 60

2.1.5 Mouse genotyping 61

2.2 Methods **62**

2.2.1 DNA techniques 62

2.2.2 Protein techniques 63

2.2.3 Histological and immunohistological techniques 65

2.2.4 Mouse work 66

2.2.5 Human tissue samples 68

2.2.6 Data analysis 68

Chapter 3: ASPP2 regulates the pancreatic response to inflammation **70**

3.1 ASPP2 deficiency does not alter pancreatic acinar development 71
3.2 Acute pancreatitis in E2F1-deficient mice results in metaplasia and persistent inflammation.....74
3.3 Acute pancreatitis upregulates ASPP2, iASPP and p53, and activates the MAPK/ERK pathway.....77
3.4 Acute pancreatitis in pancreas-specific ASPP2-deficient mice results in increased inflammation without altered recovery 80
3.5 ASPP2 expression is associated with human pancreatic inflammation and PDAC 82
3.6 Summary.....85

Chapter 4: ASPP2 suppresses metastasis and the squamous PDAC subtype 87
4.1 KC and KC;ASPP2$^{-/-}$ mice both recapitulate the histological spectrum of ADM to PDAC progression.....88
4.2 Reduced overall survival of KC;ASPP2$^{-/-}$ mice is not due to accelerated primary PDAC 90
4.3 ASPP2 may suppress early metastasis in an oncogenic Kras model of PDAC 94
4.4 ASPP2-deficiency does not impact overall survival or primary tumour-free survival in the KPC mouse model of PDAC 98
4.5 ASPP2 does not suppress metastasis in the KPC mouse model 102
4.6 ASPP2 does not regulate *ex vivo* acinar-to-ductal metaplasia 106
4.7 Inflammation potentiated oncogenic Kras driven ADM is not suppressed by ASPP2 *in vivo*.....109
4.8 ASPP2-deficiency does not alter intermittent caerulein-induced PanIN progression.....113
4.9 KC;ASPP2$^{-/-}$ mice exhibit squamous differentiation and p63 expression.115
4.10 ASPP2 represses the ΔNp63 isoform *in vivo* following inflammation and recovery.....119
4.11 Summary.....122

Chapter 5: iASPP regulates the pancreatic response to inflammation 123
5.1 iASPP is expressed in pancreatic islets in the unstressed pancreas.....124
5.2 iASPP deficiency does not alter pancreatic acinar development nor homeostasis.....127
5.3 β-cell specific iASPP-deficient mice have normal islets and glucose tolerance.....129
5.4 Acute pancreatitis in iASPP-deficient mice results in ADM and failure to recover.....131
5.5 Acute pancreatitis in pancreatic-specific iASPP-deficient mice does not result in metaplasia 134
5.6 iASPP is upregulated in human pancreatic disease 137
5.7 iASPP expression correlates with p53 from normal acini to PDAC.....141
5.8 iASPP is infrequently mutated in PDAC and iASPP amplification associates with AKT2 amplification 145
5.9 Summary.....149

Chapter 6: iASPP functions as a tumour suppressor in pancreatic tumorigenesis..... 151
6.1 KC;iASPP$^{-/-}$ mice have reduced survival and accelerated primary PDAC 152
6.2 KC;iASPP$^{-/-}$ mice have accelerated metastasis *in vivo* 156
6.3 iASPP-deficient acini have reduced ADM efficiency driven by oncogenic Kras and TGFα 160
6.4 iASPP suppresses ADM driven by inflammation and oncogenic Kras 163

6.5 iASPP suppression of inflammation-driven ADM and PanIN formation is not due to aberrant regeneration 166
6.6 KC and KC;iASPP$^{-/-}$ ADM and mPanINs do not significantly differ in senescence, apoptosis and proliferation 169
6.7 iASPP mRNA expression correlates with NF-κB, cytokeratin-19 and TGFα, markers of poor prognosis 172
6.8 iASPP expression associates with altered inflammatory mediator expression 176
6.9 KC;iASPP$^{-/-}$ mice following inflammation have upregulated p53, RelA p65 and GSDME 180
6.10 Cytokine profiling does not reveal a difference in microenvironment between KC and KC;iASPP$^{-/-}$ mice at 12-weeks 182
6.11 iASPP suppresses the pro-inflammatory cytokine response following inflammation 184
6.12 Summary 187
Chapter 7: Discussion 188
Bibliography 195

List of Figures

3.1 **ASPP2-deficiency does not result in a developmental and homeostatic phenotype**

3.2 **Acute pancreatitis in E2F1-deficient mice results in ADM and persisting inflammation**

3.3 **Acute pancreatitis induces MAPK/ERK activation and upregulation of ASPP2, iASPP and p53**

3.4 **Acute Pancreatitis in ASPP2-deficient mice demonstrates increased acute inflammatory response**

3.5 **ASPP2 is upregulated in chronic pancreatitis and well-differentiated PDAC**

4.1 **KC and KC;ASPP2$^{-/-}$ mice both recapitulate the histological spectrum from normal acini to PDAC**

4.2 **Reduced survival of KC;ASPP2$^{-/-}$ mice without accelerated primary PDAC**

4.3 **ASPP2 may suppress early metastasis in an oncogenic Kras model of PDAC**

4.4 **ASPP2-deficiency does not alter survival in KPC model of PDAC**

4.5 **ASPP2 does not suppress metastasis in the KPC mouse model of PDAC**

4.6 **ASPP2 does not regulate *ex vivo* ADM**

4.7 **Inflammation potentiated oncogenic Kras driven ADM is not suppressed by ASPP2 *in vivo***

4.8 **ASPP2-deficiency does not mediate PanIN progression following intermittent inflammation and recovery**

4.9 **KC;ASPP2$^{-/-}$ mice exhibit squamous phenotype and p63 positivity**

4.10 **ASPP2 represses ΔNp63 isoform *in vivo* following inflammation and recovery**

5.1 **iASPP is expressed in the pancreatic islets**

5.2 **iASPP-deficiency does not cause a pancreatic developmental or homeostatic phenotype**

5.3 **β-cell specific iASPP$^{\Delta 8/\Delta 8}$ have normal islets and glucose tolerance test**

5.4 Acute pancreatitis in iASPP-deficient mice results in ADM and failure to recover

5.5 Pancreatic-specific iASPP-deficiency does not result in metaplasia

5.6 iASPP expression is upregulated in pancreatic inflammation and cancer relative to normal pancreas

5.7 iASPP correlates with p53 in human pancreatic disease

5.8 iASPP is infrequently mutated in PDAC and associates with AKT2 amplification at 19q13

6.1 Reduced survival in KC;iASPP$^{-/-}$ relative to KC with accelerated primary PDAC

6.2 KC;iASPP$^{-/-}$ mice have accelerated metastasis relative to KC

6.3 iASPP is required for efficient acinar-to-ductal metaplasia

6.4 iASPP suppresses inflammation-driven ADM and PanINs

6.5 iASPP suppresses oncogenic Kras ADM in response to inflammation

6.6 iASPP metaplasia and PanIN lesions do not have a senescence, apoptotic or proliferation phenotype

6.7 iASPP mRNA expression correlates with poor prognosis markers RELA, TGFα and cytokeratin 19 in human PDAC

6.8 Comparison of iASPP mRNA levels with interleukin and cytokine signalling mediators of inflammation

6.9 KC;iASPP$^{-/-}$ mice following inflammation have upregulated p53, RelA p65 and GSDME

6.10 Cytokine profiling of KC and KC;iASPP$^{-/-}$ pancreas

6.11 iASPP suppresses the pro-inflammatory cytokine response following inflammation

7.1 Proposed mechanism for ASPP2 as a suppressor of squamous subtype of PDAC

Abbreviations

αSMA	Alpha-Smooth Muscle Actin
ADM	Acinar-to-Ductal Metaplasia
AP	Acute Pancreatitis
ASPP2	Apoptosis Stimulating Protein of p53
ASPP2$^{-/-}$	LSL-ASPP2$^{\Delta 3/\Delta 3}$; Pdx1^{Cre}
CCK	Cholecystokinin
CP	Chronic Pancreatitis
E2F1	E2F Transcription Factor 1
E2F2	E2F Transcription Factor 2
EGFR	Epithelial Growth Factor Receptor
EMT	Epithelial-Mesenchymal Transition
EYFP	Enhanced Yellow Fluorescent Protein
HRP	Horseradish Peroxidase
iASPP	Inhibitor of Apoptosis Stimulating Protein of p53
IF	Immunofluorescence
IHC	Immunohistochemistry
IL	Interleukin
KC	LSL-Kras$^{G12D/+}$; Pdx1^{Cre}
KC;ASPP2$^{-/-}$	LSL-Kras$^{G12D/+}$; LSL-ASPP2$^{\Delta 3/\Delta 3}$; Pdx1^{Cre}
KC;iASPP$^{-/-}$	LSL-Kras$^{G12D/+}$; LSL-iASPP$^{\Delta 8/\Delta 8}$; Pdx1^{Cre}
KPC	LSL-Kras$^{G12D/+}$; LSL-p53$^{R172H/+}$; Pdx1^{Cre}
KPC; ASPP2$^{-/-}$	LSL-Kras$^{G12D/+}$; LSL-p53$^{R172H/+}$; LSL-ASPP2$^{\Delta 3/\Delta 3}$; Pdx1^{Cre}
Kras	Kirsten Rat Sarcoma Viral Oncogene Homolog
MDM2	Mouse Double Minute 2
mAb	Monoclonal Antibody
MAPK	Mitogen-Activated Protein Kinase
MODY	Maturity Onset Diabetes of the Young
mPanIN	Mouse Pancreatic Intraepithelial Neoplasia
mPDAC	Mouse Pancreatic Ductal Adenocarcinoma
NF-κB	Nuclear Factor Kappa B
pAb	Polyclonal Antibody
PAMP	Pathogen-Associated Molecular Pattern

PanIN	Pancreatic Intraepithelial Neoplasia
PCR	Polymerase Chain Reaction
PDAC	Pancreatic Ductal Adenocarcinoma
Pdx1	Pancreatic Duodenal Homeobox 1
PP1	Protein Phosphatase 1
SMAD4	Mothers Against Decapentaplegic Homolog 4
SP1	Specificity Protein 1
TGFα	Transforming Growth Factor Alpha
TGFβ	Transforming Growth Factor Beta
TNFα	Tumour Necrosis Factor Alpha
WB	Western Blot

Chapter 1: Introduction

1.1 Inflammation in cancer aetiology

Inflammation is an evolutionary conserved process that serves as a primary defence mechanism against injury and infection, whilst enabling the orchestrated repair and regeneration of damaged tissue (Medzhitov 2008; Karin & Clevers 2016). In response to stress inducers such as toxins, pathogens, irritants and chemicals, an acute response is elicited by a myriad of cellular stress sensing pathways. Chronic inflammation also induces stress pathways that promote the mutations and transcriptional reprogramming that results in tumorigenesis (Grivennikov et al. 2010). The duality of inflammation-induced cancer and cancer-causing inflammation is central to understanding cancer biology and the variation in patient outcomes following diagnosis and treatment. Furthermore, there is a complex interplay between cell-intrinsic and cell-extrinsic factors that contribute to a loss of tissue homeostasis that precedes neoplasia and is exacerbated by tumour progression. Understanding the response of cells to tumour promoting chronic inflammation is central to preventing and treating cancer in an age of personalized medicine (Coussens et al. 2013).

1.1.1 The p53 family as regulators of inflammation

As ‘Guardian of the Genome’, p53 is widely understood to be a key tumour suppressor protecting cells from tumorigenesis. Originally p53 was described as an oncogene based on overexpression in tumours and the ability of p53 derived clones to transform cells. However, mutated forms of p53 were being

characterised rather than wild-type p53. Functionally, wild-type p53 acts primarily as a transcription regulator, responding to a diverse range of cellular extrinsic and intrinsic stresses. Among the range of p53-mediated responses, the induction of apoptosis or the initiation of cellular senescence are the most well-known, along with DNA repair and promoting differentiation. Regulation of p53 is achieved through complex mechanisms controlling p53 levels and target specificity. MDM2, an E3 ubiquitin ligase, reduces p53 levels in the absence of cellular stress by binding and targeting p53 for degradation (Brooks & Gu 2006).

Restoring p53 activity is hypothesised to be a therapeutic strategy in p53-wildtype tumours that will potentiate tumour apoptosis (Lu et al. 2014). However, reactivation of p53 in a p53-deficient mouse model of liver carcinoma does not result in apoptosis, rather it induces cellular senescence with differentiation and upregulation of inflammatory cytokines such as CSF1, MCP1, CXCL1 and IL-15 (Xue et al. 2007). Direct inhibition of macrophages or neutralizing antibodies to neutrophil or natural killer cell function delayed regression following p53 reactivation, suggesting a role for p53 in innate immune system mediated tumour suppression.

Inflammation can induce a stress response that activates the transcriptional network of p53. Isogenic cell lines differing in p53 status ($p53^{+/+}$ and $p53^{-/-}$), exposed to common microenvironment stresses such as nitric oxide, hydrogen peroxide, DNA replication arrest and hypoxia, demonstrate p53 stabilization and alterations in expression in hundreds of genes (Staib 2005). Mice null for p53 are more susceptible to experimental inflammatory conditions such atherosclerosis

and experimental autoimmune encephalitis (Okuda et al. 2003; Guevara et al. 1999). In a streptozotocin-induced diabetes mouse model, p53-deficient mice were more susceptible to diabetes with higher levels of IL-1, IL-6 and IL-12, potentially due to downregulation of STAT1 (Zheng et al. 2005). Lack of p53 may result in over activation of pro-inflammatory signalling either directly or indirectly, alongside delayed functional switching off of inflammatory responses (Gudkov et al. 2011). Innate immunity can also be regulated by p53. Toll-like receptors (TLR) are membrane glycoproteins that recognize pathogen-associated molecular patterns (PAMPs) to mediate innate immune responses. TLR3 induction has been shown to be p53 dependent, whilst TLR9 is less p53 dependent (Shatz et al. 2012).

1.1.2 NF-κB as regulator of inflammation

NF-κB is the central component that regulates the myriad of cell signalling pathways activated in response to inflammation. The NF-κB family of transcription factors, including NF-κB1, NF-κB2, RelA, RelB, and c-Rel, are constitutively expressed, but transcriptionally inactivated through Inhibitor of κB (IκB) binding. Three major pathways regulate NF-κB; the canonical, the alternative and atypical pathways. The canonical pathway is activated through PAMPs or cytokines such as TNFα and IL-1. Canonical activation is signalled through the IKK complex to phosphorylate IκB and facilitates nuclear translocation and transactivation of target genes to mediate survival. The functional consequence of NF-κB activation is cell type dependent. Activation of NF-κB in inflammatory cells occurs in response to bacteria, virus, cytokines, and necrotic products resulting in the production of inflammatory cytokines, growth-stimulating factors and pro-angiogenic factors (Hayden et al. 2006).

Canonical NF-κB activation through PAMPs or cytokines enhances transcription of proinflammatory cytokines such as IL-6 and IL-8. Proinflammatory cytokines are secreted to act in an autocrine or paracrine mechanism to sustain inflammation and activate immune cells. Cellular senescence, in response to oncogenic stress (oncogene-induced senescence, OIS) or chronic inflammation, requires stable cell cycle arrest and is mediated by RB and p53, acting as a barrier to tumorigenesis. NF-κB in the context of senescence is the major regulator of the senescent-associated secretory phenotype (SASP) resulting in the production of proinflammatory cytokines, chemokines and growth factors, and the alteration of the tissue microenvironment. NF-κB targets such as IL-6 and IL8, can activate the innate immune cells to eliminate senescent cells, or act in an autocrine manner to reinforce senescence (Freund et al. 2010).

1.1.3 Crosstalk between p53 & NF-κB

NF-κB and p53 share common characteristics. Both mediate cell stress responses through the transcriptional regulation of many target genes through the removal of an inhibitory protein. Activation is rapid, self-suppressing and can be pathological if excessively activated. Deregulation of NF-κB and p53 is characteristic of many cancer types. However, NF-κB and p53 mediated responses are often opposing. NF-κB promotes growth and is anti-apoptotic, whilst p53 is growth suppressive and pro-apoptotic. p53 is a tumour suppressor, frequently deleted or mutated in cancer, whilst NF-κB is rarely mutated and often activated in tumours. Generally, p53 responds to intrinsic stresses such as DNA damage and oxidative stress, while NF-κB responds to extrinsic stimuli such as pathogens.

However, p53 and NF-κB are not always in functional opposition and evidence for cooperation demonstrates the complexity of their roles. Induction of p53 can cause activation of NF-κB, independently of TNFα, while inhibition or loss of NF-κB can prevent p53-mediated apoptosis (Ryan et al. 2000). Cox-2, induced by physiological stress, stimulates proliferation and inhibits apoptosis. p53 upregulates Cox-2 by inducing NF-κB to bind to the COX-2 gene promoter, suggesting cooperation in promoting cell survival (Benoit et al. 2006). Similarly NF-κB is also required for the expression of Noxa and p53AIP1, pro-apoptotic transcriptional targets of p53 (O'Prey et al. 2010). Human macrophages can be coregulated by NF-κB and p53 for proinflammatory gene responses, through direct IL-6 promoter binding (Lowe et al. 2014). Tumour cell derived factors can upregulate p53 in macrophages to promote pro-tumorigenic cytokines such as IL-6 and IL-8, and chemokine production, for example CXCL1.

The existence of p53 and NF-κB crosstalk, either antagonistic or synergistic, or indeed whether each functions in isolation, is almost certainly cell-type and context specific. Dissecting the mechanisms that finely control the interplay and co-activation of the p53 and NF-κB networks is crucial to understand how failure to control either p53 or NF-κB results in unsuppressed inflammation and cancer.

1.2 Pancreatic ductal adenocarcinoma

1.2.1 Incidence and prognosis

In 2014, there were 9618 new cases of pancreatic cancer, ranking it the 11th most common cancer in the UK and accounting for 3% of all new cancer diagnoses (CRUK website). Low socioeconomic status is a risk factor for pancreatic cancer and it is estimated that 37% of pancreatic cancer cases are preventable through lifestyle modification. Pancreatic cancer is a malignancy of old age with 47% cases being diagnosed in patients over 75 years between 2012 and 2014. The incidence of pancreatic cancer is increasing with an additional 9% cases over a decade in the UK. This increase is not explainable by an aging population alone. Furthermore, pancreatic cancer is forecast to become the second leading cause of cancer-related death by 2030 in the United States behind lung cancer (Rahib et al. 2014).

There were 8817 deaths from pancreatic cancer in 2014, making it the 5th most common cause for cancer death and leading to 5% of all cancer deaths in the UK. Survival following a diagnosis of pancreatic cancer is less than 1% at 10 years in 2010-11 (CRUK website). Survival at five years and one year is 3% and 21% respectively, with improved survival if diagnosed below the age of 50. Patient survival following diagnosis has shown the least improvement compared to all other cancer types and remains essentially unchanged in 40 years. The dismal prognosis and outcomes following pancreatic cancer diagnosis has led CRUK to designate the disease a cancer of unmet need (CRUK website).

1.2.2 Mutational and protein expression landscape of PDAC

An oncogenic activating mutation of *KRAS* is a common oncogenic event in human cancer, typically occurring early in tumour initiation. *KRAS* mutations occur with increasing frequency with higher dysplasia grade (Löhr et al. 2005). However, mutation of *KRAS* alone is typically insufficient to initiate cancer and a second event, usually loss of wild-type tumour suppressor function is required. *KRAS* is mutated in 90% to 95% pancreatic ductal adenocarcinoma cases based on 4 sequencing projects available at cBioportal (http://www.cbioportal.org/). Oncogenic Kras mutation is the commonest activating mutation across all major tumour types. In four PDAC sequencing databases accessible in cBioportal, 92% of KRAS mutations occur at amino acid position 12 (631/685). Predominantly the change is G>D or G>V.

Understanding the key pathways altered in PDAC provides insights into the mechanisms required to facilitate tumorigenesis and metastasis. The most comprehensive whole genome sequencing (WGS) effort to date analysed 456 PDAC cases and identified 32 recurrently mutated genes that were classified into 10 pathways (Table 1.1) (Bailey et al. 2016). Consistent with previously reported WGS cohorts, activating KRAS mutations were the predominant mutational change (92%). Cell cycle alteration through mutation or loss of G1/S checkpoint regulators (TP53, CDKN2A, TP53BP2) occurred in 78% of cases. TGF-beta signalling (SMAD4, SMAD3, TGFBR1 & TGFRB2) mutations occurred in 47% of cases. DNA repair regulators (BRCA1, BRCA2, ATM and PALB2) were significantly mutated or lost, of which were 5% germline mutated and 12% were acquired somatic mutations. WGS of human PDAC supports functional studies

that demonstrate the importance of these altered pathways. Understanding how these key mutated pathways interact with non-mutated cell homeostatic regulators is central to developing an understanding of PDAC.

Significantly altered pathways	Mutated genes
KRAS	KRAS, MAPK4
Cell cycle	TP53, TP53BP2, CDKN2A
TGF-beta signalling	SMAD3, SMAD4, TGFBR1, TGFBR2, ACVR1B, ACVR2A
WNT signalling	RNF43, MARK2, TLE4
NOTCH signalling	JAG1, NF2, BCORL1, FBXW7
DNA repair	BRCA1, BRCA2, ATM, PALB2, ATF2
RNA processing	RBM10, SF3B1, U2AF1
ROBO SLIT pathway	ROBO1, ROBO2, SLIT2, MYCBP2
Chromatin	KDM6A, MLL2, MLL3, SETD2
SWI/SNF	ARID1A, ARID1B, SMARCA4, PBRM1

Table 1.1 Significantly altered pathways and mutated genes in PDAC (adapted from Bailey et al., 2016).

Expression analyses of cancer enables subtyping based on characteristic expression pathways that may relate to key mechanisms driving tumorigenesis and deregulation of homeostasis or cell identity. Expression subtyping may also inform prognosis and guide treatment and research. In PDAC, Bailey et al. proposed four subtypes: squamous, pancreatic progenitor; immunogenic; and aberrantly differentiated endocrine exocrine (ADEX). Squamous tumours were characterized by gene networks involved in inflammation, metabolic reprogramming, TGF-beta signalling, MYC pathway and upregulation of TP63ΔN.

TP63ΔN cooperates with TP53 mutation to regulate epithelial cell plasticity, tumourgenicity and epithelial to mesenchymal transition in tumours (Engelmann & Pützer 2014). The pancreatic progenitor subtype is enriched for transcription factors PDX1, MNX1, HNF4G, HNF4a, HNF1B, HNF1A, FOXA2, FOXA3 and HES1. ADEX is characterized by upregulation of genes involved in later pancreas development, such as NR5A2, MIST1 and RBPJL, important for acinar cell differentiation; pancreatitis and regeneration; as well as endocrine differentiation and MODY (INS, NEUROD1, NKX2-2 and MAFA). The immunogenic class demonstrates significant immune infiltration with associated B cell signalling pathways, antigen presentation, T cell and Toll-like receptor signalling, and upregulation of CTLA4 and PD1, along with expression profiles of infiltrating B and cytotoxic (CD8+) and regulatory T cells (CD4+ CD25+ FOXP3+ Tregs).

1.2.3 Inflammation in PDAC aetiology

Chronic pancreatitis is a risk factor for pancreatic cancer (Malka et al. 2002). Incidence of PDAC following CP is variable, with a standardized incidence ratio calculated at 14.4, and risk of malignant transformation 20 years after diagnosis at 4% (Lowenfels et al. 1993). Kras mutations are present in chronic pancreatitis cases although detectable Kras mutation may require prolonged chronic pancreatitis (van Laethem 1999; Löhr et al. 2005). However, variation in sampling method and test sensitivity contribute to reported high variability in incidence. Aetiologically, chronic pancreatitis may be the pathological consequence of alcohol abuse, hereditary chronic pancreatitis, cystic fibrosis transmembrane regulator (CFTR) gene mutation, tropical pancreatitis, autoimmune pancreatitis, hyperlipoproteinaemia or hypercalcaemia and in approximately 15% cases it is

idiopathic. Pancreatic cancer risk is reduced in randomised controlled trials in groups taking the non-steroidal anti-inflammatory aspirin compared to groups not on aspirin with the effect present from 5 year duration of treatment (Rothwell et al. 2011). Aspirin may lower the level of inflammatory stress in the pancreas that potentiates Kras mutation or disease progression following Kras mutation. Hereditary chronic pancreatitis (HCP) is the strongest risk factor for PDAC with an approximate 44-fold increase risk (Lowenfels et al. 1997). HCP is most commonly caused by a mutation in PRSS1, the cationic trypsinogen gene, that facilitates trypsin autolysis and gene mutations result in inappropriate activation of pancreatic zymogens.

Pancreatic cancer characteristically has a desmoplastic stroma composed primarily of α-smooth muscle actin (αSMA) positive myofibroblasts, also known as stellate cells. Stroma is produced by activated stellate cells in response to persistent inflammation as seen in CP or cancer. Previous studies have implicated the stroma as a physical barrier to cytotoxic chemotherapy to accessing the tumour leading to the rational to ablate stroma to potentiate cytotoxicity (Olive et al. 2009). However, genetic depletion of the αSMA+ component of PDAC led to an acceleration of the cancer and the understanding that stroma restrains cancer progression (Rhim et al. 2014; Ozdemir et al. 2014).

1.2.4 Mouse models of PDAC development

Mouse models have proved invaluable in understanding key pathways altered in PDAC development, the role of pancreatic inflammation, the contribution of the tumour microenvironment and the cellular origin of PDAC. The first mouse model

that recapitulated the preneoplastic lesions and PDAC utilized the LSL-Kras^{G12D} allele combined with either Pdx1- or P48-Cre recombinase (Hingorani et al. 2003). Pdx1-Cre;LSL-KRAS$^{G12D/+}$ (KC) mice develop additional tumours with varying penetrance including mucocutaneous papillomas, intestinal metaplasia of gastric epithelium and hyperplastic polyps of the duodenum.

Oncogenic Kras, in addition to PanIN initiation, is required for the maintenance of PanINs. The iKras mouse (*p48*-Cre;R26-rtTa-IRES-EGFP;TetO-*Kras^{G12D})* requires doxycycline to maintain Kras^{G12D} expression and reverts to wild-type Kras with doxycycline withdrawal (Collins et al. 2012). Following extended doxycycline treatment iKras mice develop complete histologic ADM and PanIN formation, with removal of doxycycline resulting in reversion of PanINs. Furthermore, αSMA- and vimentin-positive stroma becomes αSMA- and vimentin-negative following doxycycline removal as seen in non-proliferative scar tissue. The iKras mouse demonstrates the importance of oncogenic Kras for PDAC initiation and maintenance.

The long latency of approximately 12-months to PDAC development in the KC mouse corresponds to the finding that loss of tumour suppression via frequent loss of p53, p16 or SMAD4 is additionally required for tumorigenesis. The most widely utilized model of PDAC is the KPC model, combining a heterozygous p53 point mutation at R172H, equivalent to the recognized human R175 hotspot (Hingorani et al. 2005). The KPC mouse has a median survival of 6 months, at which time PDAC is present at 100% penetrance. However, KC;p53$^{R172P/+}$ is resistant to PDAC formation, as p53^{R172P} can still induce p21 and cell cycle arrest (Morton et

al. 2010). KPC exhibits similar tumour formation and median survival to KC; $p53^{flox/+}$, although metastasis is specifically enhanced *in vivo* and invasive activity *in vitro* (Morton et al. 2010). The limitation of the KPC model is that both $Kras^{G12D}$ and $p53^{R172H}$ are active embryonically rather than sequentially. Furthermore, $p53^{R175H}$ accounts for approximately 6% of human PDAC cases and conclusions drawn from the KPC mouse model may not applicable to all cases of PDAC (Bailey et al. 2016).

The $Kras^{G12D/+}$; $Ink4a/Arf^{lox/lox}$ mouse was developed to test the ability of p16 to repress the tumourgenicity of activated Kras (Aguirre et al. 2003). Within 11-weeks, all mice developed aggressive PDAC with a locally infiltrative phenotype and causing common bile duct obstruction. Metastases were less evident, lacking lung tumours, but the locally accelerated time course may have outpaced tumour cell dissemination. KC; $p53^{lox/+}$; $p16^{Ink4a\ lox/+}$ mice have increased tumour latency and metastatic burden compared to KC; $p53^{lox/lox}$ or KC; $p16^{Ink4a\ lox/lox}$ with latency the likely determinant of increased metastases (Bardeesy et al. 2006). SMAD4 deletion in the pancreatic epithelium does not alter pancreatic development. However, when combined with the oncogenic Kras, Smad4 deficiency resulted in reduced survival with terminal morbidity between 8 and 24 weeks (Bardeesy et al. 2006). Phenotypically, SMAD4-deficient tumours are more differentiated and resembled IPMNs closer than Smad4 wild-type tumours.

1.2.5 Mouse models to study inflammation in PDAC development

Mouse models utilizing the Pdx1- and p48-Cre recombinase systems are invaluable in understanding PDAC tumorigenesis particularly as the phenotypic

and signal transduction pathway changes are directly comparable between mouse and human. However, a significant limitation of the mouse model is that $Kras^{G12D}$ is expressed from embryonic day (E)9.5 and E10.5 for Pdx1 and P48 respectively. In human pancreatic disease, $Kras^{G12D}$ is not embryonically activated, rather it is acquired as an early event in tumorigenesis. The impact of embryonic activation of Kras is elegantly demonstrated by using a Tet-off strategy with a $Kras^{LSLG12Vgeo}$ under control of an elastase promoter ($Kras^{LSLG12Vgeo+/}$;*Elas*-tTA/*tetO*-Cre) (Guerra et al. 2007). Activation of $Kras^{LSLG12Vgeo}$ from P60 fails to produce PanINs and PDAC. This suggests adult pancreatic cells are refractory to oncogenic Kras mediated transformation. The de-differentiated state of embryonic development may enable oncogenic Kras expressing cells to initiate PanIN, suggesting a key barrier to tumorigenesis is the terminally differentiated tissue state.

Using the cLGL-Kras mouse, expressing $Kras^{G12V}$ under a non-endogenous promoter, resulted in higher levels of Ras activity than Ela-Cre^{ERT} and could accelerate ADM, CP and PDAC (Ji et al. 2009). Accelerating PDAC can also be achieved through over-expressing TGFα with $Kras^{G12D}$ (Siveke et al. 2007). TGFα activates the MAPK/ERK pathway through binding EGFR and resulting in a signalling cascade through Raf-Ras-Erk. Signalling that can directly or indirectly activate the MAPK pathway in presence of oncogenic Kras potentiates ADM, PanIN progression and PDAC.

Induction of pancreatitis, using intraperitoneal (IP) injection of the cholecystokinin (CCK) analogue caerulein, stimulates the secretion of pancreatic enzymes, inducing acute or chronic pancreatitis, depending on dosing schedule, and

activation of the MAPK pathway (Lampel & Kern 1977; Duan et al. 1995). Acute pancreatitis results in activation of a stress response, induction of NF-κB signalling, infiltration of immune cells, de-differentiation with expression of embryonic developmental genes, and resolution and repair of inflammation. Chronic pancreatitis similarly induces a stress response, and may additionally cause acinar-to-ductal metaplasia, and fibrosis through the persistent activation of stellate cells. In KC mice, short episodes of acute pancreatitis, without induction of chronic pancreatitis, accelerates mPanIN progression and mPDAC (Carrière et al. 2009).

In the $Kras^{LSLG12Vgeo+/}$;*Elas*-tTA/*tetO*-Cre mouse, with Kras activated at P60, chronic pancreatitis induces high-grade PanINs universally and PDAC in 30% cases at 12 months (Guerra et al. 2007). Chronic pancreatitis in the $Kras^{LSLG12Vgeo+/}$;*Elas*-tTA/*tetO*-Cre mouse appears to inhibit oncogene-induced senescence, as measured by p16 staining and inversely correlated Ki67 staining (Guerra et al. 2011). The use of nonsteroidal anti-inflammatory Sulindac, an inhibitor of COX-1 and COX-2, reduced the number and grade of lesions occurring in $Kras^{LSLG12Vgeo+/}$;*Elas*-tTA/*tetO*-Cre mice following chronic pancreatitis (Guerra et al. 2011).

The IL-6 STAT3 pathway is an example of how upregulation of a cytokine signalling pathway can initiate and sustain early pancreatic tumorigenesis. STAT3 activation is required for ADM but not pancreatic development (Miyatsuka et al. 2006). Oncogenic Kras does not directly activate STAT3, rather blocking cytokine signalling via gp130 can reduce STAT3 phosphorylation (Corcoran et al. 2011).

Gp130 is subunit of the IL-6 receptor and after complexing it is phosphorylated leading to association with JAK tyrosine kinases and STAT transcription factors. IL-6 is expressed by cancer cells and within tumour microenvironment components. In iKras; IL-6 knockout mice, pancreatitis does not alter PanIN initiation. However, iKras; IL-6 knockout mice have increased normal acini following pancreatitis recovery suggesting IL-6 is required for PanIN maintenance and cancer progression. Use of an anti-IL-6 antibody in the KPCY model results in failure of PanIN progression (Zhang et al. 2013).

Sex-determining region Y box 9 (Sox9) is required for $Kras^{G12D}$ mediated PanIN formation. $Ptf1a^{CreER};Kras^{G12D};Sox9^{fl/fl}$ mice injected at 3 weeks with tamoxifen do not form ADM and PanINs compared to $Ptf1a^{CreER};Kras^{G12D};Sox9^{+/+}$ mice (Kopp et al. 2012). $Sox9^{CreER};Kras^{G12D}$ mice only produce PanINs at extremely low frequency, thus Sox9 appears to regulate the expression of ductal genes and facilitates ADM. Furthermore, overexpression of Sox9 ($Sox9^{OE}$) in the $Ptf1a^{Cre};Kras^{G12D}$ mouse promotes ADM and PanINs. However, Sox9 overexpression alone is insufficient to induce ductal reprogramming. Injection of caerulein in $Sox9^{OE}$ mice on 2 consecutive days results in persistent ADM following injury. The $Ptf1a^{CreER};Kras^{G12D};Sox9^{fl/fl}$ mouse following inflammation does result in ADM but does not progress to PanINs (Kopp et al. 2012). Therefore, inflammation induces ADM through reactivation of developmental transcription factors with persistent expression required to promote neoplasia.

Murine evidence for the importance of inflammation in oncogenic Kras mediated PDAC provides an insight to human findings of the high incidence of Kras mutation

in CP, the greatly increased risk of PDAC in hereditary pancreatitis, and how activation of inflammatory pathways are both a hallmark of cancer and a mark of poor prognosis (Lüttges et al. 2000). Furthermore, high Ras activity is linked to induction of a senescence in cells. Senescent cells produce many factors associated with further inflammation; a process known as the senescence-associated phenotype (SASP) (Coppé et al. 2008).

In summary, the term inflammation encompasses a myriad of mechanisms linked to the stresses that potentiate Kras mutation; upregulating Ras activity to pathological levels; promoting dedifferentiation, repair and regeneration of acinar cells; activation of stellate cells in the fibrotic and tumour microenvironment; production of SASP-related inflammatory mediators; and inducing immune cells in suppressing or promoting disease progression.

1.2.6 Role of the immune response in PDAC

Tumour development is shaped by the immune system. Immune cells can be either pro- or anti-tumorigenic, forming a dynamic environment that can vary temporally and spatially alongside tumour development. At the earliest stages of pancreatic neoplasia there is an influx of leukocytes to PanINs (Clark et al. 2007). CD4+ T cells functionally contribute to the oncogenic Kras immunosuppressive environment and suppress CD8+ cytotoxic T cell activity. Elimination of CD4+ cells blocks PDAC tumorigenesis (Zhang et al. 2014). Effector T-cells are scarce in PanINs and PDAC, with little evidence of activation, while Tregs are more prominent in early PanINs (Clark et al. 2007). Tregs, characterised as CD4+CD25+ and expressing FOXP3, can inhibit immune and antitumor responses

mediated by CD4+CD25- and CD8+ cells. In PDAC, CD8+ cytotoxic T cells infiltration reduces with PanIN progression, while Tregs increase during PanIN progression (Hiraoka et al. 2006). Also, high Treg infiltration in PDAC associates with poor prognosis and distant metastasis. Tumour-infiltrating CD4+ and CD8+ T cells with lower levels of Tregs associate with longer survival (Ino et al. 2013).

Macrophage and MDSC infiltration are prominent in PDAC and is evident at the earliest stages of PanIN onset (Clark et al. 2007). Macrophage infiltration in PDAC, as with other malignancies, is associated with poor prognosis (Guerra et al. 2007; Guerra et al. 2011). Depletion of macrophages in the $p48^{Cre}$;$Kras^{G12D}$ model with gadolinium (III) chloride ($GdCl_3$) reduces PanIN formation whilst not reducing ADM (Liou et al. 2015). Similarly, targeting tumour-infiltrating macrophages (TAMs) by inhibiting colony stimulating factor-1 receptor (CSF1R) or chemokine (C-C motif) receptor 2 (CCR2) decreases tumour initiating cells and abrogates immunosuppression of cytotoxic CD8+ T cells (Mitchem et al. 2013). In PDAC, higher levels of M1 macrophages relative to M2 macrophages also associate with better prognosis (Ino et al. 2013).

Co-culture of primary acinar cells and mouse-derived macrophages promotes ADM (Liou et al. 2013). Specific cytokines are upregulated in macrophage conditioned media, of which RANTES/CCL5 and TNFα were capable in isolation of inducing ADM in explant culture studies albeit at reduced frequency compared to conditioned media. RANTES and TNFα are capable of activating NF-κB signalling, whilst RANTES is a target gene of NF-κB suggesting macrophages may potentiate a NF-κB signalling feedback loop. CD11b+ myeloid cells are

required for PDAC growth and CD11b+ cell depletion increases CD8+ T-cell infiltration, suggesting myeloid cells regulate CD8+ T-cell immunity in PDAC (Zhang et al. 2017). MAPK signalling may regulate PD-L1 expression, which could indicate a complimentary effect of dual MEKi and PD-1 inhibitor to reduced immunosuppression and enable an anti-tumoral T-cell mediated response to be achieved (Zhang et al. 2017).

Cytokines are a key factor influencing immune cell infiltration and activation in relation to inflammation and cancer. Tumour-derived GM-CSF can induce infiltration of CD45+ Gr-1+ CD11b+ cells into tumours, while GM-CSF knockdown increases activated CD8+ T cell infiltration to promote tumour necrosis (Bayne et al. 2012; Pylayeva-Gupta et al. 2012). Oncogenic Kras is central to controlling the cytokine and chemokine production that initiates and sustains the immune response to tumorigenesis. Specifically, $Kras^{G12D}$ can exert a chemoattractant effect on macrophages, whilst macrophages may secrete factors into the early neoplastic microenvironment that promote progression from ADM to PanINs. ICAM-1 is proposed as a chemoattractant candidate for macrophages as $Kras^{G12D}$ lentiviral transfection in primary acinar cells significantly upregulates ICAM-1 expression and *in vivo* administration of ICAM-1 neutralizing antibody reduces PanINs in $Kras^{G12D}$ mice (Liou et al. 2015).

The advent of immunotherapy in cancer treatment, demonstrating profound therapeutic responses in subgroups of patients, highlights the need to understand the duality of cancer-immune cell communication. Therapeutic targets could arise

from inhibiting tumour cell mediated immunosuppression, or by making cancer cells more visible to cytotoxic T cells.

1.2.7 Mechanisms of metastases

Metastasis, the growth of tumours at sites distant to the tissue of origin, is a major cause of death in PDAC cases. At death, 70% of patients have widespread metastatic disease (Iacobuzio-Donahue et al. 2009). Metastatic PDAC is often present at the time of diagnosis. The major mechanism of dissemination is haematogenous via the portosystemic blood supply resulting in liver and lung metastases. Murine models of PDAC vary in progression rate and metastatic phenotypes. Loss of p16 with oncogenic Kras results in rapidly progressive primary cancer with highly invasive and metastatic cancers (Aguirre et al. 2003). Oncogenic Kras with $p53^{R172H/+}$ (KPC) rather than $p53^{-/-}$ promotes both primary tumour and metastatic disease causing death (Hingorani et al. 2005). Mutant p53 can induce PDGFRb through inhibiting the p73/NF-Y complex to promote cell-autonomous signalling mediated metastasis (Weissmueller et al. 2014).

Epithelial-to-mesenchymal transition (EMT) is a process linking cell plasticity to cancer progression and metastasis (Nieto et al. 2016). The role of EMT in PDAC metastases is still debated as loss of EMT-specific transcription factors Snail and Twist in the KPC mouse model does not alter metastasis (Zheng et al. 2015). However, in the EMT-transcription factor ZEB1-deficient KPC model (KPCZ), epithelial PDAC tumours are promoted rather than a mesenchymal PDAC phenotype seen in KPC and human PDAC (Krebs et al. 2017).

Stromal and immune cell components are also recognised mediators of organ specific metastasis (Quail & Joyce 2013). Dense stroma produced by activated cancer-associated myofibroblasts is a key histological feature of PDAC. Stroma may be stimulating tumour progression through secreted growth factors and inhibiting chemotherapy. However, genetic ablation of PDAC cell fibrosis formation actually promoted tumour progression and metastasis (Rhim et al. 2014). PDAC metastasis to the liver is dependent on granulin-secreting inflammatory monocytes that stimulate hepatic stellate cells to promote fibrosis through periostin secretion (Nielsen et al. 2016).

1.3 NF-κB and p53 in pancreatic inflammation and PDAC

1.3.1 NF-κB in pancreatic inflammation

NF-κB activation occurs in the hyperacute response to pancreatitis and increases the expression of a plethora of proinflammatory genes. Experimental pancreatitis, induced by CCK analogue caerulein, results in measurable NF-κB activation within 30 minutes with subsequent upregulation of TNFα and NF-κB targets IL-6 and IL-8 (Gukovsky et al. 1998). NF-κB function in pancreatitis is complex and multiple lines of evidence suggests both pro- and anti-inflammatory roles (Rakonczay et al. 2008). Transgenic overexpression of p65 does not alter the pancreatic phenotype in mice due to compensatory upregulation in the inhibitory IκB subunit to abrogate dysregulation (Huang et al. 2013). However, upstream constitutive expression of IKK2 increases NF-κB activation resulting in pancreatitis (Huang et al. 2013). Conversely, pancreatic specific inactivation of the RELA encoding p65 increases

susceptibility of acinar cells to acute pancreatitis induced necrosis and systemic complications (Algül et al. 2007).

1.3.2 NF-κB in pancreatic ductal adenocarcinoma

As previously discussed, NF-κB signalling can result in tumour promoting and suppressive effects. Central to PDAC is constitutive NF-κB signalling, suggesting either a shift towards tumour-promoting downstream NF-κB effectors, or a specific NF-κB mediated mechanism that favours tumorigenesis. Deregulated NF-κB signalling may function by cell-autonomous or non-cell-autonomous mechanisms to regulate tumorigenesis. Progressive activation of NF-κB signalling has proposed to result from feedforward activation that potentiates Ras activity (Daniluk et al. 2012). *In vitro* upstream signalling through p38 MAPK activation can result in AP-1 mediated transcription of IL-1α to activate NF-κB thus feeding forward to promote further IL-1α transcription (Niu et al. 2004). IL-1α overexpression associates with poor prognosis in human PDAC and genetic ablation of upstream NF-κB regulator IKK2 in the KC mouse of PDAC effectively blocks PanIN and PDAC development (Ling et al. 2012). Also, genetic ablation of IKK complex member NEMO (IKKγ) in the KC model results in drastically reduced mPanIN, inflammation and fibrosis (Maier et al. 2013). However, inactivation of NF-κB family member RelA (p65) increases PDAC and decreases survival in a oncogenic Kras mouse. Mechanistically this is attributed to RelA deficiency compromising oncogene-induced senescence mediated by RelA target CXCL1 signalling via CXCR2 (Lesina et al. 2016). The phenotypic difference between loss of IKK2 and RelA in the oncogenic Kras mouse model is attributed to a greater number of cellular process controlled by IKK2 rather than p65/RelA alone, where

inactivation specifically promoted cellular stress and differentiation pathways (Lesina et al. 2016). NF-κB p65/RelA is a master regulator of SASP gene regulation and NF-κB p65/RelA inhibition generally promotes an aggressive cancer phenotype (Chien et al. 2011). However, the NF-κB pathway has been shown to be either pro- or anti-tumorigenic depending of the level of NF-κB pathway loss or inhibition. Members of the NF-κB family are rarely mutated or lost in PDAC suggesting other mechanisms of regulation exist in the context of PDAC tumorigenesis.

1.3.3 p53-family in pancreatic ductal adenocarcinoma

TP53 is altered in 66% of PDAC cases (Bailey et al. 2016). Most commonly, the alteration is a missense mutation (64%) with the five most common hotspots being R175G/H, R273C/H, R248Q/W, R282W, G245A/C/D/S. Missense mutations are almost exclusive to the DNA binding region of p53. TP53 truncating alterations occur throughout the TP53 gene, presumably resulting in p53-null heterozygous or homozygous phenotypes occurring in 32% of TP53 altered tumours. Interestingly the $p53^{R175H}$ mutation occurs in 10% of p53 missense mutations, and only contributes to approximately 4% of total PDAC cases. The contribution of the KrasG12D; $p53^{R175H}$ phenotype to our understanding of PDAC may be exaggerated by the focus on the KPC mouse as the most frequently utilized PDAC model.

When first described, the KPC mouse was found to replicate the spectrum of disease progression through preinvasive to metastatic cancer (Hingorani et al. 2005). Chromosomal instability, evaluated as aneuploidy, chromosomal

aberrations, chromatid breaks and fragmentation were cardinal genomic features of advanced and metastatic disease in the KPC model. However, the lack of concurrent $p16^{Ink4a}$ or TGF-beta-SMAD4 pathway mutations highlighted that Kras oncogene activation and loss of wild-type p53 were sufficient for PDAC onset. Mutant p53 (R172H) alters the metastatic incidence in mouse model of PDAC. The Pdx1-Cre-GFP, LSL-$Kras^{G12D/+}$, LSL-$Trp53^{loxP/+}$ ($KP^{fl}C$) model results in no macrometastases while the Pdx1-Cre-GFP, LSL-KrasG12D/+, LSL-$Trp53^{R172H/+}$ (KPC) model results in liver metastases in 65% mice. These results are suggestive of a distinct prometastatic role for R172H compared to loss of p53. Accumulation of p53 correlates with p53 mutation status, and higher immunohistological p53 staining scores correlated with lymph node metastasis in human samples (Rosenfeldt et al. 2013). These data are consistent with the mutant p53 status enhancing metastases either through gain of function or through a dominant negative effect on wild-type p53.

Autophagy, the cellular homeostatic process for intracellular degradation to deliver cytoplasmic components to the lysosome, can function in a tumorigenic or tumour suppressive way in PDAC. Genetic loss of autophagy genes Atg5 or Atg7 in the KC mouse model blocks the transition from low-grade neoplastic lesions to high-grade PanINs and PDAC (Rosenfeldt et al. 2013). However, when combined with p53 loss, Atg5 or Atg7 loss does prevent tumour progression. Also, the use of autophagy inhibitors as a potential antitumor strategy accelerated tumorigenesis in the p53-null state. The $p53^{R172P}$ mutation promotes p21 gene transactivation but not of other p53 target genes. Pdx1-Cre-GFP, LSL-$Kras^{G12D/+}$, $Trp53^{R172P/+}$ ($KP^{p21}C$) mice do not form PDAC, despite forming similar numbers of PanINs

compared to KC mice (Morton et al. 2010). Therefore, p21 suppression is required for PDAC development through bypass of growth arrest and senescence.

Loss or mutation of p53 is the commonest genetic event in the addition to the activating Kras mutation. Loss of wild-type p53 function is an important barrier to facilitate the progression from high-grade PanIN to PDAC, but is not universal. Understanding the mechanisms of p53-mediated suppression of PanIN progression, and aberrant cell-autonomous tumour pathways with both p53 loss and mutation is crucial to make progress in the prevention and treatment of PDAC. In p53 wild-type PDAC, p53 tumour suppression bypass may occur at the level of p53 expression and transcription. Restoration of wild-type p53 activity may be a therapeutic strategy to target PDAC (Lu et al. 2014).

1.4 ASPP2

ASPP2 is encoded by the TP53BP2 gene, located at human chromosomal position 1q41. ASPP2 was discovered by a screen for p53 interactors using a yeast two-hybrid system in which a protein termed 53BP2 was found (Iwabuchi et al. 1994). Full-length ASPP2, at 1128 amino acids, includes both 53BP2 and BBP variants, specifically stimulates the apoptotic function of p53 (Samuels-Lev et al. 2001). Subsequently, there have been numerous interacting partners of ASPP2 identified, leading to various p53-family-dependent and -independent functions regulating cancer, inflammation and development (Table 1.2).

Interacting Partner	**Reference**
p53	(Iwabuchi et al. 1994; Samuels-Lev et al. 2001)

p63	(Bergamaschi et al. 2004)
p73	(Bergamaschi et al. 2004)
Bcl-2	(Naumovski & Cleary 1996)
PP1	(Helps et al. 1995; Liu et al. 2011)
p65/RelA	(J.-P. Yang et al. 1999)
APCL	(Nakagawa et al. 2000)
CagA	(Buti et al. 2011)
Ras	(Wang et al. 2013)
YAP1	(Espanel & Sudol 2001)
PAR3	(Sottocornola et al. 2010)

Table 1.2 Published ASPP2 interacting partners

ASPP2 is regulated in three main ways; transcriptionally, epigenetically, and proteasomally. ASPP2 is a transcriptional target of E2F1, a transcription factor that regulates the cell cycle, DNA replication and apoptosis (Chen et al. 2005; Fogal et al. 2005). ASPP2 is also a transcriptional target of STAT1, a transcription factor regulating interferon expression, in response to LPS and IFN signalling (Turnquist et al. 2014). ASPP2 gene control may also be achieved through promoter CpG island methylation status (Liu et al. 2005). Hypermethylation of tumour suppressor gene promoters occurs in cancer. ASPP2 down-regulation through promoter methylation may function to bypass wild-type p53 mediated apoptosis and tumour suppression (Schittenhelm et al. 2013). Finally, ASPP2 levels are also controlled by proteasomal degradation (Zhu et al. 2005). Proteasomal inhibitors increase ASPP2 protein levels but not RNA levels. Like p53, ASPP2 can be ubiquitinated, most likely in the central region, consistent with a proteasomal substrate. Itch, an E3 ubiquitin ligase, recognises the PPXY motif of ASPP2 to result in binding that mediates ubiquitination and subsequent degradation (Gao et al. 2015).

1.4.1 ASPP2 as a regulator of apoptosis and inflammation

ASPP2 specifically enhances the apoptotic function of p53, while not effecting p53 mediated G1 arrest (Samuels-Lev et al. 2001). Along with ASPP1, ASPP2 provides an example of how p53 functional selectivity is achieved through promoting an apoptotic cell fate over senescence. *In vitro* ASPP2 is generally not found to be mutated in various cell lines, but mRNA levels are highly variable. Cell line viability, following exposure to DNA-damaging agents, such as irradiation and *cis*-diamine-dichloroplatinum, correlate with low ASPP2 expression, supporting a pro-apoptotic role (Mori et al. 2000). In cell lines engineered for conditional expression, ASPP2 lowers the apoptotic threshold following irradiation, while ASPP2 silencing enhances clonogenic survival following UV irradiation (Lopez et al. 2000).

Epithelial tissues, such as the colon, require maintenance of polarity for homeostasis and regeneration following injury. Yes-associated protein (YAP) is a critical regulator of tissue regeneration following inflammatory injury and may be potentially oncogenic if deregulated (Cai et al. 2010). ASPP2 localisation at the apical-lateral domain may act as molecular scaffold for regulating YAP activity and consequently the Hippo pathway (Royer et al. 2014). ASPP2$^{\Delta 3/\Delta 3}$ mice have abnormal regeneration following dextran sodium sulfate (DSS) treatment, possibly due to abnormal YAP activity (Koch, unpublished).

ASPP2 deficiency has also been linked to neuroinflammation. ASPP2 expression is upregulated in response to the TLR4 ligand lipopolysaccharide (LPS) and IFNγ

in human monocytes, murine macrophage and microglial cell (Turnquist et al. 2014). Induction is independent of NF-κB RELA/p65 and is via a STAT1-dependent pathway. It was proposed that ASPP2 acts at the blood-cerebral spinal fluid barrier, as ASPP2-deficient mouse brains exhibit enhanced inflammation.

Helicobacter pylori, a bacterium that can establish persistent stomach infection in humans, increases risk of gastrointestinal cancers and myeloid and B-cell lymphomas, and is classified as Group 1 carcinogen by the World Health Organization. Cytotoxin-associated gene A (CagA) is injected by *H. pylori* into epithelial cells to manipulate host cellular processes, including cytoskeleton integrity, epithelial polarity and apoptosis. Intriguingly, CagA binds ASPP2 with subsequent binding to p53 resulting in proteasomal degradation of p53 (Buti et al. 2011). Degradation of p53 thus favours cell survival in the presence of chronic infection and promotes transformation. *In vitro* knockdown of ASPP2 in *H. pylori* infected cells potentiates apoptosis.

1.4.2 ASPP2 in development

The discovery and characterization of ASPP2 as a proapoptotic binding partner of p53 resulted from *in vitro* experiments. A developmental role of ASPP2 was subsequently elucidated through the creation of a transgenic mouse deficient for ASPP2 (Vives et al. 2006). In the C57/B6 background, targeted disruption of exon 3 of the TP53BP2 gene resulted in a homozygous birth rate of 6.4% (expected 25%) from heterozygous mating. Most live mice born died between 6 and 30 days with a presumed hydrocephalus or cardiac-related cause of death. Double homozygous knockout mice for ASPP2$^{-/-}$ and p53$^{-/-}$ were prenatal lethal. In the

BALB/c background the majority of mice survive to weaning, and developed hydrocephalus and retinal dysplasia (Sottocornola et al. 2010). ASPP2 localization to the cell junction and colocalization with apical-junctional complex (AJC) components Par-3 and ZO-1 crucial for cellular polarity supported a p53 independent role for ASPP2 in development. ASPP2-deficiency in neural progenitors results in loss of polarity and failure of asymmetric division (Sottocornola et al. 2010). In humans, ASPP2 has been associated with a 1q41q42 microdeletion syndrome, characterized by dysmorphic features, intellectual disability and brain abnormalities (Zak et al. 2016). TP53BP2 was proposed as a candidate for the clinical features associated with 1q41q42 microdeletion syndrome.

1.4.3 ASPP2 in tumorigenesis and cancer

ASPP2, encoded by TP53BP2, regulates key pathways involved in tumorigenesis and cancer progression. However, TP53BP2 is infrequently mutated in human cancer, with the exception of pancreatic ductal adenocarcinoma where TP53BP2 is one of 32 significantly mutated genes (Bailey et al. 2016). ASPP2-null mice on the C57BL/6 background die soon after birth or weaning. ASPP2 heterozygotes develop normally and can be used for tumour studies. Heterozygosity of ASPP2 predisposes mice to spontaneous tumours with an increased incidence of lymphoma, sarcoma and carcinoma, and a reduced tumour-free survival (Vives et al. 2006). ASPP2 heterozygotes also have increased incidence of lymphomas following gamma-radiation, analogous to $p53^{+/-}$ mice. Double $ASPP2^{+/-}$ and $p53^{+/-}$ heterozygous mice have increased spontaneous tumour incidence, most frequently lymphomas, relative to single heterozygous mice. Tissue ASPP2 protein

or RNA expression forms the basis of linking ASPP2 downregulation to poor prognosis and mechanisms of tumour suppression (Table 1.3).

Tumour type	Putative Role	Proposed Mechanism	Reference
Hepatocellular carcinoma	Tumour suppressor	Inhibits EMT Inhibits autophagy	(Wang et al. 2014) (Chen et al. 2016)
Pancreatic ductal adenocarcinoma	Tumour suppressor	Inhibits autophagy and chemosensitizer	(Song et al. 2015)
Squamous cell carcinoma	Tumour suppressor	Facilitates NF-κB–mediated repression of p63	(Tordella et al. 2013)
Breast cancer	Tumour suppressor	Promotes apoptosis Inhibits metastasis	(Samuels-Lev et al. 2001) (Sgroi et al. 1999)
Diffuse large B-cell lymphomas	Tumour suppressor	Promotes apoptosis	(Lossos et al. 2002)
Gastric cancer	Tumour suppressor	Inhibits invasion and TGF-β1 induced EMT via Smad7	(Gen et al. 2017)

Table 1.3 Published cancers with ASPP2 associates and proposed mechanism of tumour suppression

Squamous cell carcinoma (SCC) develops from squamous epithelia, such as the skin, oral cavity, oesophagus, and cervix. Modelling SCC in mice requires multiple genetic mutations or is most commonly induced with chemical carcinogens to induce *RAS* mutation. Expression of p63 in squamous tissue occurs in the basal layers where stem cells reside, and is lost with squamous differentiation, whereas ASPP2 is expressed in differentiated but not basal epidermis cells (Tordella et al. 2013). Overexpression of p63 is a hallmark of SCCs, while the p63 isoform

ΔNp63 is considered oncogenic through capability to regulate genes for basal cell proliferation. BALB/c ASPP2$^{\Delta 3/+}$ mice develop SCC spontaneously by potentiating NF-κB mediated repression of p63. Mechanistically, ASPP2 binds IκB to enhance nuclear p65 that inhibits p63. In human head and neck SCC, ASPP2 and p63 expression were inversely correlated, with lowest ASPP2 levels in metastatic disease (Tordella et al. 2013). ASPP2$^{+/-}$ mice created in the B6 background by removing exons 10-17 displayed increased spontaneous tumour incidence with age, occurring at over 1-year, with no specific increase in lymphoma, sarcoma or carcinoma (Kampa et al. 2009).

ASPP2 induces the mesenchymal-to-epithelial transition (MET) in mouse kidney, that is required for nephrogenesis, through formation of an ASPP2-β-catenin-E-cadherin ternary complex that prevents β-catenin from inducing ZEB1 expression (Wang et al. 2014). Reduced ASPP2 expression favours epithelial-to-mesenchymal transition (EMT) that associates with poor prognosis in hepatocellular carcinoma and breast cancer patients (Sgroi et al. 1999). ASPP2 is also linked to the regulation of autophagy. In hepatocellular carcinoma (HCC), ASPP2 inhibits autophagy by regulating the translocation of p65/RelA to the nucleus and reducing *BECN1* transcription (Chen et al. 2016). Additionally, ASPP2 binds BECN1 to inhibit formation of a complex with UVRAG and PIK3C3 (Complex II) in autophagosome formation.

1.4.4 Hypothesized role of ASPP2 in pancreatic ductal adenocarcinoma

ASPP2 may function in a cell-context and tissue-type specific manner, but no study has yet attempted to study the role of ASPP2 in tumour type-specific model.

PDAC is the only cancer with significantly mutated TP53BP2. One study to date has investigated a role for ASPP2 in PDAC. *In vitro* cell line work and ASPP2 staining of a cohort of pancreatic cancer patients made the connection between ASPP2 and down-regulation of autophagic activity through the AMPK-mTOR pathway (Song et al. 2015). ASPP2 may suppress epithelial plasticity and plasticity through inhibiting β-catenin regulated ZEB1 expression, as demonstrated in nephrogenesis *in vivo* (Wang et al. 2014).

The TP63 transcriptional network is associated with a squamous expression profile and poor prognosis in PDAC (Bailey et al. 2016). ASPP2 may bind IκB to enhance nuclear p65 that represses p63 expression. ASPP2 could potentiate Kras induced senescence, a key roadblock in PDAC development, or facilitate PanIN apoptosis, prior to PDAC onset. Alternatively, ASPP2 may function on multiple pathways, and thus provide insights into crosstalk between key cancer pathways. For example, concurrent analysis of the p53-family and NF-κB pathways may provide insights to how these critical tumour pathways are deregulated in cancer.

1.5 iASPP

iASPP, an 828 amino acid protein, is encoded by the PPP1R13L gene, located at position 19q13.32 in humans. iASPP, also known as RAI (RelA-associated inhibitor), is evolutionarily conserved from *Caenorhabditis elegans* (*C. elegans)* to humans. iASPP specifically inhibits p53-mediated apoptosis *in vivo* and *in vitro.* In *C. elegans*, iASPP RNAi increases apoptotic germ cell corpses, a phenotype absent in p53-null worms (Bergamaschi et al. 2003). iASPP has a number of interacting partners, and like ASPP2, results in a number of p53-dependent and -

independent functions regulating cancer, inflammation and development (Table 1.3).

iASPP Interacting Partner	Reference
p53	(Bergamaschi et al. 2006)
p63	(Notari et al. 2011)
p73	(Cai et al. 2012)
p65	(J. P. Yang et al. 1999)
PP1	(Llanos et al. 2011)
SP1	(Takada et al. 2002)

Table 1.3 Published iASPP interacting partners

Regulation of iASPP occurs through phosphorylation, transcriptionally, and through localisation. Cyclin B1/CDK1 mediated phosphorylation of iASPP at S84/S113 increases iASPP nuclear localization by preventing self-interaction (Lu et al. 2013). Phosphorylated iASPP is more potent in inhibiting p53 than unphosphorylated iASPP. The iASPP promoter has a conserved E2F-binding site and E2F1 can bind to the iASPP promoter, as well as binding the ASPP1 and ASPP2 promoters (Pandolfi et al. 2015). In melanoma, hedgehog signalling, through GLI1/2 regulates both Cyclin B1 and E2F1 to upregulate iASPP thus inhibiting wild-type p53 *in vivo*. RelA also binds a putative iASPP promoter that links constitutive NF-κB/p65 activation with upregulation of iASPP in hepatocellular carcinoma (Lu et al. 2010). The biological function of iASPP is context dependent with phenotypes described in development and related to cellular stress events such as inflammation, apoptosis and cancer.

1.5.1 iASPP as a regulator of apoptosis and inflammation

iASPP was initially characterised as an inhibitor of p53-mediated apoptosis and an oncoprotein (Bergamaschi et al. 2003). iASPP also inhibits apoptosis independently of p53 in tumour cells by inhibiting the transcription of apoptotic genes of p63/p73 (Cai et al. 2012). Evidence for iASPP as a functional inhibitor of apoptosis predominantly exists *in vitro,* with limited *in vivo* models (Wilson et al. 2014). iASPP links the regulation of both RelA/p65 and p53, which can be induced or activated by similar stresses, but result in differing cellular responses. Caspase 3-mediated cleavage of iASPP, resulting in an 80 kDa fragment can translocate to the nucleus where it can inhibit RelA or p53 more efficiently than full-length iASPP (Hu et al. 2015).

Patient skin-derived fibroblasts (PDFs) from humans with a premature stop codon in the *PPP1R13L* gene express higher mRNA levels of NF-κB target genes including IL-1β, TNFα, IL-6 and MCP1, but not MMP9 and IκB, when stimulated with LPS (Falik-Zaccai et al. 2017). Similar increase in inflammatory mediators were seen with *PPP1R13L* knockdown in control fibroblasts with LPS stimulation. In *PPP1R13L* deficient PDFs, inhibition of NF-κB with BOT-64 abolished LPS induced upregulation of IL-1β, IL6 and TNFα to confirm NF-κB dependence.

1.5.2 iASPP in development and tissue homeostasis

Developmental roles for iASPP were first discovered in Poll Hereford calves and mice with spontaneous iASPP mutations (Simpson et al. 2009; Herron et al. 2005). The Poll Hereford cattle displayed a lethal, autosomal recessive cardiomyopathy

and woolly haircoat syndrome, while mice, termed waved-3 (wa3) possess similar heart and skin abnormalities. Using transgenic mice with exon 8 of iASPP deleted (*iASPP*$^{\Delta 8/\Delta 8}$), the phenotype of arrhythmogenic right ventricular cardiomyopathy (ARVC) was described and matches wa3 (Notari et al. 2015). In five related Arab-Christian patients with a homozygous premature stop codon in *PPP1R13L* gene, who all died before 3-years of age, all had evidence of structural heart defects and cardiomyopathy (Falik-Zaccai et al. 2017). Examination of wa3 mouse hearts demonstrated increased levels of IL-1β without extrinsic stimulation. RNA-Seq of wa3 hearts from new-born to 12 weeks, demonstrated a progressive upregulation of genes associated with fibrosis, immune function, signal transduction, TGFβ and NF-κB signalling (Falik-Zaccai et al. 2017). The iASPP$^{\Delta 8/\Delta 8}$ mouse epidermis is thicker than wild-type due to expansion of the early-differentiation layers. iASPP is predominantly expressed in the basal keratin 14-expressing layers and co-localizes with p63. iASPP binds p63 to inhibit transcriptional targets that promote epithelial differentiation independently of NF-κB/p65 and p53 (Notari et al. 2011). In humans with a premature stop codon in *PPP1R13L*, two out of three assessments described skin with ichthyosis-like fine scale and erythema (Falik-Zaccai et al. 2017).

Waved-1 (wa1) and waved-2 (wa2) mice, named prior to the discovery of waved-3, possess wavy hair due to follicular abnormalities and a variable incidence of eyes open at birth depending on mouse background (Luetteke et al. 1993; Luetteke et al. 1994). Eyes open at birth occurs in wa3 and *iASPP*$^{\Delta 8/\Delta 8}$ mice. Wa1 has a disrupted TGFα gene and does not produced functional TGFα protein, whilst wa2 has a V742G point mutation that reduces EGFR tyrosine kinase activity. Wa1 and

wa2 do not possess a cardiac phenotype. Waved with open eyes (woe) shares the wa3 phenotype with wavy hair, eyelids open at birth, and enlarged heart (Hassemer et al. 2010). Woe mice possess a C794T substitution in the *Adam17* gene in the protein metalloprotease domain rendering it functionally inactive. Woe2 is another waved with open eyelids and heart abnormalities arising as a spontaneous mouse phenotype due to a 1308 base pair deletion in *PPP1R13L* resulting in a C-terminal end loss of 223 amino acids (Toonen et al. 2012). Wa1, wa2 and woe share phenotypes related to hypoactivation of the EGFR pathway. However, it is unknown whether mutant iASPP, including the wa3 and woe2 mice, sharing the wavy fur and eyelids open at birth phenotype, is also due to abnormalities in EGFR pathway activation.

1.5.3 iASPP in tumorigenesis and cancer

Following the identification of iASPP as an inhibitor of the p53 family, studies have consistently linked iASPP expression in tumours to poor prognosis. iASPP is rarely deleted or mutated in cancer, with expression intensity and location linking iASPP to prognosis. High levels of nuclear iASPP associates with reduced survival in melanoma (Lu et al. 2013). Nuclear and cytoplasmic iASPP are upregulated in prostate cancer, while high iASPP expression is associated with metastatic disease and reduced survival (Morris et al. 2014). Multiple studies link iASPP overexpression in human tumours with *in vitro* work proposing inhibition of p53 and anti-apoptosis as the predominant mechanism (summarized in Table 1.4). It has been hypothesized that iASPP could be a target to restore wildtype p53 function, promote apoptosis and treat cancer (Lu et al. 2014).

Tumour type	Putative Role	Proposed Mechanism	Reference
Melanoma	Oncogene Oncogene	Inhibition of p53-mediated apoptosis p53 inhibition	(Pandolfi et al. 2015) (Lu et al. 2013)
Hepatocellular carcinoma	Oncogene Oncogene	Promotes proliferation Promotes proliferation and is antiapoptotic	(Lin et al. 2011) (Lu et al. 2010)
Bladder	Oncogene	Inhibition of p53 family mediated apoptosis	(Wu et al. 2017)
Ovarian	Oncogene	Chemoresistance by inhibiting mitotic catastrophe	(Jiang et al. 2011)
Colorectal	Oncogene	Promotes proliferation and inhibits apoptosis	(Gan et al. 2017)
Prostate	Oncogene	Inactivates wild-type p53	(Morris et al. 2014)
Glioma	Oncogene	Inhibits apoptosis and	(Liu et al. 2015)

Table 1.4 Published cancers with iASPP associations with proposed role

No mouse model exists to examine whether iASPP functions as an oncogene *in vivo*. The germline *iASPP*$^{\Delta 8/\Delta 8}$ mouse median survival of 6 months precludes its use in murine tumour studies. An unpublished study using a cytokeratin 14 specific iASPP-deficient mouse (*iASPP*$^{\Delta 8/\Delta 8}$*;KRT14*^{Cre}) exposed to chemical tumour promoter 12-O-tetradecanoylphorbol-13-acetate (TPA) found iASPP-deficient mice are more susceptible to papilloma formation (Chung, unpublished thesis).

1.5.4 Hypothesized role of iASPP in pancreatic ductal adenocarcinoma

iASPP expression is consistently associated with poor prognosis in human cancer. Direct binding and transcriptional inhibition of the tumour suppressor function of p53-family members, primarily p53-mediated apoptosis, is the proposed mechanism through which iASPP functions as an oncogene. However, no model

exists to test whether loss of iASPP protects from tumorigenesis or progression, and whether it functions primarily by potentiating p53-regulated apoptosis. *In vitro* studies lack two key elements in tumorigenesis; the ability to study initiating events of tumorigenesis, and the tumour-microenvironment interactions involving non-cancer cell types such as stroma and immune cells.

Oncogenic Kras-mediated pancreatic tumorigenesis is inhibited by EGFR- and Adam17-knockout, suggesting that a feedforward mechanism through the MAPK pathway is essential for pathological MAPK activation (Ardito et al. 2012). Interestingly, iASPP, TGFα, EGFR and Adam17 mutant mice all share the developmental wavy hair and eyes open at birth phenotype. If iASPP also functions to negatively regulate MAPK feedforward activation, then iASPP may be a pathological player in PDAC initiation.

Central to pancreatic cancer tumorigenesis is loss of tumour suppression, through p53, SMAD4, or CKDN2 deletion or mutation, thought to be the barrier between PanIN and PDAC onset, and subsequent metastasis. TP53 has been demonstrated to be mutated or deleted in approximately 50% cases, but there remains a significant proportion of cases with wild-type p53. Functional inhibition of wild-type p53 may be achieved through elevated iASPP, as proposed in other tumour types. Loss of iASPP may potentiate apoptosis to protect from conversion of high-grade PanIN into PDAC.

1.6 Aim of the study

ASPP2 and iASPP are classified as a tumour suppressor and oncogene respectively primarily based on expression in human cancer linked to prognosis; *in vitro* evidence consistent with mechanisms of tumourgenicity; and as a known regulators of both p53-family function and NF-κB. No study has systematically determined the roles of ASPP2 and iASPP in inflammation and tumorigenesis, and the primary mechanism through which the ASPPs regulate cancer. The aim of this study is to evaluate the roles of ASPP2 and iASPP in the regulation of pancreatic ductal adenocarcinoma and pancreatitis.

Chapter 2: Materials and methods

2.1 Materials

2.1.1 Reagents

All reagents were purchased from Sigma or VWR unless stated otherwise.

5x Agarose Sample Buffer

50% (w/v)	Sucrose
100 mM	EDTA, pH 8.0
0.1% (w/v)	Bromophenol blue
0.1% (w/v)	Xylene cyanol

Agarose Gel for DNA Electrophoresis

Agarose gel (Gibco BRL, UK) was dissolved in 1x TAE buffer at an appropriate percentage (w/v). The mixture was heated in a microwave until dissolved, then ethidium bromide was added (1:50,000). The solution was poured into a casting tray with a comb and left to solidify to room temperature.

Alcian Blue

1% (w/v) final solution of Alcian Blue 8G was prepared in 3% glacial acetic acid. pH was adjusted to 2.5.

Ammonium Persulfate (APS)

10% (w/v) stock solution was prepared in water, aliquoted and stored at -20°C degrees.

Blocking Solution

5% (w/v) fat-free milk (Marvel, UK) or 5% (w/v) bovine serum albumin (BSA) was prepared in Tris-buffered saline and Tween 20 (1x TBS-T).

Caerulein

Caerulein (>97% HPLC) (Sigma, C9026) solubilised in PBS for IP injection at the required concentration.

COmplete™ Protein Inhibitor Cocktail

One COmplete™ protein inhibitor (Boehringer Mannheim, UK) tablet was dissolved in 2 mL of sterilized water as a 20x stock solution and stored at -20 degrees for up to 12 weeks.

Citric Acid Buffer

10 mM citric acid solution was prepared in water and pH adjusted to 6.0 with NaOH.

DAPI Staining Solution

1000x stock solution of 10 mg/mL was prepared by dissolving 4',6'-Diamidino-2-phenylindole (DAPI) dihydrochloride hydrate in water and stored at -20°C.

DNA marker

100bp and 1kb DNA ladders were purchased from New England Biolabs (UK).

EDTA Solution

A 0.5 M stock solution of ethylenediaminetetracetic acid (EDTA) was prepared by dissolving 18.6 g of EDTA in 70 mL distilled water. pH was adjusted to pH 8.0 with NaOH and volume made to 100 mL with distilled water.

Ethidium Bromide

A 10 mg/mL stock solution was prepared by dissolving 0.2 g ethidium bromide in 20 mL of distilled water and then stored protected from light at room temperature.

GNT Buffer

50 mM	KCl
1.5 mM	$MgCl^{2+}$
10 mM	Tris-HCl (pH 8.5)
0.01%	Gelatine
0.45%	NP-40
0.45%	Tween-20

Adjust pH 8 with HCl then store in fridge.

Mouse Cytokine Antibody Array

R&D Systems Mouse Cytokine Array, Panel A (Catalog #ARY006) was used per manufacturer's instructions.

Paraformaldehyde (PFA) Fixation Solution

4% (w/v) solution was prepared by dissolving paraformaldehyde in water and heating to 65°C. pH was adjusted to 7.0 with 1 M HCl and solution stored at 4°C.

Phosphate Buffered Saline (PBS)

PBS (10X), pH 7.4, Gibco was diluted to 1X with distilled water. Sterile PBS was prepared and autoclaved by the Ludwig laboratory support team.

Primers used in PCR

All primers were synthesized by Operon (Germany). The lyophilized primers were dissolved in nuclease-free water to a stock concentration of 100 mM.

Protein Molecular Weight Markers

Pre-stained protein markers were purchased from New England Biolabs (UK) and used as a size standard for SDS-PAGE.

SDS Solution

10% (w/v) solution of sodium dodecyl sulphate (SDS) was dissolved in water and stored at room temperature.

5x SDS-Page Loading Buffer

250 mM	Tris-HCl
10% (w/v)	SDS
50% (v/v)	Glycerol
12.5% (v/v)	β-Mercaptoethanol
0.5% (w/v)	Bromophenol blue

10x SDS-PAGE Running Buffer

720 g Glycine

150 g Tris-Base

50 g SDS

Final volume adjusted to 5 L with distilled water.

10x SDS-PAGE Transfer Buffer

725 g Glycine

145 g Tris

Final volume adjusted to 5 L with distilled water. The buffer was used with 20% methanol as 1x solution.

50x TAE (Tris-Acetate-EDTA) Buffer

242 g Tris base

57.1 ml Glacial acetic acid

100 ml 0.5 M EDTA

The final volume was adjusted to 1 L with distilled water and pH adjusted to 8.5, before using at a 1x concentration. For making agarose gel, 2 μl of 10 mg/ml ethidium bromide solution per 100 ml was added to the 1x TAE buffer.

Tris Stock solutions

Tris base was dissolved in water to provide 0.5 M, 1 M and 1.5 M solutions which were pH adjusted with concentrated HCl.

10x Tris Buffered Saline Tween (TBS-T)

121 g	Tris base
36.53 g	NaCl
10 ml	Tween-20

pH adjusted to 7.6 with around 60 ml HCl in a total volume of 5 L. Used at 1x concentration.

Urea Buffer

8 M	Urea
1 M	Thiourea
0.5%	CHAPS
50 mM	DTT (dithiothreitol)
24 mM	Spermine

Stored at -20°C short term.

2.1.2 *Ex vivo* ADM assay materials

3D-culture medium

10x	RPMI 1640; Gibco 31800-022
1%	Fetal bovine serum (FBS)
1%	Penicillin-Streptomycin (Pen)
0.1 mg/mL	Soybean Trypsin Inhibitor (STI); Sigma T6522
1 µg/mL	Dexamethasone; Sigma D4902

Dissolve 1 package of RPMI 1640 powder in 100 ml ddH_2O. Add 2 g NaHCO3, pH to 7.2. Add FBS, Pen, STI and Dexamethasone at required concentrations. Filter sterilized, stored at 4°C.

Collagenase P

Collagenase P (Roche, 11213857001) dissolved in 10 ml ddH_2O to make a 10 mg/mL stock. Filter sterilized, aliquoted and stored at -80°C.

Sodium Bicarbonate

4.2% $NaHCO_3$, as 4.2 g $NaHCO_3$ dissolved in 100 mL ddH_2O and filter sterilized.

Rat Tail Collagen I

Rat tail collagen I (Invitrogen, A10483) stored at 4°C.

TGFα

Human recombinant TGFα (Peprotech) dissolved in sterile water at a working concentration of 50 ng/mL and stored at -20°C.

2.1.3 SDS-Polyacrylamide Gels

Preparation of SDS-polyacrylamide gels

	Resolving Gels				Stacking Gel
	6%	8%	10%	12%	4%
Acryl/Bis (30%)	2 mL	2.7 mL	3.3 mL	4 mL	1.3 mL
1.5 M Tris HCl pH8.8	2.5 mL	2.5 mL	2.5 mL	2.5 mL	-
1 M Tris HCl pH6.8	-	-	-	-	2.5 mL
10% SDS	100 µL	100 µL	100 µL	100 µL	100 µL
10% APS	100 µL	100 µL	100 µL	100 µL	100 µL
TEMED	10 µL	8 µL	5 µL	5 µL	10 µL
Distilled Water	5.3 mL	4.6 mL	4 mL	3.3 mL	6.1 mL

Total Volume	10 mL	10 mL	10 mL	10 mL	10 mL

Table 2.1 Preparation of SDS-Polyacrylamide gels. Abbreviations: APS, ammonium persulfate; TEMED, N,N,N′,N′-Tetramethylethylenediamine; Tris, Tris(hydroxymethyl)aminomethane; SDS, sodium dodecyl sulphate.

2.1.4 Antibodies

Antigen	Clone	Host/Source	Application
ASPP2	DX54.10 (Ludwig)	Mouse mAb	IHC 1:200
ASPP2	S32 (Ludwig)	Rabbit pAb	WB 1:1000; IHC 1:200
CK19	TROMAIII (DSHB)	Mouse mAb	IHC 1:400
Cleaved-Caspase 3 (Asp175)	#9661 (CST)	Rabbit pAb	IHC 1:200
p44/42 MAPK (ERK1/2)	#9102 (CST)	Rabbit pAb (purified)	WB 1:1000
GFP	D5.1 (CST)	Rabbit mAb	IHC 1:200
iASPP	LX49.3 (Ludwig)	Mouse pAb (purified)	WB 1:1000; IHC 1:400; IF 1:400
Ki67	SP6 (Abcam, ab16667)	Rabbit mAb	IHC 1:400
MDM2	C-18 (Santa Cruz, sc-812)	Rabbit pAb	WB 1:1000
p53 (Murine)	CM5 (Novocastra)	Rabbit pAb	WB 1:2000; IHC 1:500
p53 (Human)	DO-1 (Santa Cruz, sc-126)	Mouse mAb	IHC 1:500
p97/VCP	NB100-1557 (Novus)	Rabbit pAb	WB 1:5000
Phospho-p44/42 MAPK (ERK1/2)	#9101 (CST)	Rabbit pAb	WB 1:1000
β-Tubulin	#2146 (CST)	Rabbit pAb (purified)	WB 1:2000

Table 2.2 Primary antibodies

Antigen	Source	Application
BP-HRP Anti-Mouse IgGκ	Vector Labs	IHC 1:100 WB 1:1000
Biotinylated Anti-Rabbit IgG	Vector Labs	IHC 1:400
Biotinylated Anti-Rat IgG	Vector Labs	IHC 1:400
Anti-Mouse Immunoglobulins/HRP	DAKO	WB 1:3000
Anti-Rabbit Immunoglobulins/HRP	DAKO	WB 1:3000
Alexa Fluor 488 Anti-Rabbit or Mouse	Invitrogen	IF 1:400
Alexa Fluor 647 Anti-Rabbit or Mouse	Invitrogen	IF 1:400

Table 2.3 Secondary antibodies

2.1.5 Mouse genotyping

ASPP2$^{\Delta 3/\Delta 3}$ mice were genotyped with primers SDL1s, 5'-TGGACAGGCTGAGCTGTTAG-3'; SDL2s, 5'-ACACTTTCACCAACCCTAGGTC-3'. iASPP$^{\Delta 8/\Delta 8}$ mice were genotyped with primers: FRANT9, 5'-GGGTAGGAAAAAGGGCTGAG-3'; FLP2, 5'-CCGAATTGGAGAAGTGAAGC-3'. LSL-Kras^{G12D} mice were genotyped with the following primers: Y116, 5'-TCCGAATTCAGTGACTACAGATG-3'; Y117, 5'-CTAGCCACCATGGCTTGAGT-

3'; Y118, 5'-ATGTCTTTCCCCAGCACAGT-3'. EYFP mice were genotyped with primers: YFPcommon, 5'-AAAGTCGCTCTGAGTTGTTAT-3' and YFPwildtype, 5'-GGAGCGGGAGAAATGGATATG-3'; or YFPcommon and YFPmutant, 5'-AAGACCGCGAAGAGTTTGTC-3'. LSL-Trp53^{R172H} mice were genotyped with primers: p53common, 5'-CTTGGAGACATAGCCACACTG-3' and p53wt, 5'-TTACACATCCAGCCTCTGTGG-3'; or p53commmon and p53mut, 5'-AGCTAGCCACCATGGCTTGAGTAAGTCTGCA-3'.

2.2 Methods

2.2.1 DNA techniques

Agarose gel electrophoresis

Agarose was dissolved in 1X TAE buffer at required percentage, boiled until completely dissolved, and ethidium bromide was added to a final concentration of 20 μg/ml. Gels were set then run in a Bio-Rad Sub-Cell GT cell running tanks at 100V and visualised in an UV-imaging system. DNA samples were mixed with 5X loading buffer to a final concentration of 1X and run alongside the appropriate-sized DNA ladder.

DNA extraction from ear biopsies

Mice ear biopsies were obtained with an ear-punch and the resulting tissue was used for genotyping. Biopsy tissue was digested overnight at 55°C in 100 μl of extraction buffer GNT and 7.8 mg/ml of proteinase K (Qiagen). The digested tissue was boiled for 10 minutes at 97°C and 1 μl was used for PCR analysis.

Polymerase Chain Reaction

PCR reactions were performed with 0.5 μl of sample DNA, 0.05 μl appropriate primers, 5 μl GoTaq Green Master Mix 2X, and nuclease-free water made up to 10 μl reaction volumes.

2.2.2 Protein techniques

Sample Preparation

Tissue was dissected and snap frozen in 1.5 ml Eppendorf tubes in liquid nitrogen immediately and stored at -80°C. Tissue was homogenized in a pestle and mortar on dry ice and lysed in urea lysis buffer for 10 minutes. Lysates were sonicated 10 seconds x3 then rotated for 1 hour at 4°C. Lysates were centrifuged 12,000 g at 4°C for 30 minutes with resulting lysate transferred to a fresh Eppendorf and the cell debris discarded.

Protein Concentration Determination

Protein concentrations of tissue lysates were determined using the Bio-Rad protein assay reagent system. 1 μl tissue lysate was mixed with 200 μl of 1x Bio-Rad assay reagent and measured at 595 nm in a spectrophotometer (Anthos Labtech instrument). All samples were measured in duplicate and the absorbance was compared against a standard curve at the same time as known concentrations of bovine serum albumin (BSA).

SDS-polyacrylamide gel electrophoresis (PAGE)

All plates were cleaned with water and detergent, dried and assembled in the casting trays (Bio-Rad). The acrylamide content of the gels varied between 6% and 12% depending on size of protein of interest. The acrylamide gels were overlaid with 70% isopropanol solution and left to polymerize. After polyermizerization, the isopropanol was removed and a 4% stacking gel set with the appropriate number and size wells. Known concentrations of protein were mixed with appropriate volumes of 5x SDS-PAGE loading buffer and boiled for 5 minutes. Tissue lysates and a protein molecular weight marker were loaded onto SDS-polyacrylamide gels in a 1x SDS-PAGE running buffer and the proteins electrophoresed at a constant voltage of 100-200 V. Equal amounts of protein were loaded into each lane as determined by the Bio-Rad assay system.

Immunoblotting

After sample separation by SDS-PAGE, the gel was placed in a wet transfer unit containing 1x SDS-PAGE transfer buffer for electrophoretic transfer of proteins onto a nitrocellulose membrane (Schleicher and Schill, Germany) for 2 hours at a constant voltage in a Hoefer Transphor Electrophoresis unit. Membranes were washed in water and incubated in 5% fat-free milk (Marvel, UK) or 1% BSA in 1x TBS-Tween at room temperature for 60 minutes. Primary antibody was added at recommended concentrations, diluted 5% milk or 1% BSA in 1x TBS-Tween for 3 hours room temperature (RT) or overnight at 4°C. After three 15 minute washes in 1x TBS-Tween, the secondary HRP-labelled antibody was added for 1 hour at RT (1:2000 to 1:5000). Membranes were washed for a further 3 times for 15 minutes in 1x TBS-Tween. The membranes were visualised using enhanced

chemiluminescent detection, ECL (Amersham Biosciences) using X-ray films (Fujifilm).

2.2.3 Histological and immunohistological techniques

Haematoxylin and Eosin (H&E) staining

Slides were deparaffinised and hydrated in distilled water. Haemotoxylin staining for 3 minutes, washed, then dipped ten times in 1% acid alcohol. Thirty seconds in Scott's water, further washing, then eosin for 5 minutes. Dehydration with alcohol, cleared in histoclear and mounted.

Alcian Blue Staining

Slides were deparaffinised and hydrated in distilled water. Alcian blue solution staining for 30 minutes then washed. Slides counterstained with nuclear fast red solution for 5 minutes. Dehydration with alcohol, cleared in histoclear and mounted.

Tissue Immunohistochemistry (IHC)

Slides were deparaffinised and hydrated in distilled water. Antigen retrieval was performed using either boiling citric acid pH6 or EDTA pH9 and left to cool. Endogenous peroxidases were inactivated using 3% H_2O_2 in methanol. Sections were washed and blocked with either 5% normal goat serum or sheep serum in TBS-T for 1 hour. Sections were incubated with primary antibody diluted in either 5% goat serum or CST SignalStain® Antibody Diluent #8112 overnight. Following 3 x 5 minute washing in PBS, slides were incubated for 30 minutes in primary

matched secondary biotinylated antibody. Sections were washed 3 x 5 minutes then incubated with Vectastain Elite® ABC-HRP Kit for 15 minutes, and washed for 3 x 5 minutes. Sections were incubated with a DAB Peroxidase (HRP) Substrate Kit (varying time). Slides were washed in water and counterstained with haemotoxylin for 15 seconds. Slides were dehydrated through alcohols concentrations and cleared with histoclear for 10 minutes prior to mounting.

Tissue Immunofluorescence (IF)

Slides were deparaffinised and hydrated in distilled water. Antigen retrieval was performed using boiling citric acid pH6 and left to cool. Sections were blocked with either 5% normal goat serum or sheep serum in TBS-T for 1 hour. Sections were incubated with primary antibody diluted in either 5% goat serum. Following 3 x 5 minute washing in PBS, slides were incubated for 60 minutes in primary matched fluorescent probe linked secondary antibody with DAPI. Sections were washed 3 x 5 minutes then mounted with Fluoroshield Mounting Medium. The slides were kept at 4°C, protected from light and imaged using a Zeiss 710 confocal microscope.

2.2.4 Mouse work

Acute Pancreatitis

Caerulein was prepared in PBS and administered via peritoneal injection in alternate flanks hourly, between 8 to 12 times in one day or up to 16 times in two days during day time.

Chronic Pancreatitis

Chronic pancreatitis, unless stated specifically, was performed in 6- to 8-week old mice by six weekly intraperitoneal injections of 250 μg/kg caerulein. Where feasible, equal number of male and females were used and d

Mouse Maintenance

All mice were housed at the FGF Unit at the Wellcome Trust Centre for Human Genetics, University of Oxford. Humane mouse endpoints were used according to Home Office Animal Scientific Procedures Act 1986 licence of Professor Lu.

Histological Classification

Histological classification of mouse pathology were based on a consensus report from a 2004 meeting international workshop to establish a nomenclature for transgenic mouse models of pancreatic neoplasia (Hruban et al. 2006).

Acinar-to-Ductal Metaplasia *ex vivo* assay

Adapted from Pancreatic Acinar Cell 3-Dimensional Culture (http://www.bio-protocol.org/e930) and Shi et al. (Shi et al. 2013). 24-well plates were coated with 250 μl/well rat tail collagen gel mixture. Rat tail collagen (3 mg/mL) (Life Technologies, A1048301) was mixed with 10x RPMI 1640 medium in a 9:1 ration. 4.2% $NaHCO_3$ was added (~80 - 100 μl) to give a light pink/yellowish mixture colour.

Mice were sacrificed by cervical dislocation and the pancreas was immediately dissected and washed in HBSS. The pancreas with then transferred to 5 mL cold HBSS and minced with dissection scissors. 100 μl Collagenase P (10 mg/mL) was

added to the tissue suspension and mixture was placed a 37°C for approximately 20 minutes with regular agitation until suspension is cloudy. 5 mL cold HBSS and 5% FBS was added to the suspension and then pelleted by centrifugation at 4°C. The pellet was resuspended and centrifuged again for 3 times and filtered with a 100 μm mesh. The cell suspension is gently placed on top of a 50 mL Falcon tube in 20 mL HBSS and 30% FBS and centrifuged to pellet individual acini clusters. The pellet was resuspended in 3D-culture medium (RPMI 1640, 1% FBS, 1% Penicillin/Streptomycin, 0.1 mg/mL soybean trypsin inhibitor (Sigma) and 1 μg/mL dexamethasone, and then mixed with equal amount of rat tail collagen mix. The acini mixture is then plated at 0.5 mL/well and left to solidify for 1 hour at 37°C. 5% CO_2, before 1 mL 3D-culture medium is added with or without 50 ng/mL human recombinant TGFα (Peprotech). Media was changed at 24 hours and every 48 hours thereafter. Conversion from acini to ductal cysts was counted on day 5.

2.2.5 Human tissue samples

Human pancreatic tissue samples were obtained from Professor Robert Goldin, Imperial College, London.

2.2.6 Data analysis

Computer Images

All autoradiographs were scanned using an Epson 1660 photo scanner. Histological or immunohistological slides were scanned using Hamamatsu slide scanner. Slide scanned images were viewed and captured using NDP.view2 software.

Statistical Analysis

Kaplan-Meier survival analyses was performed using GraphPad Prism 7 with log rank tests. Assessment of differences in counts between different mice was performed in GraphPad Prism 7 using non-parametric Mann-Whitney U tests.

Chapter 3: ASPP2 regulates the pancreatic response to inflammation

ASPP2 is a binding partner of key regulators of apoptosis, inflammation and regeneration. Understanding the function of ASPP2 in tissue homeostasis and response to physiological stress may provide key insights into mechanisms that control the balance between cell death, survival, and regeneration. However, the inherent complexity of overlapping cell signalling mechanisms and regulation requires a systematic approach to delineate a functional role for ASPP2. Murine injection of cholecystokinin analogue caerulein results in pancreatitis that is reproducible and self-limiting. Consequently, injections of caerulein can be used to study murine responses to pancreatitis stress, and in combination with knockout mouse models, to determine the roles of key inflammation regulators in tissue response to pancreatitis. In this chapter, ASPP2-deficient mouse models are studied to assess whether ASPP2 functions as a regulator of the pancreatic response to pancreatitis.

3.1 ASPP2 deficiency does not alter pancreatic acinar development

ASPP2 expression is regulated by the transcription factor E2F1 (Chen et al. 2005; Fogal et al. 2005; Pandolfi et al. 2015). E2F1 knockout ($E2F1^{-/-}$) mice have developmental defects with reduced pancreatic size due to impaired growth and hyperglycaemia due to reduced insulin secretion (Fajas et al. 2004). Therefore, I need to exclude the possibility of a developmental or homeostatic phenotype resulting from ASPP2 deficiency is required prior to investigating the effects of altered ASPP2 levels in response to pancreatitis.

Hydrocephalus and retinal dysplasia due to central nervous system abnormalities are the predominant phenotype in ASPP2 exon 3 deleted mice ($ASPP2^{\Delta3/\Delta3}$) (Sottocornola et al. 2010). $ASPP2^{\Delta3/\Delta3}$ is *in utero* lethal in the C57BL/6 (B6) background, whilst in the mixed 129/Sv x B6 background, the pups have a severe phenotype resulting in failure to wean in 100% cases (Sottocornola et al. 2010). BALB/c $ASPP2^{\Delta3/\Delta3}$ mice have a less severe phenotype with survival up to 1 year and most mice surviving beyond weaning. I initially assessed the adult $ASPP2^{\Delta3/\Delta3}$ pancreases. BALB/c $ASPP2^{\Delta3/\Delta3}$ mice do not have a histological pancreatic phenotype compared to litter mate controls ($ASPP2^{+/+}$), with normal acinar and islet structure, and absence of spontaneous metaplasia at 12-months (n=3) (Figure 3.1A).

A pancreatic-specific ASPP2 deficiency is achieved by crossing the B6 LSL-$ASPP2^{\Delta3/+}$ mouse with a B6 Pdx1 Cre-recombinase expressing mouse (Pdx1-Cre). *PDX1* encodes pancreatic duodenal homeobox 1, also known as insulin promoter factor 1, which is required for the developmental specification of the pancreas.

Expressed from E9.5, loss of Pdx1 results in agenesis of the pancreas. Pdx1 is also expressed in the foregut and liver. Pdx1-Cre is the most utilized method of achieving pancreatic specificity and results in cellular specific knockout in the acini, islets and ductal cells of the pancreas. ASPP2$^{\Delta 3/\Delta 3}$;Pdx1-Cre mice, subsequently termed ASPP2$^{-/-}$ in this thesis, survived over 1 year with no overt acinar nor islet phenotype (n=3) (Figure 3.1B). These results demonstrate that ASPP2 deficiency does not result in a developmental or homeostatic phenotype in the pancreas. Absence of spontaneous metaplasia, fibrosis, inflammation and tissue loss suggests that the ASPP2 does not function to maintain tissue homeostasis in the absence of pancreatic stress. Therefore demonstrates that ASPP2$^{-/-}$ mice are suitable models to study the effects of pancreatic specific inflammation and oncogene induced tumorigenesis.

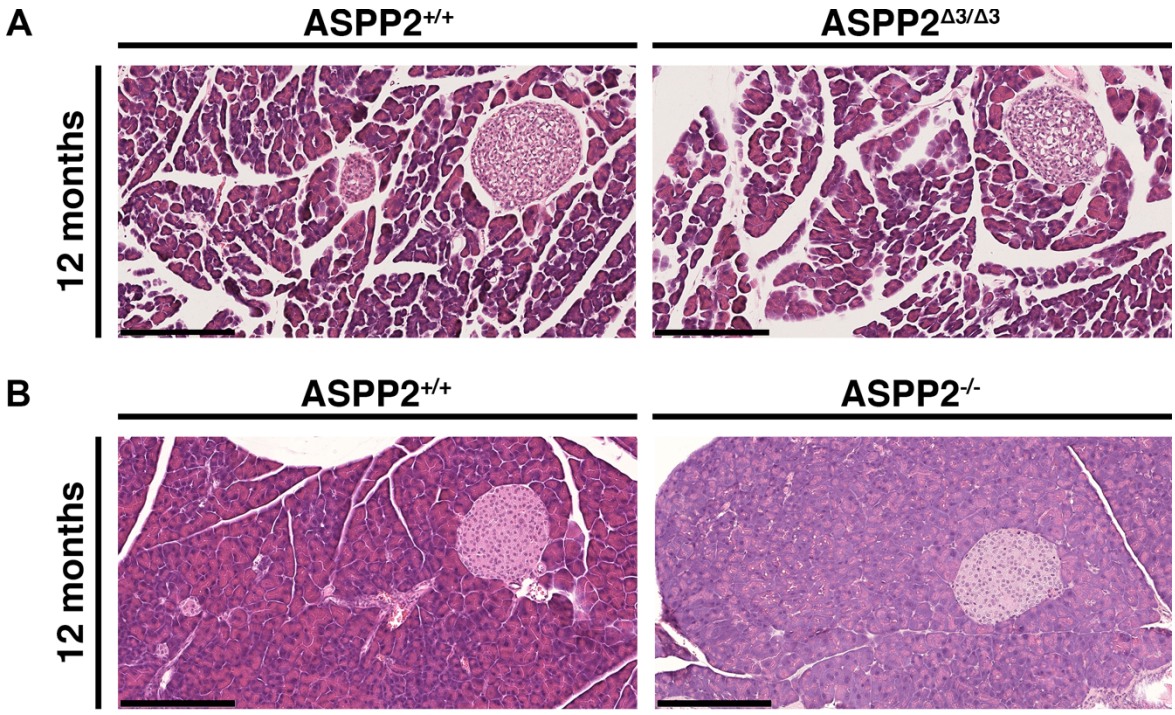

Figure 3.1 ASPP2-deficiency does not result in a developmental and homeostatic phenotype in the pancreas

A Representative pancreas sections of 12-month old constitutive transgenic mice on a BALB/c background. ASPP2 wild-type (left) and ASPP2-deficient (right). Scale bar 100μm.

B Representative pancreas sections of 12-month old pancreatic-specific (Pdx1-Cre) mice on B6 background. ASPP2 WT (left) and ASPP2-deficient (right). Scale bar 100μm.

3.2 Acute pancreatitis in E2F1-deficient mice results in metaplasia and persistent inflammation

E2F1 transactivates the promoters of iASPP and ASPP2 to provide transcriptional level control of ASPP expression (Fogal et al. 2005). E2F1$^{-/-}$ mice exhibit exocrine gland dysplasia, defective thymocyte apoptosis and increased tumour incidence consistent with a tumour suppressive role *in vivo* (Field et al. 1996; Yamasaki et al. 1996). An E2F1/E2F2 compound (DKO) mutant mice develops nonautoimmune insulin-deficient diabetes and exocrine dysfunction (Iglesias et al. 2004). Increased rates of DNA replication and apoptosis are present in the DKO pancreas with reduction of number of acini and islets with age, with progressive replacement by ductal ADM-like structure, and fibrosis reminiscent of chronic pancreatitis. Additional p53$^{-/-}$ deficiency protected E2F1/E2F2 DKO mice from organ involution and diabetes (Iglesias-Ara et al. 2015). I hypothesized that the E2F1-null mouse (with wild-type E2F2) would be more susceptible to inflammatory stress than E2F1 wild-type mice. To test this six-week old E2F1$^{+/+}$ and E2F1$^{-/-}$ litter mates were intraperitoneally injected hourly with caerulein or PBS 12 times in one day, then left to recover, with predetermined culling time points of 24-hour and 14-day recovery (Figure 3.2A). Histological evaluation of the tissue was performed with H&E staining. The PBS injected mice had no clear phenotypic change in acinar structure (Figure 3.2B). Prominent acinar cell nuclei were noted in the E2F1$^{-/-}$ tissue but no ADM or fibrosis was evident. Caerulein injected E2F1$^{+/+}$ and E2F1$^{-/-}$ mice at 24-hours displayed acinar degranulation, immune cell infiltration and oedematous tissue (Figure 3.2C). No overt difference histologically was noted. At day 14, E2F1$^{+/+}$ mice were virtually indistinguishable from PBS injected mice with complete resolution of inflammation, whereas E2F1$^{-/-}$ mice had evidence of

extensive damage with loss of acinar mass, fat necrosis, oedema and duct-like structures in place of acini (ADM) (Figure 3.2D). Between days 1 and 14 following the inflammatory stimulus, the E2F1-deficient mice experienced either an increased extent of inflammation, a failure of tissue repair or abnormal tissue recovery. As E2F1 is a transcriptional regulator of iASPP and ASPP2, I speculated that iASPP or ASPP2 may share a proinflammatory or regeneration defect if the role of ASPPs is to protect from inflammatory pancreatic stresses mediated by p53 or NF-κB.

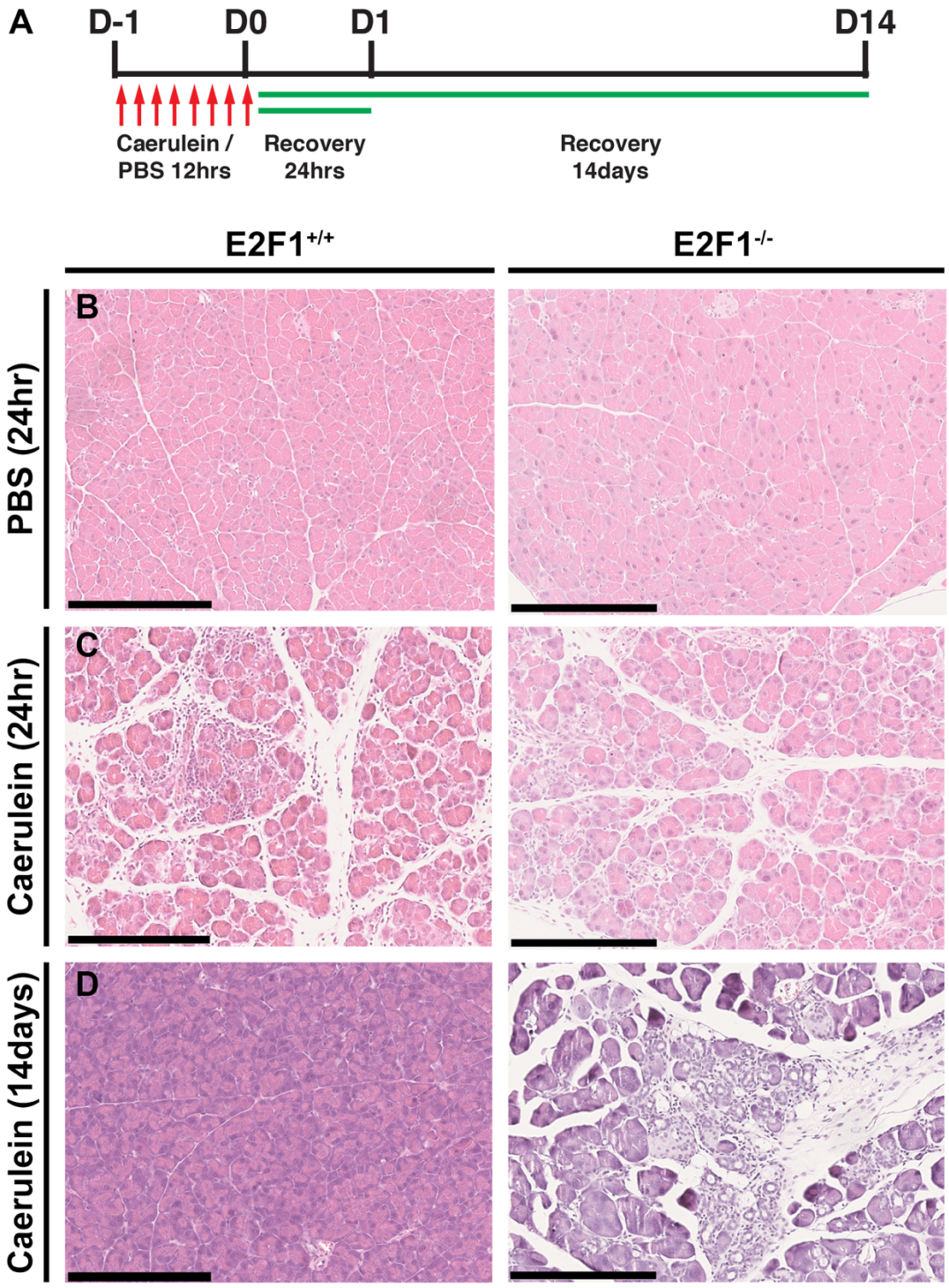

Figure 3.2 Acute pancreatitis in E2F1-deficient mice results in ADM and persisting inflammation

A Injection schedule. Hourly caerulein/PBS injections on Day -1 (total 12 injections). Mice culled following either 24-hours or 14-days recovery following final injection.

B Representative H&E sections of $E2F1^{+/+}$ and $E2F1^{-/-}$ mice following 24-hour recovery after 12 injections of PBS. Scale bar 250 μm.

C Representative H&E sections of $E2F1^{+/+}$ and $E2F1^{-/-}$ mice following 24-hour recovery after 12 injections of caerulein. Scale bar 250 μm.

D Representative H&E sections of $E2F1^{+/+}$ and $E2F1^{-/-}$ mice following 14-days recovery after 12 injections of caerulein. Scale bar 250 μm.

3.3 Acute pancreatitis upregulates ASPP2, iASPP and p53, and activates the MAPK/ERK pathway

Acute pancreatitis (AP) involves a multi-step process of amylase degranulation, activation of an acute stress response, immune cell infiltration, oedema, cell death or survival, and subsequent recovery and regeneration. AP is associated with transient activation of the MAPK/ERK pathway and the induction of a NF-κB mediated stress response (Daniluk et al. 2012). A p53 response, defined as upregulation of p53 in the context of downregulation of MDM2, classically occurs in response to DNA-damage and genotoxic stress (Levine & Oren 2009). Less is known about the role of the p53 family in acute inflammation. It is also unknown whether ASPP2 and iASPP levels are altered in response to acute pancreatitis. Furthermore, timing of protein expression would indicate a specific role such as acutely regulating apoptosis/survival or regenerative processes following AP resolution. To investigate these processes, I performed a time course of AP induced by hourly caerulein intraperitoneal injections over 2-days in wild-type BALB/c mice (Figure 3.3A).

In control mice injected with PBS and sacrificed following one hour recovery (Day 0) ASPP2 and iASPP protein levels are low (Figure 3.3B). MDM2 is present with p53 barely detectable, and low levels of phosphorylated ERK1/2 (pERK1/2) representing low activation of the MAPK/ERK pathway. One hour (Day 0) following the cessation of caerulein injections ASPP2 levels are upregulated. A classic p53 response is detectable with downregulation of MDM2 and upregulation of p53. Also, ERK1/2 is phosphorylated with an appreciable decrease in ERK1/2 levels. Following one day of recovery, ASPP2 and iASPP levels remain raised with a

persisting p53 response and pERK1/2 levels have returned to baseline. After two days of recovery, ASPP2 and iASPP levels peak, with MDM2 protein level returning to baseline with persisting p53 levels. MAPK activation is at baseline with barely detectable levels of pERK1/2 (Figure 3.3B).

These data suggest ASPP2 and iASPP are upregulated in acute pancreatitis, alongside the transient upregulation of p53 and activation of MAPK pathway. The upregulation of ASPP2 in response to inflammation, without a developmental phenotype, supports further investigation into ASPP2 as a regulator of pancreatic inflammatory stress. It is unknown how ASPP2 is upregulated in response to AP, although the focus remains on the functional role of ASPP2.

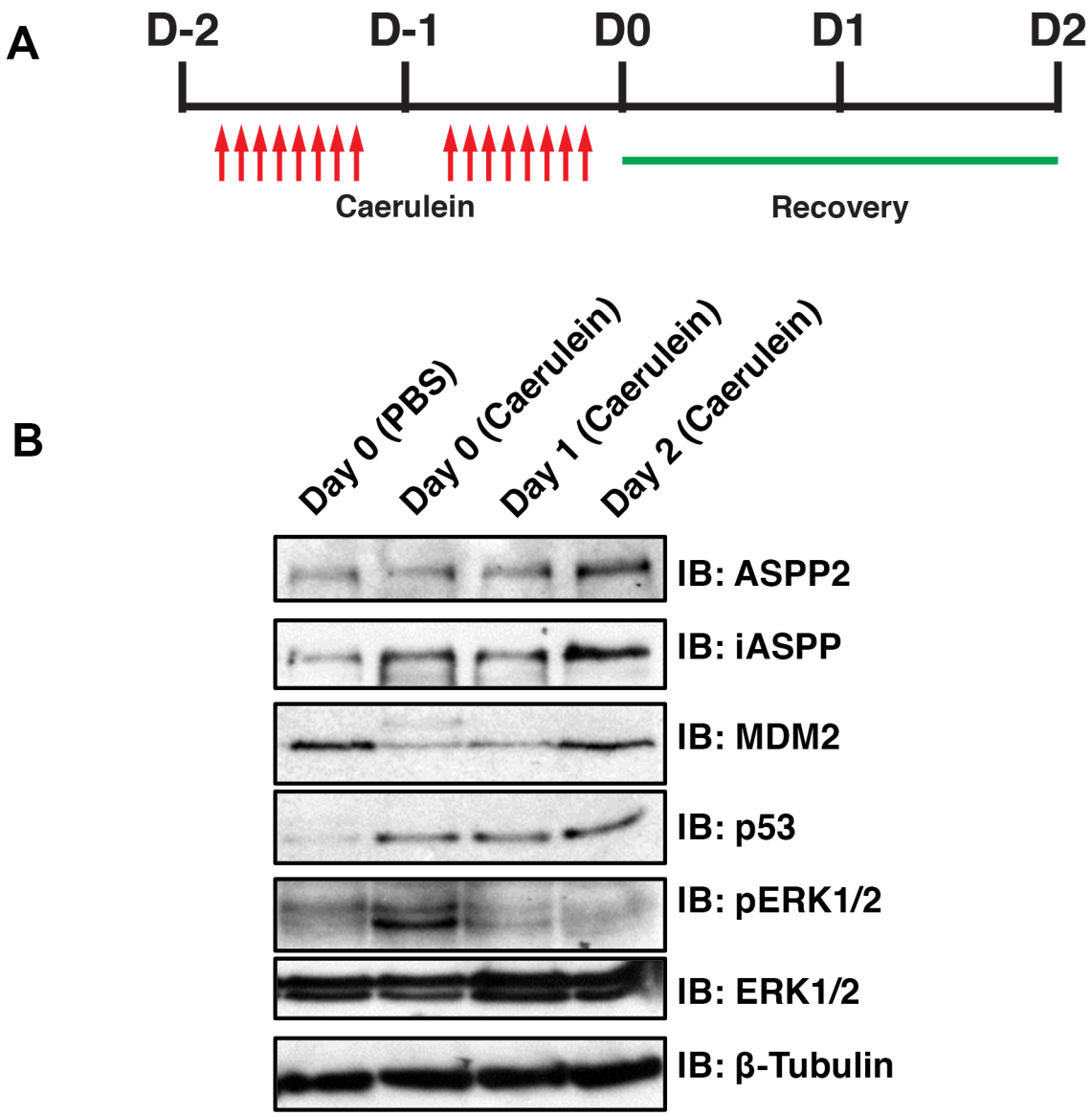

Figure 3.3 Acute pancreatitis induces MAPK/ERK activation and upregulation of ASPP2, iASPP and p53

A Injection schedule. Hourly caerulein/PBS injections on Day -2 (total 16 injections, 8 per day). Mice culled following either 1-hour (Day 0), 24-hours (Day 1) or 48-hours (Day 2) following the final injection.

B Western blot for ASPP2 (S32), iASPP (LX49.3), MDM2 (C18), p53 (CM5), and MAPK pathway activation (phosphorylated ERK1/2 and total ERK1/2). Loading control is β-tubulin.

3.4 Acute pancreatitis in pancreas-specific ASPP2-deficient mice results in increased inflammation without altered recovery

E2F1 regulates the pancreatic response to acute inflammation (Figure 3.2D) while RelA knockout mice demonstrate the functional importance of the NF-κB pathway in the inflammatory response (Algül et al. 2007). ASPP2, as a transcriptional target of E2F1, a regulator of NF-κB and p53, and which is upregulated in AP, is a good candidate for a mediator of the pancreatic response to inflammation. To examine this, I utilized the pancreatic-specific ASPP2-deficient ($ASPP2^{-/-}$) mice described in chapter 3.1. $ASPP2^{-/-}$ and littermate controls ($ASPP2^{+/+}$) at 6-weeks were injected 16 times over 2 days (Figure 3.4A). Following 14-days recovery, no clear histological differences between $ASPP2^{+/+}$ and $ASPP2^{-/-}$ mice were apparent (Figure 3.4B). Analysis at the 48-hour recovery time point was also performed (Figure 3.4C). Western blot demonstrates higher levels of p53 at 48-hours in the $ASPP2^{-/-}$ mouse suggesting a more severe stress than in $ASPP2^{+/+}$ (Figure 3.4D). Histological evidence supported the presence of increased stress in $ASPP2^{-/-}$ mice as there is greater oedema, acinar degranulation, and immune cell infiltration (Figure 3.4E).

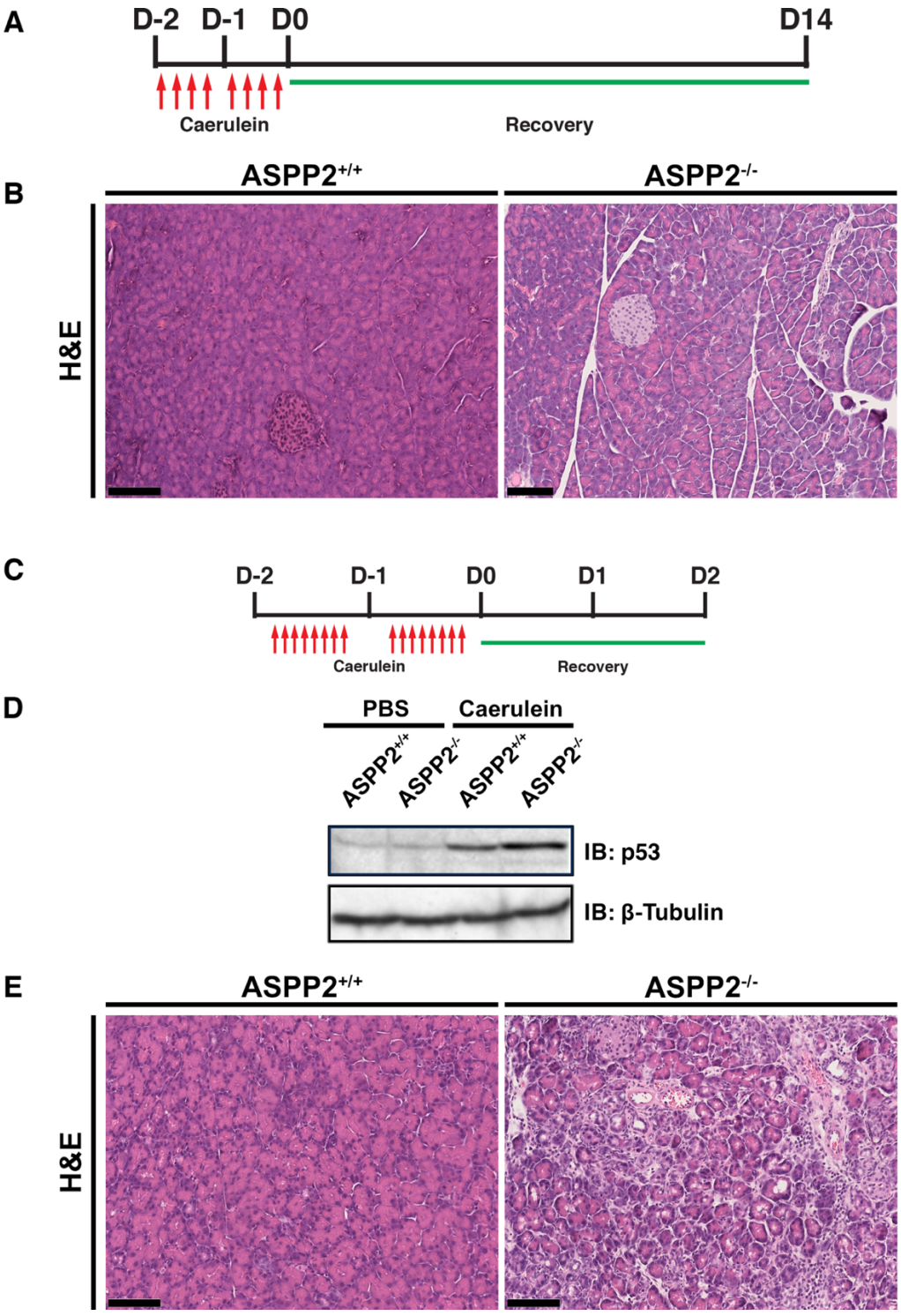

Figure 3.4 Acute pancreatitis in ASPP2-deficient mice demonstrates increased acute inflammatory response

A Injection schedule. Caerulein/PBS injections on Day -2 (total 16 injections, 8 per day). Mice culled after 14-days recovery following final injection.

B Representative H&E sections of ASPP2$^{+/+}$ and ASPP2$^{-/-}$ mice following 14-days recovery. Scale bar 100 μm.

C Injection schedule. Caerulein/PBS injections on Day -2 (total 16 injections, 8 per day). Mice culled after 48-hours recovery following final injection.

D Western blot of p53 (CM5) after 48-hours recovery from PBS or caerulein.

E Representative H&E sections of ASPP2$^{+/+}$ and ASPP2$^{-/-}$ mice following 48-hours recovery. Scale bar 100 μm.

3.5 ASPP2 expression is associated with human pancreatic inflammation and PDAC

In a murine model of acute pancreatitis, ASPP2 is upregulated as a result of physiological pancreatitis stress but the functional consequence is unclear (Chapter 3.4). Histologically, following acute pancreatitis, ASPP2$^{-/-}$ acini do not readily undergo metaplasia similar to E2F1$^{-/-}$ mice, nor have an overt regeneration defect. A single study has reported on ASPP2 expression in human PDAC. ASPP2 levels were found to be lower in tumour then para-cancerous cells at the mRNA and protein level (Song et al. 2015). Also, high ASPP2 tumour expression on IHC associated with longer overall survival and disease-free survival.

To understand whether ASPP2 levels are altered in human disease, I analysed a batch of human pancreatic tissue from various pathological conditions. Human chronic pancreatitis had areas of fibrotic stroma, normal acinar, inflamed acini, ADM and PanINs (Figure 3.5A). Stroma and fibrotic tissue were largely negative for ASPP2 staining, inflamed areas had moderate staining intensity, whilst PanINs were generally negative (Figure 3.5B). In cases of PDAC, ASPP2 staining was more prominent in well-differentiated areas of disease, and often correlated with nuclear p53 staining in a wild-type pattern (Figure 3.5C, D & E). In poorly differentiated PDAC, ASPP2 staining intensity was generally weak, whilst in adjacent slides, iASPP staining was strong (Figure 3.5F, G & H). In the small cohort of human pancreatic disease samples analysed, it is clear that ASPP2 expression is variable but associates with inflamed tissue and well-differentiated PDAC. Limited availability of samples prevented an analysis of ASPP2 expression and correlation with clinical outcomes or tumour histotype.

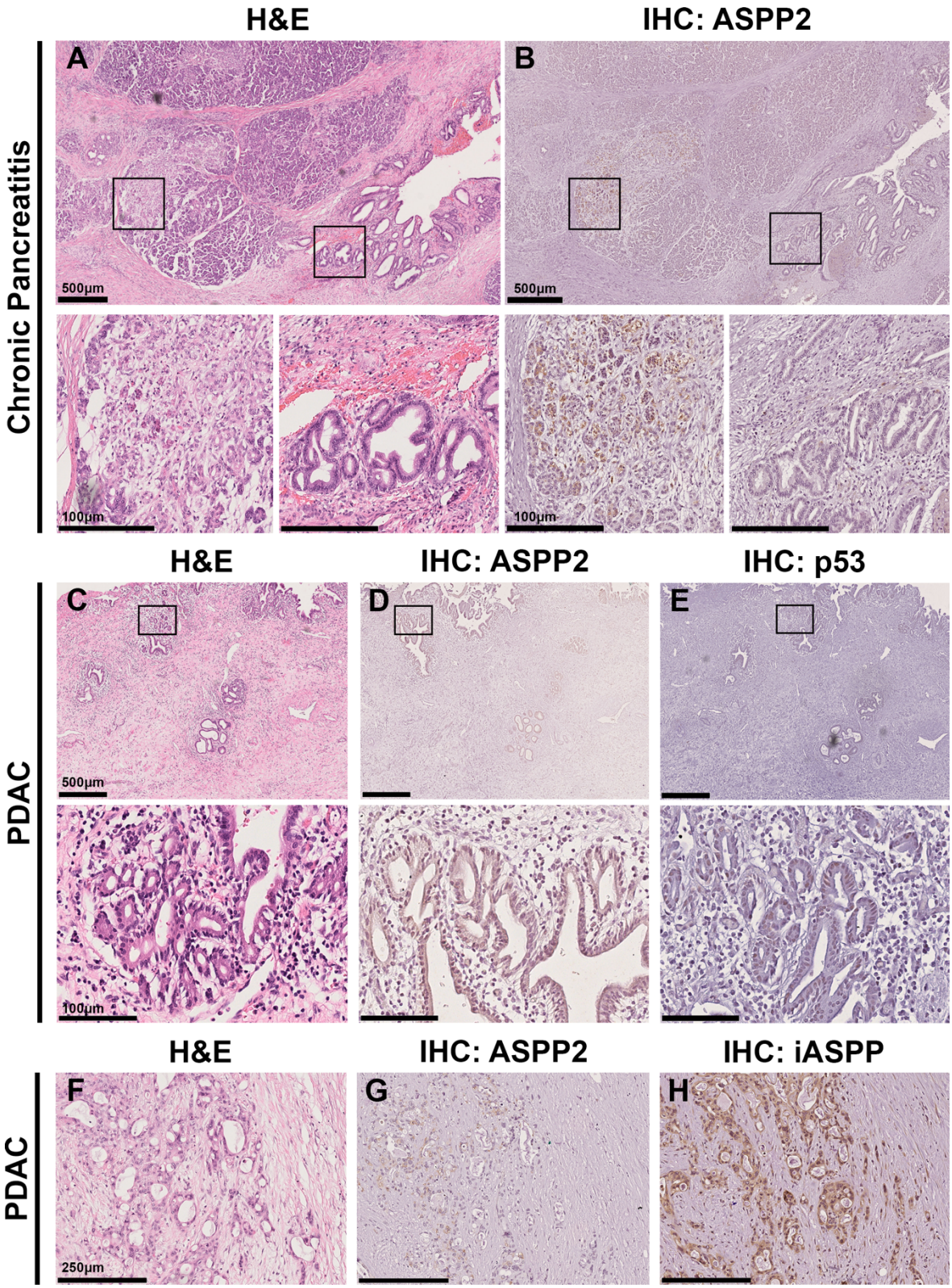

Figure 3.5 ASPP2 is upregulated in chronic pancreatitis and well-differentiated PDAC

A H&E staining of a case of chronic pancreatitis with areas of normal acini, stroma, ADM and PanINs present (Upper image). Area of inflamed pancreas with ADM (Lower left image).Area of PanIN (Lower right). Upper scale bar 500 μm. Lower scale bars 100 μm.

B ASPP2 (DX54.10) IHC staining in a case of chronic pancreatitis, adjacent to 3.5A (Upper image). Area of inflamed pancreas with ADM (Lower left image).Area of PanIN (Lower right). Upper scale bar 500 μm. Lower scale bars 100 μm.

C H&E staining of a case of pancreatic cancer with dense stroma and areas of well differentiated PDAC (Upper image, scale bar 500 μm). Area of well-differentiated PDAC (Lower image, scale bar 100 μm).

D ASPP2 (DX54.10) IHC staining of a case of pancreatic cancer (Upper image, scale bar 500 μm). Area of well-differentiated PDAC (Lower image, scale bar 100 μm).

E p53 (DO-1) IHC staining of a case of pancreatic cancer (Upper image, scale bar 500 μm). Area of well-differentiated PDAC (Lower image, scale bar 100 μm).

F H&E staining of a case of poorly differentiated PDAC (Scale bar 250μm).

G ASPP2 (DX54.10) IHC staining of a case of poorly differentiated PDAC (Scale bar 250 μm).

H iASPP (LX49.3) IHC staining of a case of poorly differentiated PDAC (Scale bar 250 μm).

3.6 Summary

In this chapter I sought to investigate whether ASPP2 is a regulator of pancreatic inflammation based on the *a priori* understanding that ASPP2 is a regulator of cellular response to NF-κB and p53, key regulators of inflammation, regeneration and apoptosis. Absence of phenotype in both constitutive ASPP2-deficient and pancreatic-specific ASPP2-deficient mouse pancreas suggests ASPP2 does not regulate pancreatic development nor homeostasis, unlike E2F1. Interestingly, double knockout E2F1$^{-/-}$ and E2F2$^{-/-}$ mice (DKO) develop frank diabetes, features of chronic pancreatitis and shortened lifespan (Iglesias et al. 2004). Combining DKO with p53$^{-/-}$ protected the pancreas from diabetes and chronic pancreatitis features but reduced survival due to accelerated thymic lymphomas (Iglesias-Ara et al. 2015). Exposing the E2F1$^{-/-}$ mouse to caerulein has never been reported in the literature. Following AP and recovery, the E2F1$^{-/-}$ pancreases have prominent acinar-to-ductal metaplasia (ADM), and persisting inflammation that is otherwise absent in wild-type mice following inflammation. I confirmed that neither overt ADM occurs nor features of abnormal inflammation following recovery occur in ASPP2$^{-/-}$ mice. There is possibly a greater acute stress response and higher p53 levels is present in ASPP2$^{-/-}$ mice apparent in the acute onset phase of pancreatitis.

Acute pancreatitis, induced by supramaximal intraperitoneal injections caerulein, is a robust method to screen for physiological regulators of inflammation, in particular p53 stabilization and MAPK/ERK pathway activation. I demonstrate through the murine model of AP and in IHC analysis of human pathological pancreatic tissue, that ASPP2 may regulate the tissue response to inflammation. However, the lack of a clear phenotype in absence of ASPP2 deficiency alone when exposed to mild-

to-moderate pancreatitis suggests ASPP2 may be more relevant in chronic inflammation or in the presence of oncogenic stress.

Chapter 4: ASPP2 suppresses metastasis and the squamous PDAC subtype

ASPP2 is classified as a tumour suppressor in a plethora of cancers via p53-dependent and -independent mechanisms. High expression of ASPP2 in human cancers consistently associates with better prognosis relative to low ASPP2 expressing tumours. Mutation of the ASPP2 gene, *TP53BP2*, is rare in human cancer. PDAC is the only cancer in which *TP53BP2* mutation was identified as recurrently mutated (Bailey et al. 2016). However, the functional consequence of *TP53BP2* mutation in PDAC is unknown. Together with TP53 loss or mutation and p16 mutation, ASPP2 mutation is classified as a disruption of G1/S checkpoint machinery. To determine whether ASPP2 functions as a regulator of cell cycle in PDAC or influences the progression of PDAC, I created two ASPP2-deficient models of PDAC to study tumour development and metastasis. Furthermore, by studying the role of inflammation in the oncogenic Kras mouse model of PDAC I will be able to determine whether ASPP2 regulates PDAC at the level of oncogenic Kras alone, or in combination with inflammation-driven tumorigenesis.

4.1 KC and KC;ASPP2$^{-/-}$ mice both recapitulate the histological spectrum of ADM to PDAC progression

To investigate the role of ASPP2 in oncogenic Kras-mediated progression from acini to PDAC, I used a mouse model that recapitulates the histological characteristics of the human pancreatic acinar-to-ductal metaplasia (ADM), PanIN progression and subsequent PDAC with metastasis (Hingorani et al. 2003). LSL-Kras$^{G12D/+}$; Pdx1-Cre (KC) mice carry a single copy of the oncogenic Kras codon 12 point mutation point found in over 90% of PDAC cases (Bailey et al. 2016). These mice were crossed with the ASPP2$^{\Delta 3/\Delta 3}$; Pdx1-Cre mice to form a colony termed KC;ASPP2$^{-/-}$ (LSL-Kras$^{G12D/+}$; Pdx1-Cre; ASPP2$^{\Delta 3/\Delta 3}$). The KC and KC;ASPP2$^{-/-}$ colonies were maintained in parallel, and both mice were born at expected Mendelian ratios (data not shown).

I found that ADM, histologically defined as metaplastic conversion from eosinophilic acini to small-round ductal morphology with an empty lumen, is evident in all both KC and KC;ASPP2$^{-/-}$ mice post-weaning (Figure 4.1A and B). Low-grade PanINs (PanIN-1A and PanIN-1B) are also universally present post-weaning as flat epithelial lesions with basally located nuclei, commonly with abundant mucin present. High-grade PanIN-3 are usually not present until age 6-months or later and exhibit cribriforming with budding, loss of nuclear polarity and occasional mitoses (Figure 4.1C and D). Macroscopic or histological evidence of PDAC is evident in both KC and KC;ASPP2$^{-/-}$ mice at variable latency but typically only over 6 months of age.

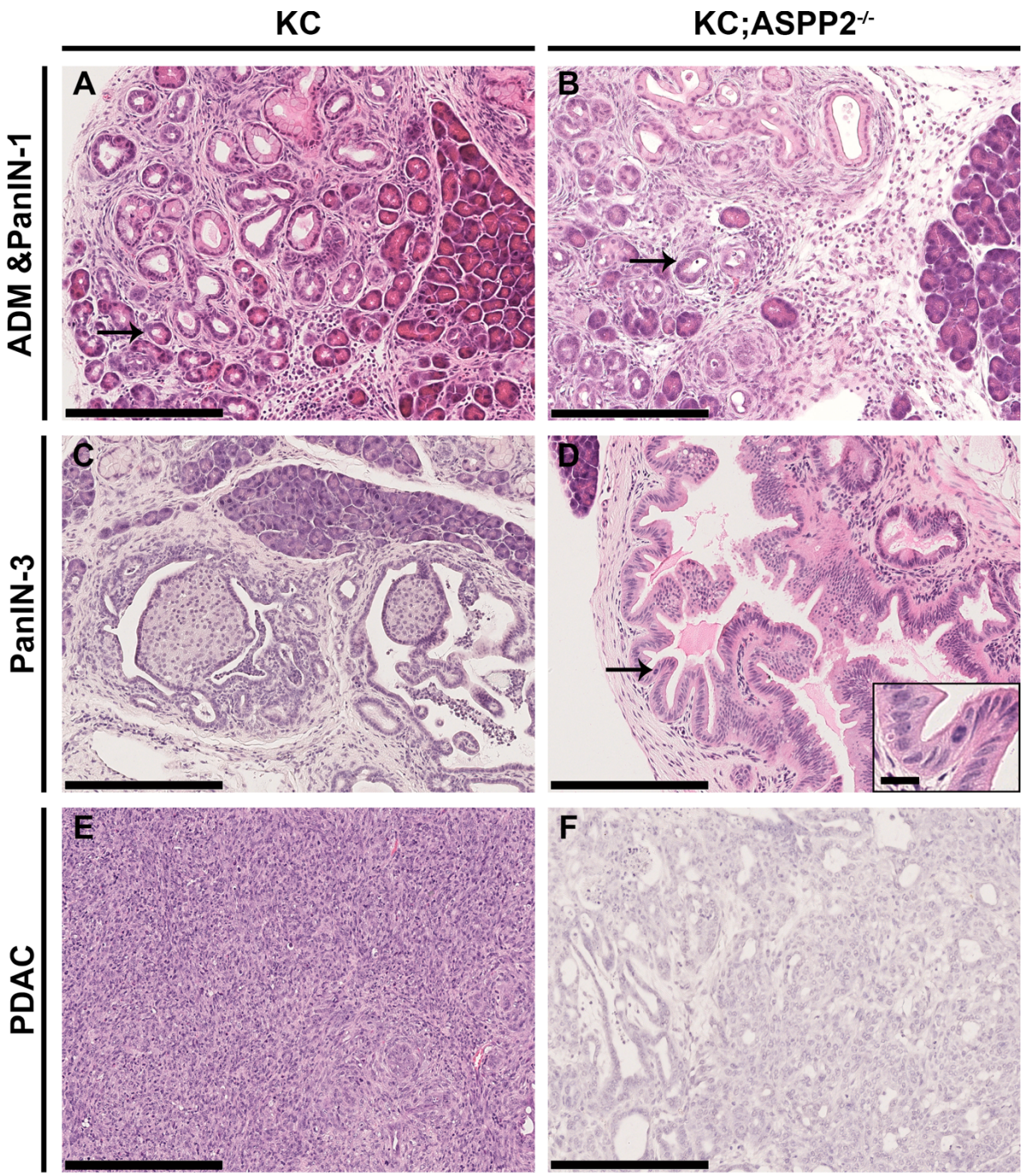

Figure 4.1 KC and KC;ASPP2$^{-/-}$ mice both recapitulate the histological spectrum from normal acini to PDAC

A 6-month old KC mouse with normal acini, ADM, and mPanIN-1A and mPanIN-1B with ADM in-progress (black arrow). Scale bar 250 μm.

B 6-month old KC;ASPP2$^{-/-}$ mouse with normal acini, ADM, and mPanIN-1A and mPanIN-1B with ADM in-progress (black arrow). Scale bar 250 μm.

C 9-month old KC mouse with high-grade mPanIN-3. Scale bar 250 μm.

D 5-month old KC;ASPP2$^{-/-}$ mouse with high-grade mPanIN-3 with mitosis identifiable (black arrow and inset, scale bar 20 μm). Scale bar 250 μm.

E 12-month old KC mouse with mPDAC. Scale bar 250 μm.

F 11-month old KC;ASPP2$^{-/-}$ mouse with mPDAC. Scale bar 250 μm.

4.2 Reduced overall survival of KC;ASPP2$^{-/-}$ mice is not due to accelerated primary PDAC

To investigate whether ASPP2 deficiency on the KC background (KC;ASPP2$^{-/-}$) impacts the time course of PDAC progression, I performed a Kaplan-Meier analyses on the KC and KC;ASPP2$^{-/-}$ cohorts. Overall survival was measured from birth to death, occurring when the mouse met predetermined humane endpoints as defined by the Home Office Licence under which the mice were kept or were found dead. A total of 40 KC and 29 KC;ASPP2$^{-/-}$ mice contributed to the overall survival Kaplan-Meier plot (Figure 4.2A). KC mice had a median survival of 267 days while KC;ASPP2$^{-/-}$ mice had a median survival of 183 days (P = 0.0078, log rank) (Figure 4.2B). However, the mice were culled for various reasons, including keratoacanthomas of anal and oral mucosae, non-healing or persistently bleeding lesions, assessed as being unwell or hunched, subcutaneous masses causing distress, significant weight loss, and rapid breathing. The majority of mice were electively culled as there were assessed as reaching a humane endpoint (88% and 97% for KC and KC;ASPP2$^{-/-}$ respectively).

To determine whether the reduced overall survival was attributable to accelerated onset of primary pancreatic cancer, I performed histological evaluation of all available tissues. 32 KC (32/40) and 28 KC;ASPP2$^{-/-}$ (28/29) pancreases were analysed for primary mPDAC (Figure 4.2C). Surprisingly, 41% of KC mice had evidence of primary mPDAC at death while only 14% of KC;ASPP2$^{-/-}$ had primary mPDAC. Median primary tumour-free survival for KC or KC;ASPP2$^{-/-}$ with primary mPDAC at death was 358 and 327 days respectively. Median survival was not

significantly different ($p>0.05$) suggesting ASPP2 does not accelerate primary PDAC progression (Figure 4.2D).

A

Mouse Genotype	*N* =	Median Survival (Days)	Mouse Fate			Cause of Death		
			Elective Cull	Found Dead	Alive	Unwell	Lesion/Mass	Unknown
KC	40	267	35 (88%)	4 (10%)	1 (2%)	23 (59%)	12 (31%)	4 (10%)
KC;ASPP2$^{-/-}$	29	183	28 (97%)	1 (3%)	0 (0%)	11 (38%)	14 (48%)	4 (14%)

B

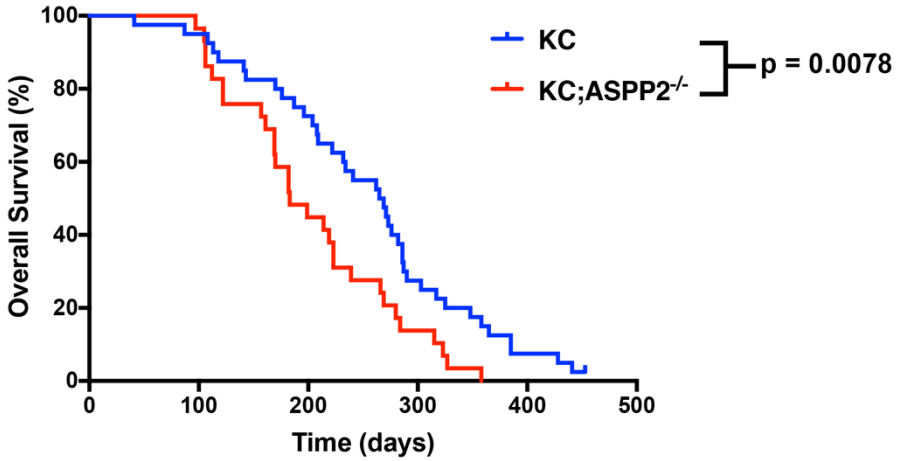

C

Mouse Genotype	Primary Tumor Incidence		Median Survival (Days)
	Primary Tumour	No Primary Tumour	
KC	13 (41%)	19 (59%)	358
KC;ASPP2$^{-/-}$	4 (14%)	24 (86%)	327
	Fisher's exact test P = 0.0428		

D

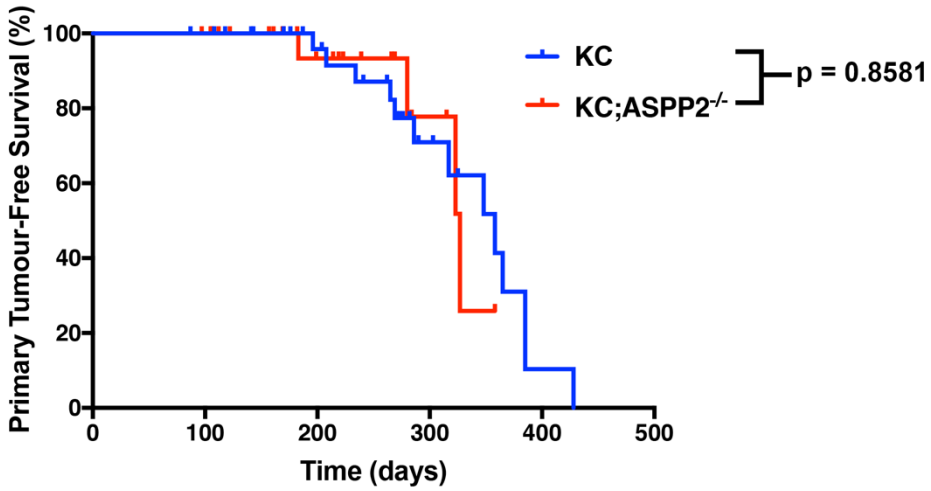

Figure 4.2 Reduced survival of KC;ASPP2$^{-/-}$ mice without accelerated primary PDAC

A Table for KC and KC;ASPP2$^{-/-}$ cohorts: number of mice analysed, median survival, mouse fate and cause of death for mice contributing the overall survival analysis.

B Kaplan-Meier analysis of overall survival comparing KC (n=40) and KC;ASPP2$^{-/-}$ (n=29) cohorts ($p < 0.01$).

C Comparison of primary tumour incidence and median survival between KC and KC;ASPP2$^{-/-}$ cohorts.

D Kaplan-Meier analysis of primary tumour-free survival comparing KC and KC;ASPP2$^{-/-}$ cohorts ($p > 0.05$).

4.3 ASPP2 may suppress early metastasis in an oncogenic Kras model of PDAC

KC;ASPP2$^{-/-}$ mice had a significantly reduced overall survival with a significantly reduced incidence of primary PDAC, but not an altered median survival. In human PDAC, 30% die with locally destructive cancer, while 70% die with widespread metastatic disease (Iacobuzio-Donahue et al. 2009). Both KC and KC;ASPP2$^{-/-}$ mice had macroscopic metastatic disease at necropsy that was subsequently confirmed histologically. To address whether ASPP2 loss altered metastasis, I classified mice as having metastasis or no metastasis on the basis of macroscopic or histological diagnosis of metastases at necropsy. KC mice had a 50% incidence of metastasis and KC;ASPP2$^{-/-}$ had a 39% incidence. Median metastatic-disease free survival was 317 days in KC mice and 315 days in KC;ASPP2$^{-/-}$ mice (Figure 4.3A). However, in KC;ASPP2$^{-/-}$ mice with metastatic disease, median survival was shorter at 182 days, whilst 296.5 days in KC mice. Shorter survival in KC;ASPP2$^{-/-}$ mice with metastatic disease may suggest a subtype of KC;ASPP2$^{-/-}$ mice with more aggressive early metastatic disease. Location of metastasis demonstrates a favouring of lung over liver in KC;ASPP2$^{-/-}$ whilst KC mice metastases occurred more frequently in the liver. Kaplan-Meier analysis showed a non-significant trend to difference between KC;ASPP2$^{-/-}$ and KC mice generated by earlier death in KC;ASPP2$^{-/-}$ mice (Figure 4.3B). Histologically I found no clear difference between KC and KC;ASPP2$^{-/-}$ metastases (Figure 4.3C). Single- and multiple-foci of lung and liver metastases were noted.

In summary, KC;ASPP2$^{-/-}$ is the first tumour-type specific mouse model to study ASPP2 function in the context of oncogene driven tumorigenesis. KC;ASPP2$^{-/-}$

mice may generate a subset of mice with accelerated early metastatic disease that reduces survival in a mouse model of PDAC tumorigenesis. The KC;ASPP2$^{-/-}$ versus KC comparison provides *in vivo* evidence for ASPP2 as tumour suppressor of metastatic PDAC. However, the high incidence of metastatic disease in KC;ASPP2$^{-/-}$ mice without overt primary PDAC should raise concerns as to whether leakiness of the Cre-model could potentiate primary lung or liver tumours rather than specific pancreatic metastases.

A

Mouse Genotype	Metastasis Status		Metastatic Median Survival	Metastasis Location		
	Metastasis	No Metastasis	(Days)	Lung	Liver	Other
KC	16 (50%)	16 (50%)	317	5/16	12/16	1/16
KC;ASPP2$^{-/-}$	11 (39%)	17 (61%)	315	6/11	3/11	2/11

B

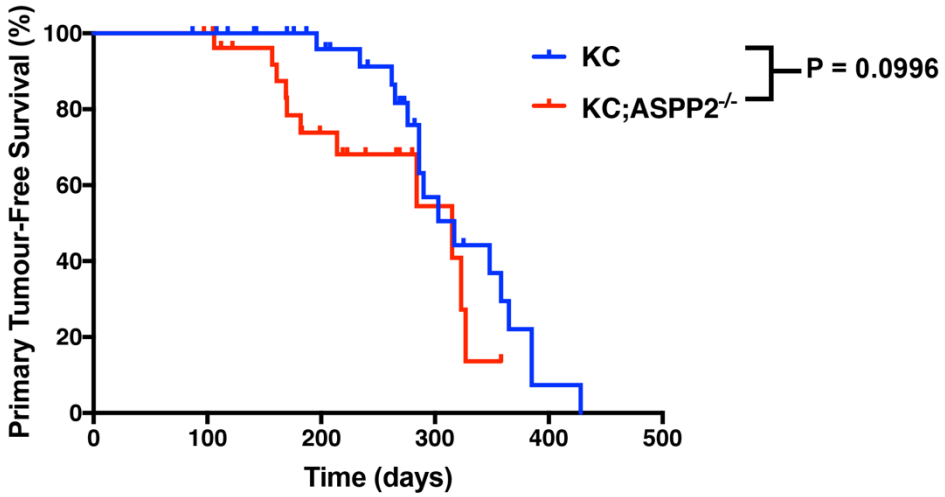

C

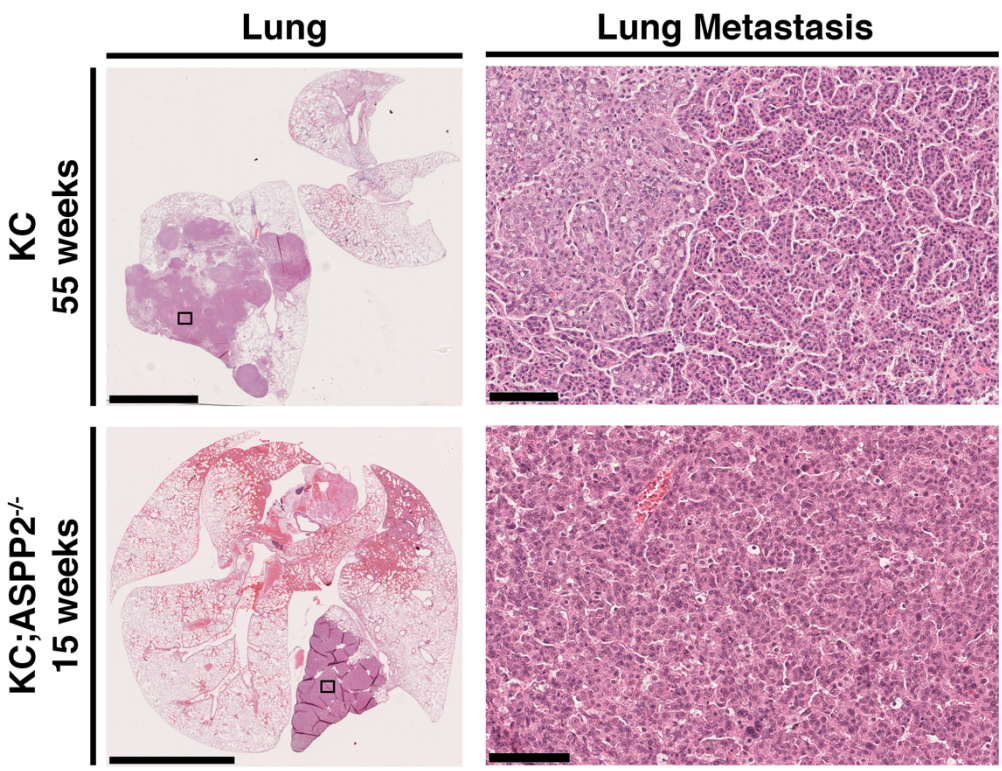

Figure 4.3 ASPP2 suppresses metastasis in KC mice

A Metastasis status of KC and KC;ASPP2$^{-/-}$ mice, median survival with metastatic disease and metastasis location.

B Kaplan-Meier plot for metastasis-free survival in the KC (n=16) and KC;ASPP2$^{-/-}$ (n=11) mouse cohorts. ($P > 0.05$).

C H&E scan whole lung of KC lung metastasis at 55-weeks (upper left, scale bar 5 mm) and representative image of tumour (upper right, scale bar 100 μm). H&E scan whole lung of KC;ASPP2$^{-/-}$ 15-week old mouse with lung

metastasis (lower left, scale bar 5 mm) and representative image of tumour (lower right, scale bar 100 μm).

4.4 ASPP2-deficiency does not impact overall survival or primary tumour-free survival in the KPC mouse model of PDAC

The KC mouse, despite the limitation of embryonic activation of $Kras^{G12D}$ not observed in human PDAC development, is a good model to study tumorigenesis from ADM to low- then high-grade PanINs, and eventually PDAC with or without metastases. However, due to prolonged onset of PDAC and metastases, typically reported as over 1 year, the $Kras^{G12D/+}$; $p53^{R172H/+}$; Pdx1-Cre (KPC) PDAC mouse model is more commonly utilised to study cancer and metastasis. KPC has a median survival of 6 months, with a reported 100% incidence of PDAC at 6 months (Hingorani et al. 2005). To further investigate whether ASPP2 also suppresses metastasis in the KPC mouse model, I crossed the KC;$ASPP2^{-/-}$ mouse with PC mice ($p53^{R172H/+}$; Pdx1-Cre), to produce KPC;$ASPP2^{-/-}$ ($Kras^{G12D/+}$; $p53^{R172H/+}$; $ASPP2^{\Delta3/\Delta3}$; Pdx1-Cre). The resultant mice were born at expected Mendelian ratios (data not shown).

I found that overall survival was not different between KPC and KPC;$ASPP2^{-/-}$ cohorts, with a trend towards increased survival in the KPC;$ASPP2^{-/-}$ cohort relative to KPC (Figure 4.4A). Similar levels of elective culling and being found dead were observed, as were causes of death being due to mouse being unwell, or as a complication of lesion or mass. Kaplan-Meier analysis demonstrated no difference in survival between KPC and KPC;$ASPP2^{-/-}$ (Figure 4.4B). Incidence of macroscopic or histologically diagnosed primary PDAC showed no difference between KPC and KPC;$ASPP2^{-/-}$ (Figure 4.4C). The Kaplan-Meier analysis of

primary tumour-free survival found no difference between KPC and KPC;ASPP2$^{-/-}$ mice (Figure 4.4D).

A

Mouse Genotype	*N* =	Median Survival (Days)	Mouse Fate		Cause of Death		
			Elective Cull	Found Dead	Unwell	Lesion/Mass	Unknown
KPC	23	117	20 (87%)	3 (13%)	4 (35%)	17 (59%)	2 (6%)
KPC;ASPP2$^{-/-}$	27	128	23 (85%)	4 (15%)	8 (29%)	14 (52%)	5 (19%)

B

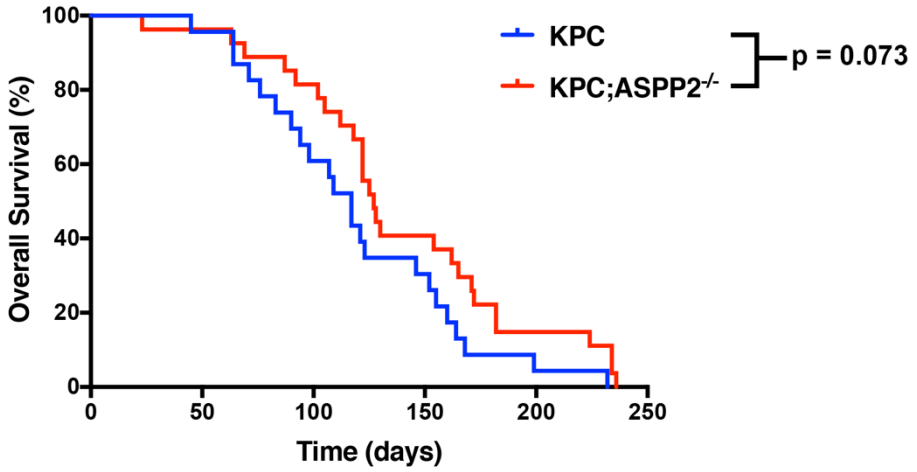

C

Mouse Genotype	Primary Tumor Incidence		Median Survival (Days)
	Primary Tumour	No Primary Tumour	
KPC	10 (56%)	8 (44%)	123
KPC;ASPP2$^{-/-}$	16 (64%)	9 (36%)	130
	Fisher's exact test P = 0.753		

D

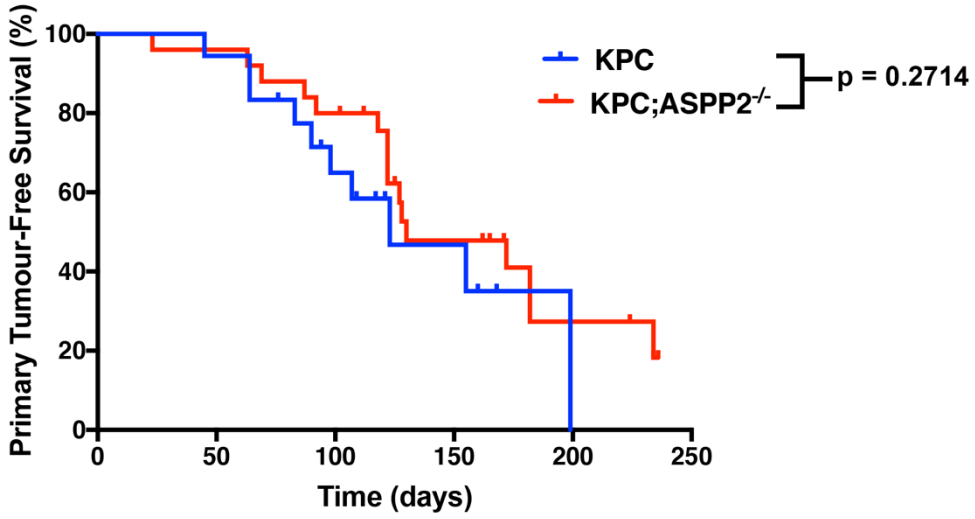

Figure 4.4 ASPP2-deficiency does not alter survival in KPC model of PDAC

A Table for KPC and KPC;ASPP2$^{-/-}$ cohorts: number of mice analysed, median survival, mouse fate and cause of death for mice contributing the overall survival analysis.

B Kaplan-Meier overall survival plot of KPC (n=23) and KPC;ASPP2$^{-/-}$ (n=27) ($P > 0.05$).

C Comparison of primary tumour incidence and median survival between KPC and KPC;ASPP2$^{-/-}$ cohorts.

D Kaplan-Meier analysis of primary tumour-free survival comparing KPC (n=18) and KPC;ASPP2$^{-/-}$ (n=25) cohorts ($P > 0.05$).

4.5 ASPP2 does not suppress metastasis in the KPC mouse model

Metastatic disease macroscopically evident at death is a key feature of the KPC mouse. The distribution of metastases in the KPC mouse is liver (80%), lung (50%), adrenals (20%), and peritoneum (20%) (Hingorani et al. 2005). Potential early metastasis in the KC;ASPP2$^{-/-}$ mouse, relative to the KC mouse, suggested a suppressive role for ASPP2 in the development of metastasis. Whilst the KPC;ASPP2$^{-/-}$ mouse had a trend to live longer than the KPC mouse, I performed a comparison of the metastatic outcomes between the KPC and KPC;ASPP2$^{-/-}$ cohorts.

Macroscopic or histologically diagnosed metastatic mPDAC occurred in 22% and 32% of KPC and KPC;ASPP2$^{-/-}$ cohorts respectively with no clear predilection to lung or liver (Figure 4.5A). Median metastatic-disease survival was 234 days in KPC;ASPP2$^{-/-}$ whilst KPC did not meet incidence to calculate median metastasis-free survival. Kaplan-Meier analysis of metastasis-free survival demonstrates no difference between KPC and KPC;ASPP2$^{-/-}$ cohorts (Figure 4.5B). In almost all cases, metastatic disease was accompanied by primary mPDAC either as a macroscopic tumour or following histological evaluation. I was unable to determine any clear trend in pattern, number or histology on H&E evaluation of metastatic disease in the KPC and KPC;ASPP2$^{-/-}$ cohorts (Figure 4.5C and D).

A lack of difference between KPC and KPC;ASPP2$^{-/-}$ mice in overall, metastatic-free and primary-free survival is incongruent with reduced overall survival in the KC;ASPP2$^{-/-}$ cohorts relative to the KC cohort. Therefore, ASPP2 role in pancreatic

cancer onset may be subtle and centred around the early events of PDAC tumorigenesis. Prior to pursuing a specific mechanism for ASPP2 suppressing metastatic PDAC, evaluating whether ASPP2 regulates ADM is required to understand whether ASPP2 influences the initiating steps in the PanIN to PDAC continuum.

A

Mouse Genotype	Metastasis Status		Metastatic Median Survival	Metastasis Location		
	Metastasis	No Metastasis	(Days)	Lung	Liver	Other
KPC	4 (22%)	14 (78%)	Undefined	3/4	1/4	0/4
KPC;ASPP2$^{-/-}$	8 (32%)	17 (68%)	234	6/8	4/8	0/8

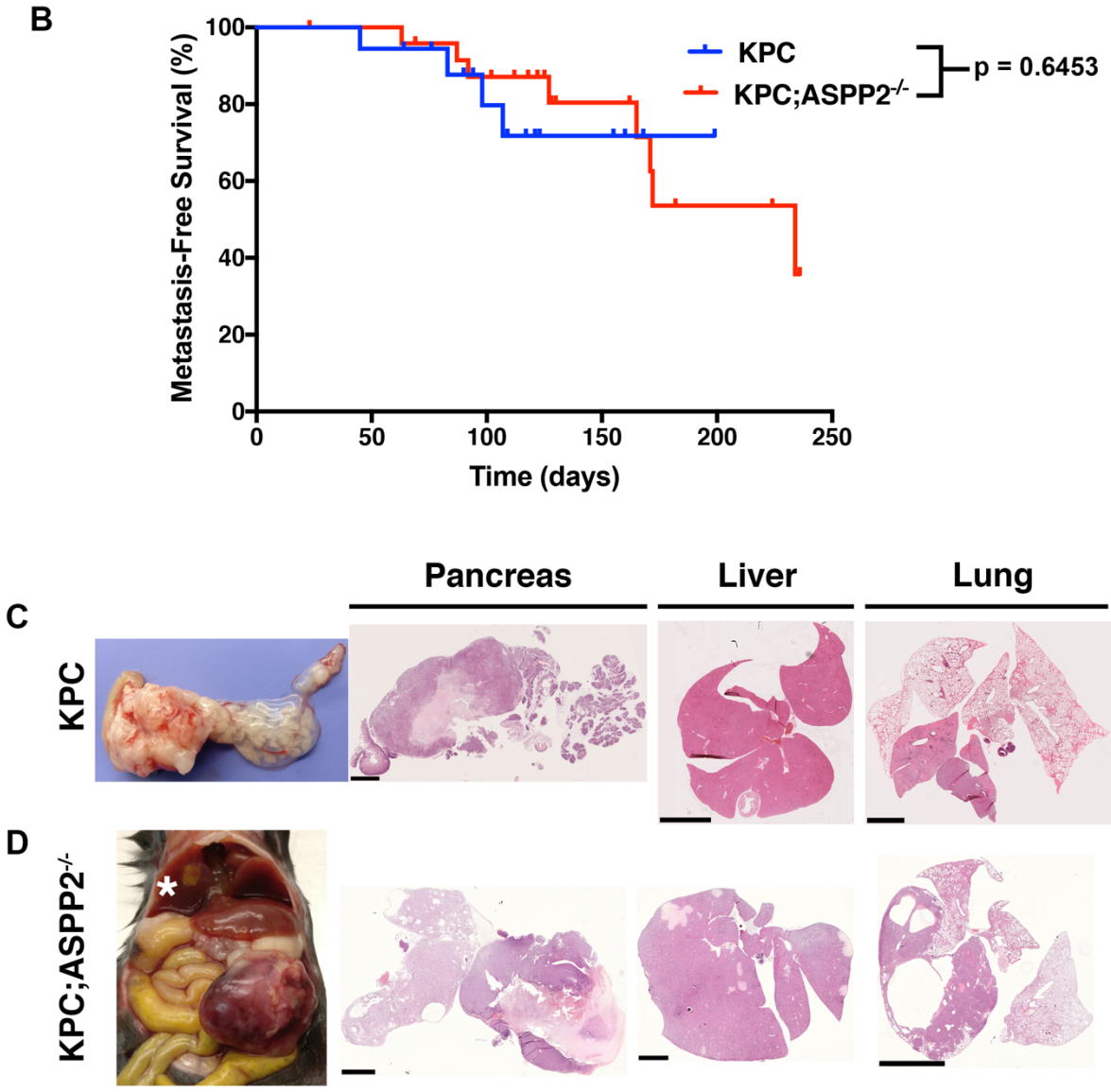

Figure 4.5 ASPP2 does not suppress metastasis in the KPC mouse model of PDAC

A Metastasis status of KPC and KPC;ASPP2$^{-/-}$ mouse cohorts, median metastasis-free survival and metastasis location.

B Kaplan Meier analysis of metastasis-free survival for the KPC (n=4) and KPC;ASPP2$^{-/-}$ (n=8) cohorts ($P > 0.05$).

C Example of 18-week old KPC macroscopic PDAC at necropsy with corresponding H&E pancreas section (scale bar 2.5 mm); a KPC liver metastasis at 6-weeks (scale bar 5 mm); and a 12-week old KPC lung metastasis (scale bar 2.5 mm).

D Example of 9-week old KPC;ASPP2$^{-/-}$ mouse at necropsy with large vascular mPDAC with liver metastasis (white star) with corresponding H&E

section (scale bar 2.5 mm); KPC;ASPP2$^{-/-}$ liver multiple metastases (scale bar 2.5 mm); KPC;ASPP2$^{-/-}$ lung metastasis (scale bar 5 mm).

4.6 ASPP2 does not regulate *ex vivo* acinar-to-ductal metaplasia

ADM is a critical initiating step in the onset of PDAC. Acini, the exocrine cells of the pancreas, are the prime candidates of the cell of origin of PDAC. ADM requires dedifferentiation that switches on developmental genes, such as Pdx1, that reprograms acini to a ductal phenotype. Pancreatic ducts are highly resistant to PanIN and PDAC formation, and can only form features of PanIN in models with severe genetic drivers or stimulated conditions. Consequently, to evaluate possible extrinsic factors and genetic drivers or blocks, I measured the efficiency of *ex vivo* ADM in these models. Activation of the MAPK pathway is central to ADM and 5-day cell culture in TGFα containing media results in a reported ADM efficiency of 60 to 80%. Similarly, expression of oncogenic Kras, results in an ADM efficiency of 70-90% (Shi et al. 2013). ADM marks the down-regulation of acini specific genes, such as amylase and MIST1, with upregulation of developmental and ductal genes, such as Pdx1 and Sox9. Morphologically these expression changes coincide with a switch from homogeneous ball of acinar cells, to a round halo-like structure with cells orientated in a loop with an empty centre (Figure 4.6A).

Wild-type acini (Pdx1-Cre+ only) and AC (ASPP2$^{-/-}$) acini essentially form no ducts after 5-days in culture. Following 5-day culture in TGFα containing media, efficiency in both genotypes is over 60% without a significant difference in genotypes (Figure 4.6B). In oncogenic Kras mice (KC and KC;ASPP2$^{-/-}$), the is no difference in ADM efficiency in the absence of TGFα at over 80%. TGFα

stimulated KC and KC;ASPP2$^{-/-}$ acini has little effect on ADM efficiency, with a statistically significant difference between KC and KC;ASPP2$^{-/-}$.

Ex vivo evaluation of ADM efficiency can demonstrate the effects of EGFR inhibition and Sox9 in the pathway dedifferentiation and redifferentiation with a ductal morphology. My data suggests ASPP2 does not regulate ADM, and therefore, ASPP2 functions in PDAC development at another point in the PDAC developmental pathway.

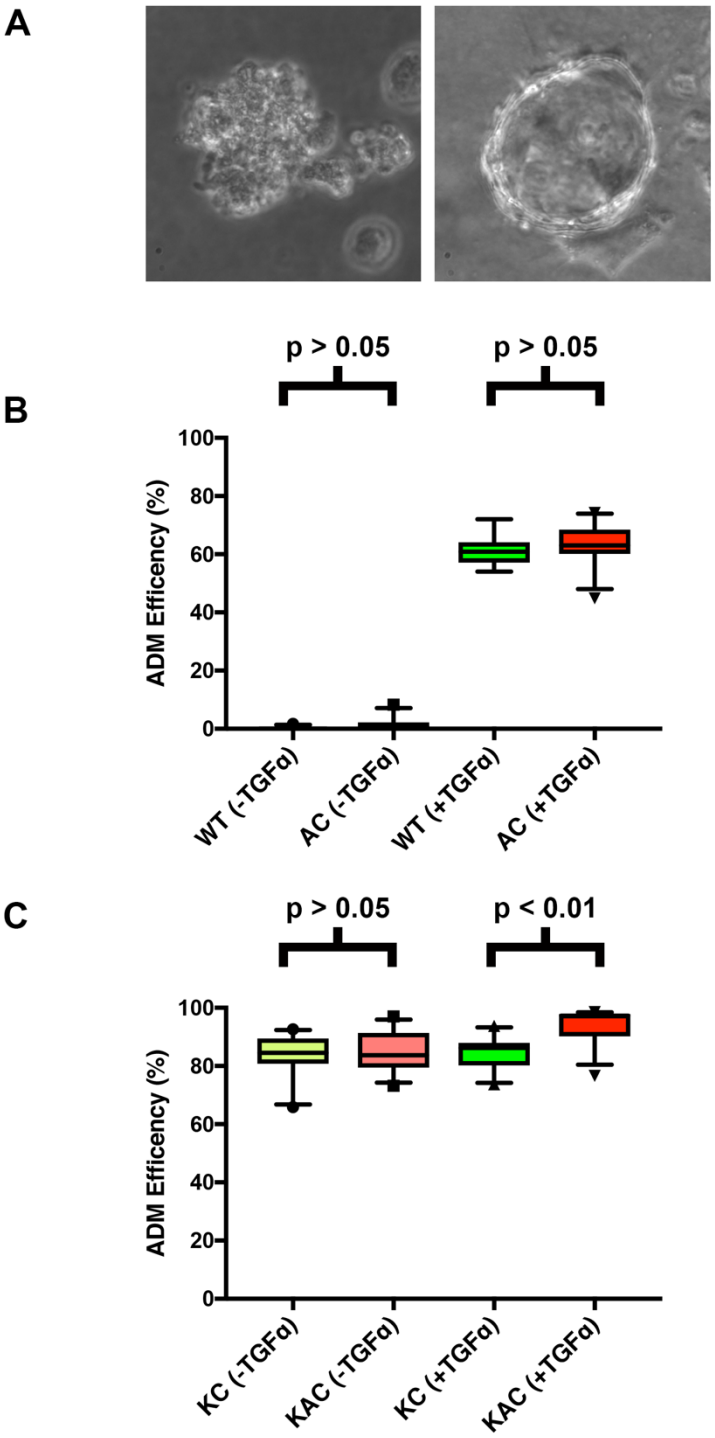

Figure 4.6 ASPP2 does not regulate *ex vivo* ADM

A Whole acinus at day 0 (left) and acinus following ADM at day 5 (right).

B ADM efficiency after 5 days in wild-type (WT) and ASPP2$^{-/-}$ (AC) mice with and without TGFα stimulation. Symbols represent data points outside the plotted 10-90% error bars.

C ADM efficiency after 5 days in KC and KC;ASPP2$^{-/-}$ (KAC) mice with and without TGFα stimulation. Symbols represent data points outside the plotted 10-90% error bars.

4.7 Inflammation potentiated oncogenic Kras driven ADM is not suppressed by ASPP2 *in vivo*

Activation of the MAPK pathway is critical for ADM, and sustained MAPK activation is required for progression through PanIN to PDAC. The almost ubiquitous presence of oncogenic Kras in PDAC supports these observations. However, oncogenic Kras is not enough for progression through ADM to PDAC. ADM requires further stimulation by factors that activate MAPK with the literature suggesting TGFα, EGF, IL-1α, TNFα, among others are capable of stimulating the pathway *in vivo*. Furthermore, the extrinsic factors may function in an autocrine, direct paracrine, or indirect paracrine mechanism requiring stromal components or immune cells to amplify MAPK activation. In the oncogenic Kras mouse model this is likely to occur via a feedforward mechanism. Inflammation is also central to ADM and PDAC onset. Adult (>P60) oncogenic Kras activation does not result in significant ADM and progression to PDAC (Guerra et al. 2007). Pancreatic inflammation, produced by intraperitoneal injection of cholecystokinin analogue caerulein, causes pancreatitis and additionally stimulates MAPK alongside oncogenic Kras to facilitate progression. However, the effect of caerulein inflammation will vary depending on dosing, injection intervals and recovery timing. Furthermore, depending on the role of ASPP2, injection schedule may alter the phenotype demonstrated.

To investigate the role of persistent pancreatic inflammatory stress, 8-week old mice KC and KC;ASPP2$^{-/-}$ were injected with low-dose caerulein (30 μg/Kg body weight) or PBS daily (5 days each week) for 4 weeks (Figure 4.7A). PBS-injected control mice, culled at 12-weeks, had few areas of ADM and PanINs, with the vast

majority of acini indistinguishable from wild-type acini (Figure 4.7B). Both KC and KC;ASPP2$^{-/-}$ caerulein injected mice had almost complete loss of morphologically normal acini, replaced with multiple examples of ADM, PanINs and a dense stroma. H&E staining did not reveal a phenotypic difference between KC and KC;ASPP2$^{-/-}$ (Figure 4.7C). Alcian blue staining was used to detect acidic mucins expressed in PanINs. No clear difference in abundance of alcian blue positive lesions was present (Figure 4.7C). Immunohistochemical staining of p53 demonstrated a greater abundance of p53-positive nuclei in KC;ASPP2$^{-/-}$ relative to KC (Figure 4.7D).

Daily caerulein injections for a month (20 injections in total) resulted in profound ADM and acquisition of PanIN morphology. To investigate recovery, parallel KC and KC;ASPP2$^{-/-}$ mice after 4-week of injections were allowed to recover to see if the onset of PDAC was accelerated. KC with 4-weeks caerulein, died spontaneously at 12 days following cessation of injection, whilst a KC;ASPP2$^{-/-}$ mouse survived until 15 weeks following cessation of injections (data not shown). My conclusion is that daily caerulein is too severe to evaluate the role of ASPP2$^{-/-}$ in potentiating inflammation driven PDAC.

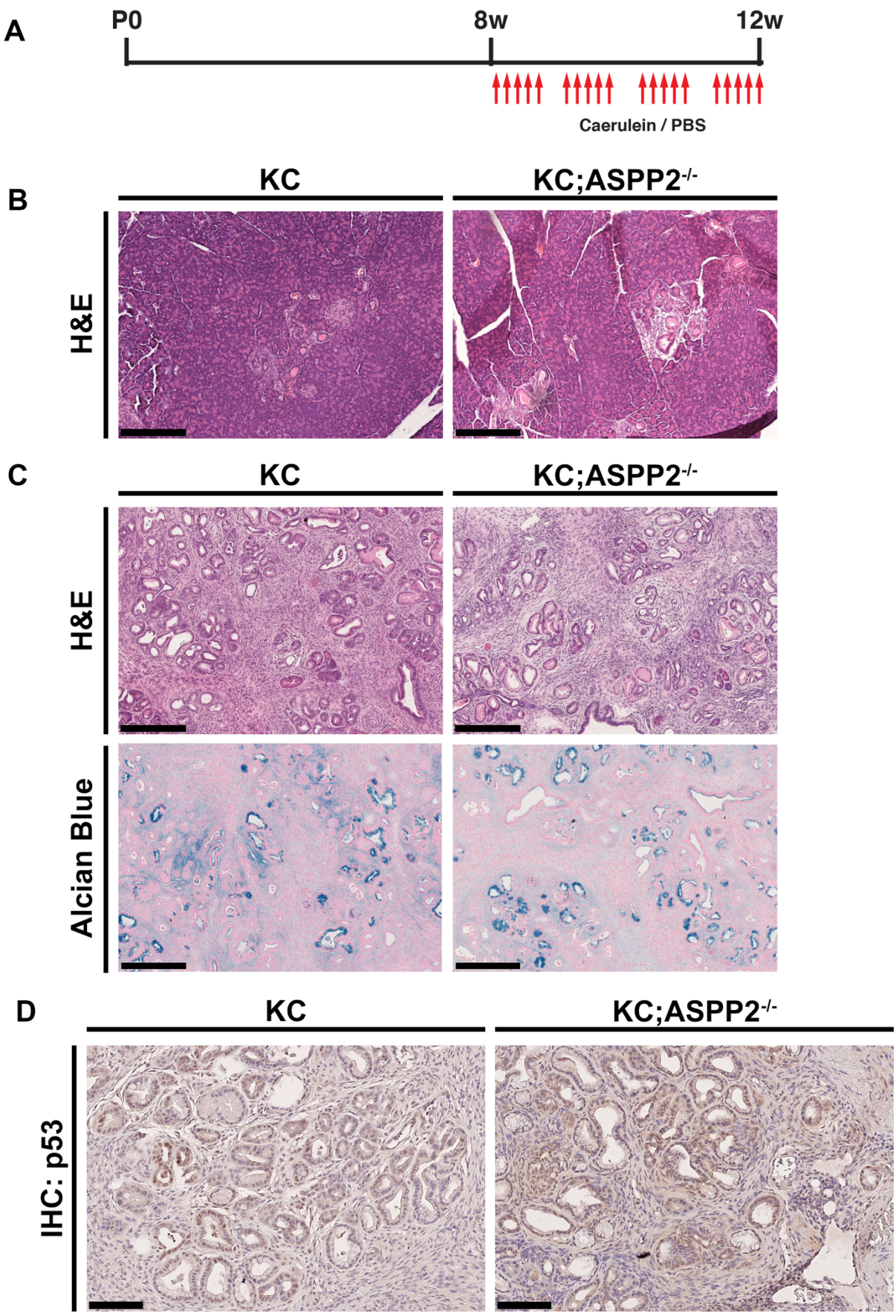

Figure 4.7 Inflammation potentiated oncogenic Kras driven ADM is not suppressed by ASPP2 *in vivo*

A Injection schedule. KC and KC;ASPP2$^{-/-}$ mice were injected with PBS or caerulein daily (5 days out of 7 per week) for 4 weeks.

B Representative H&E staining of KC and KC;ASPP2$^{-/-}$ mouse pancreas injected with daily PBS. Scale bar 250 μm.

C Representative H&E and alcian blue of KC and KC;ASPP2$^{-/-}$ mouse pancreas injected with daily caerulein. Scale bar 250 μm.

D p53 IHC for KC and KC;ASPP2$^{-/-}$ mice injected with daily caerulein. Scale bar 100 μm.

4.8 ASPP2-deficiency does not alter intermittent caerulein-induced PanIN progression

Daily IP caerulein injection results in a severe phenotype in which almost all acini undergo metaplasia and survival of KC mice is limited without induction of cancer. I speculated that an intermittent IP injection schedule administering weekly caerulein rather than daily could produce a less severe phenotype whilst enabling a longer term study of the effects of intermittent stress followed by recovery in the context of ASPP2-deficiency in the presence of oncogenic Kras. To determine this, a weekly dose of 250 μg/Kg was administered over 6 weeks, then the mice proceeded into a recovery phase of varying length (Figure 4.8A).

Following 48 hours recovery after 6-weekly injections between 6- and 12-weeks, there is no histological difference between the KC and KC;ASPP2$^{-/-}$ mice. The majority of acini undergo metaplasia with a ductal phenotype and abundant stroma (Figure 4.8B). After 6 weeks of recovery, during which no further caerulein has been administered, there is no clear progression to high-grade lesions, with increased normal acini present suggestive of regeneration. Finally, elective culling at 32-weeks, following 20-week recovery, demonstrated high-grade lesions, with stroma and abundant normal acini. In summary, ASPP2-deficiency in the context of intermittent inflammation and oncogenic Kras did not alter the progression of primary pancreatic tumorigenesis.

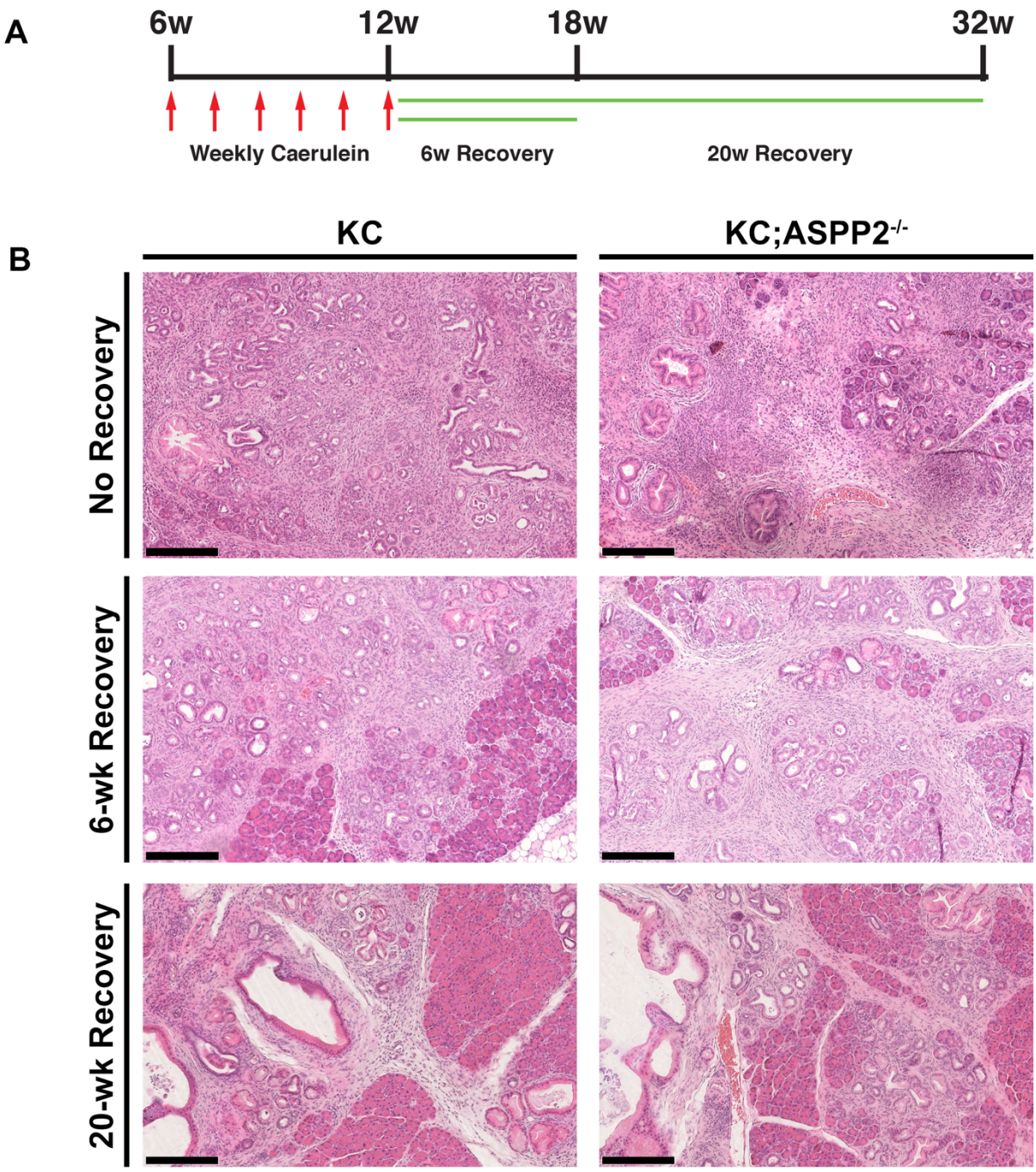

Figure 4.8 ASPP2-deficiency does not mediate PanIN progression following intermittent inflammation and recovery

A Injection Schedule. Weekly IP caerulein (250 μg/Kg) between 6-weeks and 12-weeks, with endpoints at 48-hours following final injection, following 6-week recovery and 20-weeks recovery.

B Representative H&E sections of KC and KC;ASPP2$^{-/-}$ pancreas sections. Scale bars 250 μm. Top row, majority of acini undergone metaplasia at 48-hours following final injection. Middle row, recovery at 6-weeks following last injection. Regeneration of normal acini present with multiple areas of low-grade PanIN, dense stroma and occasional high-grade areas. Bottom row, recovery at 20-weeks following last injection. Further regeneration evident with enlarged ductal areas, stroma and areas of high grade lesions.

4.9 KC;ASPP2$^{-/-}$ mice exhibit squamous differentiation and p63 expression

Classification of pancreatic cancer subtypes based on expression of transcription factors and important downstream targets for differentiation and lineage specification identified squamous, pancreatic progenitor, immunogenic and aberrantly differentiated endocrine exocrine (ADEX) subtypes (Bailey et al. 2016). Squamous subtype tumours associated with poor prognosis and gene networks linked to inflammation, metabolic reprogramming, TGF-β signalling, autophagy and upregulated ΔNp63. Adenosquamous carcinoma of the pancreas has previously been proposed as a histologic variant of pancreatic cancer. Characterised by loss of p16, presence of mutant p53, expression of p63 and squamous morphology, often adjacent to ductal PanINs, this subtype is particularly aggressive with poor prognosis and metastasis (Brody et al. 2009). ΔNp63 expression is a reliable marker of squamous differentiation in the pancreas (Basturk et al. 2005). Pure squamous pancreatic cancer is a rare entity, with an incidence reported between 0.5% to 3%. No mouse exists for the squamous or adenosquamous subtype of pancreatic cancer. ASPP2 expression is mutually exclusive to p63 in keratinocytes and functions to regulate squamous differentiation (Tordella et al. 2013). ASPP2 is a potent repressor of p63 expression via NF-κB. Therefore, I speculated that ASPP2-deficiency may favour a squamous or an adenosquamous phenotype PDAC phenotype.

Analyses of all cases KC and KC;ASPP2$^{-/-}$ tumours identified a case of pure squamous pancreatic cancer defined as squamous morphology and keratin pearls

clearly evident in a KC;ASPP2$^{-/-}$ mouse (Figure 4.9B). Immunohistochemical staining of p63 demonstrates positivity in basal cells of the squamous differentiation. The importance of ΔNp63 expression linked to poor prognosis may be derived from the accelerated or more aggressive metastatic disease related the squamous transcriptional profile. Further screening of p63 positivity in PDAC metastatic disease found no examples of KC metastasis with p63+ staining by IHC, only KC;ASPP2$^{-/-}$ in liver and neck metastases demonstrated nuclear p63+ cells (Figure 4.9C-F). In the case of p63+ neck metastasis, no squamous morphological changes were evident (Figure 4.9F).

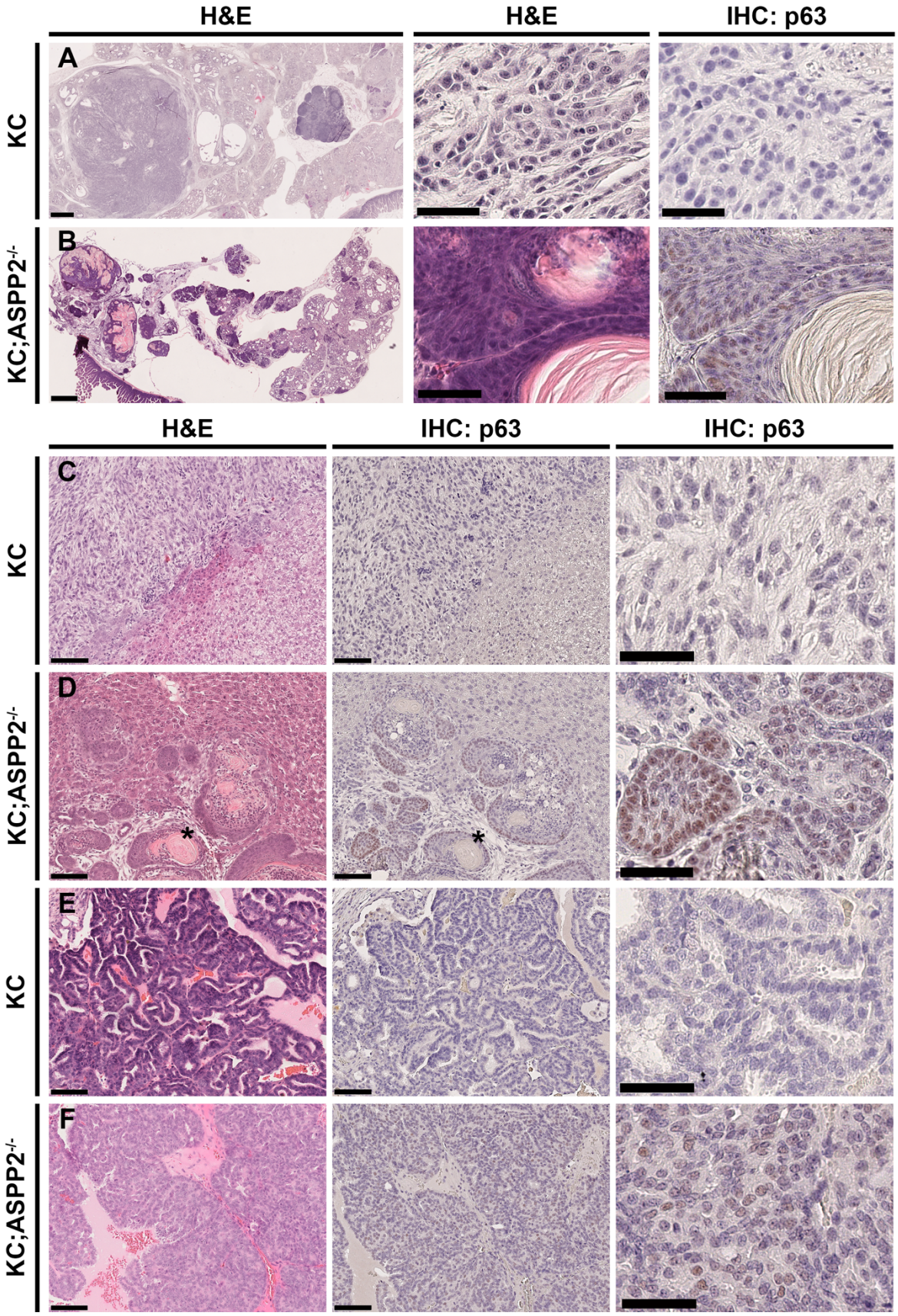

Figure 4.9 KC;ASPP2$^{-/-}$ mice exhibit squamous phenotype and p63 positivity

A KC 50-week old primary mPDAC with poorly- and well-differentiated morphology. H&E PDAC and PanIN section left panel (scale bar 1 mm);

representative H&E area of PDAC with ductal morphology middle panel (scale bar 50 μm). Representative IHC for p63 (4A4) of PDAC right panel (scale bar 50 μm).

B KC;ASPP2$^{-/-}$ 46-week old primary mPDAC with squamous pancreatic cancer and abundant PanINs. H&E squamous cancer and PanIN section left panel (scale bar 1 mm); representative H&E area of cancer with squamous morphology middle panel (scale bar 50 μm). Representative IHC for p63 (4A4) of squamous cancer right panel with basal p63 expression (scale bar 50 μm).

C KC 38-week old liver metastasis. H&E liver metastasis and liver tissue interface left panel; IHC for p63 (4A4) centre panel (scale bars 100 μm). IHC for p63 of PDAC right panel (scale bar 50 μm).

D KC;ASPP2$^{-/-}$ 46-week old liver metastasis with squamous differentiation and keratin expression. H&E liver metastasis and liver tissue left panel, with keratin pearls (*) and IHC for p63 centre panel (scale bar 100 μm). IHC for p63 (4A4) demonstrating basal expression of p63 right panel (scale bar 50 μm).

E KC 33-week old neck metastasis. H&E neck metastasis with ductal morphology left panel with IHC for p63 (4A4) negative (scale bar 100 μm). IHC for p63 demonstrates negative p63 expression (scale bar 50 μm).

F KC;ASPP2$^{-/-}$ 26-week old neck metastasis. H&E neck metastasis without squamous morphology left panel with IHC for p63 (4A4) positivity (scale bar 100 μm). IHC demonstrates variable nuclear p63 expression (scale bar 50 μm).

4.10 ASPP2 represses the ΔNp63 isoform *in vivo* following inflammation and recovery

Histological and immunohistochemical evidence for a subset of KC;ASPP2$^{-/-}$ mice expressing a squamous phenotype of metastatic PDAC is consistent with previous work demonstrating ASPP2 is a repressor of p63 (Tordella et al. 2013). Mechanistically this is achieved by ASPP2 binding NF-κB regulator IκB to enhance nuclear RelA/p65 that mediates repression of p63. Therefore, I speculated that ASPP2 repression of p63 may be potentiated by inflammation that requires activation of p65. Using tissue obtained from KC and KC;ASPP2$^{-/-}$ mice following inflammation and recovery described in chapter 4.8, I assessed relative levels of p63 and p53 (Figure 4.10A).

Age-matched control KC and KC;ASPP2$^{-/-}$ mice at 32-weeks without a 6-week course of caerulein-induced inflammation found no difference in relative expression of p63 and p53 (Figure 4.10B). Following 6-weekly IP injections of caerulein followed by recovery (6-weeks and 20-weeks), there is no difference in relative expression of p53 between KC and KC;ASPP2$^{-/-}$ mice. However, at both 6-week and 20-week recovery time points, there is greatly increased expression of p63 in KC;ASPP2$^{-/-}$ tissue compared to KC.

The monoclonal pan-p63 antibody clone 4A4 recognizes all mouse p63 isoforms. The p63 gene expresses at least six major transcripts, three of which contain the transactivation (TA) domain (TAp63α, TAp63β, and TAp63γ) capable of transactivating p63 reporter genes and induce apoptosis. Three other p63 isotypes

lack the N-terminal TA domain (ΔNp63α, ΔNp63β, and ΔNp63γ) and typically function as dominant-negative factors to suppress both p53 and TAp63 isotypes. Differentiating p63 isotypes using 4A4 is not completely possible but size indicates that the blot may be demonstrating a ΔNp63 isoform. A single p63 band was obtained at approximately 55kDa and may represent the most abundant form of p63 in tissue, ΔNp63.

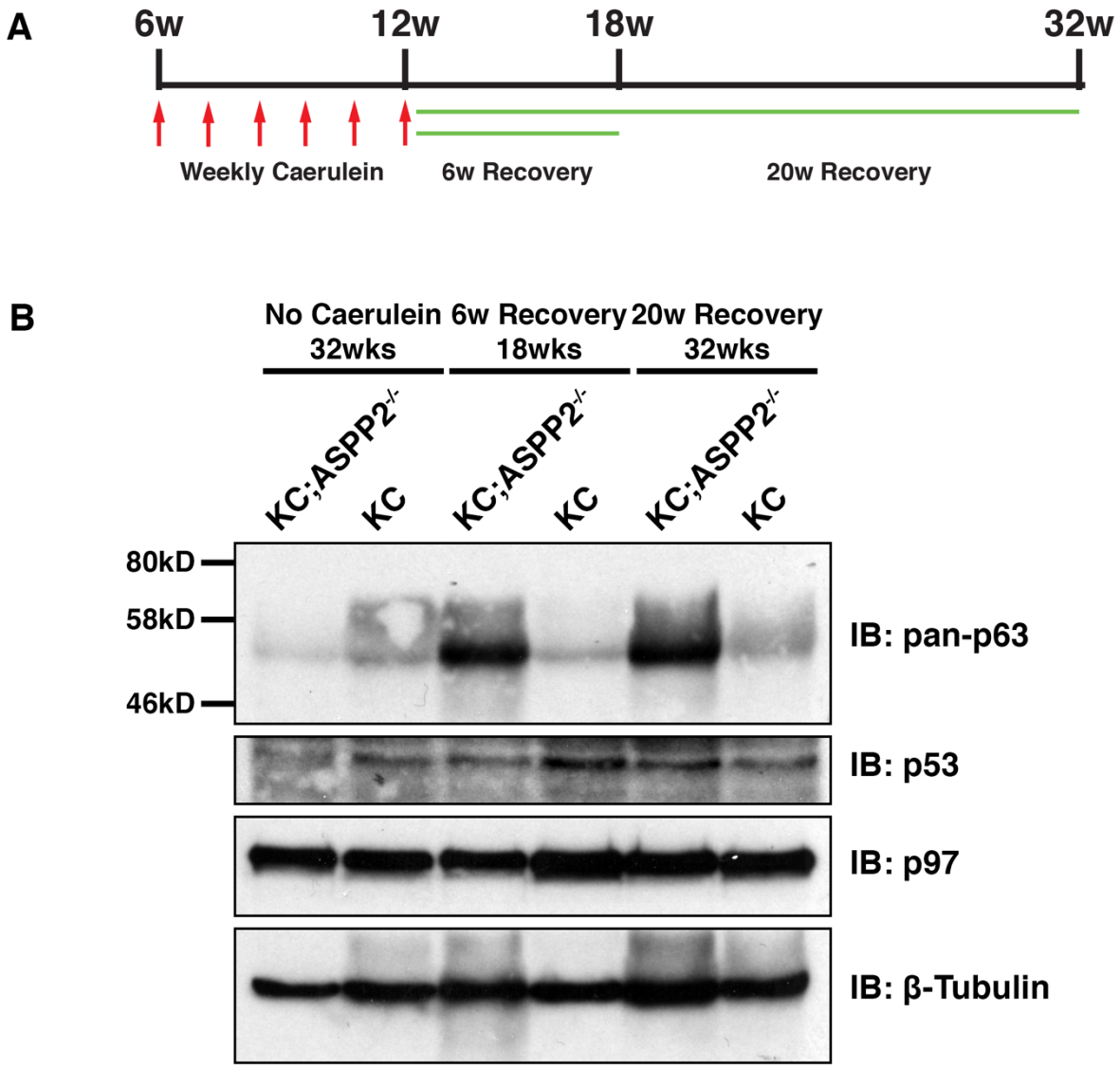

Figure 4.10 ASPP2 represses ΔNp63 isoform *in vivo* following inflammation and recovery

A Injection Schedule. Weekly IP caerulein between 6-weeks and 12-weeks, with endpoints at 48-hours following final injection, following 6-week recovery and 20-weeks recovery.

B Western blot for p63 (4A4) and p53 (CM5). Loading controls are p97 and β-Tubulin.

4.11 Summary

The KC;ASPP2$^{-/-}$ mouse is the first tissue specific ASPP2-deficient mouse model of cancer. Importantly KC;ASPP2$^{-/-}$ can examine potential roles of ASPP2 in regulating all stages of pancreatic cancer development from metaplasia to metastatic cancer. Consistent with tumour suppressor function of ASPP2, KC;ASPP2$^{-/-}$ mice have a reduced median survival compared with KC mice. However, rather than potentiating ADM or the progression through PanIN to PDAC, the reduced survival in KC;ASPP2$^{-/-}$mice appears to be due to earlier metastatic disease requiring elective culling of the mice. Both inflammation and recovery does not alter the histological extent of metaplasia and onset of PDAC.

The KC;ASPP2$^{-/-}$ mouse exhibits a spontaneous squamous phenotype, a rare occurrence in human pancreatic cancer, and not described in murine models of pancreatic cancer. The squamous subtype of human PDAC is defined by expression of ΔNp63 and has a poor prognosis relative to other PDAC subtypes. The KPC model is considered to be the closest murine model of squamous PDAC. Mechanistically there is evidence for the role of ASPP2 as suppressor of p63 via IκB and p65. Therefore, the evidence presented in this chapter is supportive of KC;ASPP2$^{-/-}$ representing a novel model for squamous PDAC.

Chapter 5: iASPP regulates the pancreatic response to inflammation

The ASPP family member iASPP is the most evolutionary conserved member of the family. In numerous cancers high expression of iASPP is associated with poor prognosis relative to low levels of iASPP. Also, nuclear iASPP associates with poorer prognosis than cytoplasmic iASPP localization. Similar to ASPP2, iASPP has multiple interacting partners, with the inhibition of the apoptotic function of p53 as main mechanism proposed for poor prognosis. Previous work in the Lu Lab examined the role of iASPP-deficiency in an epidermal (cytokeratin 14-Cre) mouse model of squamous cell cancer potentiated by TPA to induce Ras mutation (K Chung, unpublished). However, rather than inhibiting apoptosis as a main phenotypic consequence of iASPP loss, the mouse demonstrated upregulation of inflammatory mediators and infiltration of immune cells. In fibroblasts derived from patients with an iASPP premature stop mutation, iASPP-deficiency results in elevated pro-inflammatory genes (Falik-Zaccai et al. 2017).

To date, no mouse model of cancer exists that tests whether iASPP functions as an oncogene *in vivo*. Similar to the approach to study ASPP2 in inflammation and in response to oncogenic Kras, I therefore have systemically analysed the phenotype of iASPP deficiency in a mouse model for PDAC development.

5.1 iASPP is expressed in pancreatic islets in the unstressed pancreas

The pancreas consists of three functionally and morphologically distinct tissue types developing from the distal foregut endoderm. Exocrine acinar cells, accounting for over 90% pancreatic mass, produce the digestive enzymes secreted into the intestine. Endocrine cells, arranged into islets of Langerhans making up 5% of pancreatic cells, secrete hormones into the blood; including α-cells (glucagon), β-cells (insulin), δ-cells (somatostatin), ε-cells (ghrelin), and γ-cells (pancreatic polypeptide). Control of the developmental specification of the various tissue types is regulated by spatiotemporal expression of developmental transcription factors, in particular PDX1, FOXA2, GATA4, NKX6.1 and SOX9. Pancreatic ductal cells, expressing cytokeratin 19, account for approximately 5% of pancreatic cells and are also derived from Pdx1+ cells.

To determine expression of iASPP in the pancreatic cell populations, I performed immunohistochemical analyses of adult human and mouse pancreatic tissue. In human tissue, strong iASPP staining is demonstrated in the pancreatic islets (Figure 5.1A). Weak-to-moderate expression occurs in acini, with negative staining in the stroma. Similarly, in the adult mouse, iASPP is expressed most strongly in the islets, with weaker staining in the acini (Figure 5.1B). Pancreatic ductal cells are generally negative for iASPP expression.

Islet endocrine cell type specific expression was determined using immunofluorescence double-staining of mouse tissue. iASPP colocalizes with

insulin expression β-cells of the pancreas (Figure 5.1C). iASPP does not colocalize with somatostatin expressing δ-cells expressing cells (Figure 5.1D).

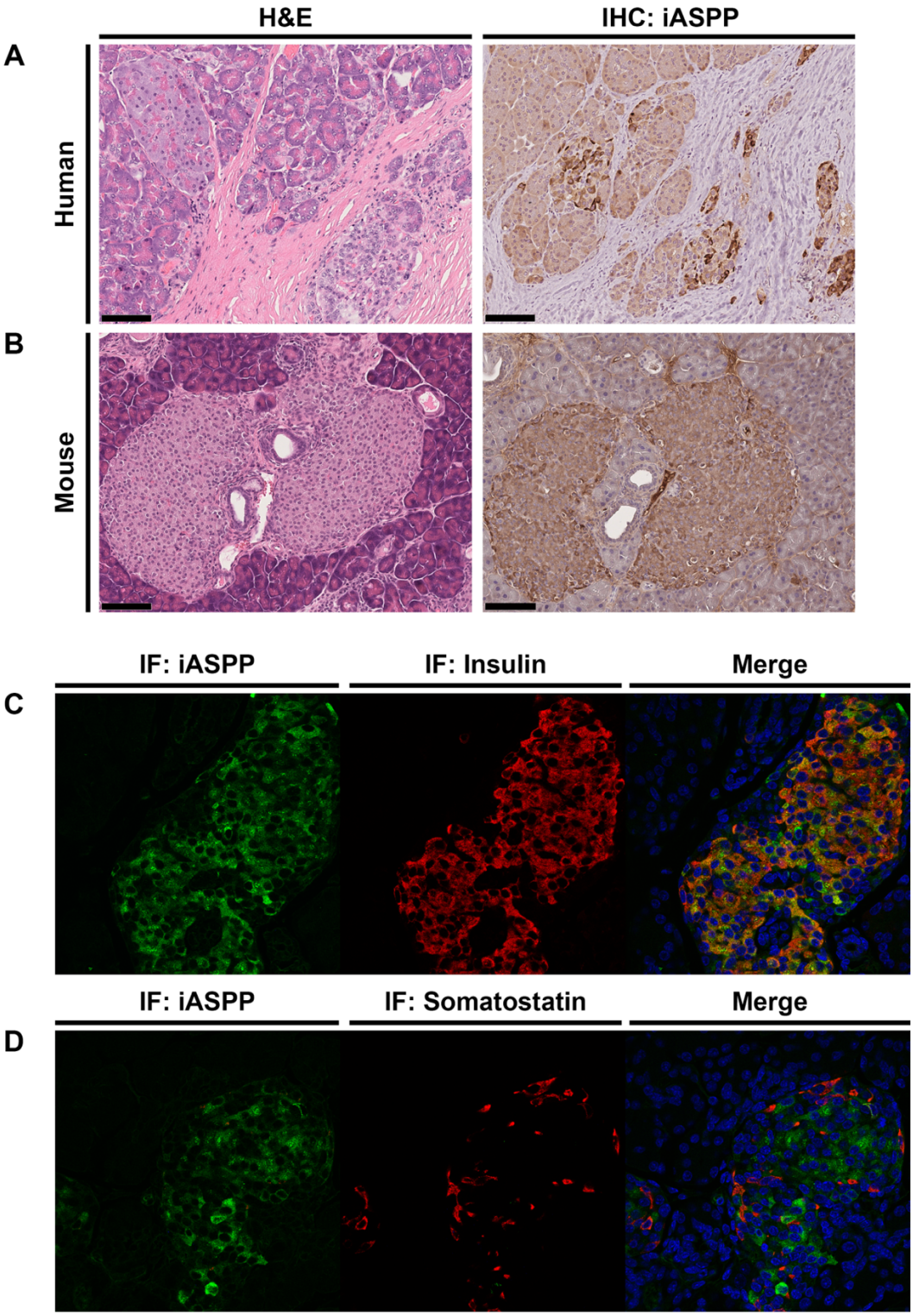

Figure 5.1 iASPP is expressed in the pancreatic islets

A Human pancreas section with fibrosis, acini and islets. H&E stained pancreas (left) and IHC for iASPP (LX49.3). Scale bar 100 μm.

B Mouse pancreas section islets, acini and ducts. H&E stained pancreas (left) and IHC for iASPP (LX49.3). Scale bar 100 μm.

C Immunofluorescence double staining of mouse pancreas for iASPP (green), insulin (red) and DAPI (blue).

D Immunofluorescence double staining of mouse pancreas for iASPP (green), somatostatin (red) and DAPI (blue).

5.2 iASPP deficiency does not alter pancreatic acinar development nor homeostasis

iASPP expression is regulated by the transcription factor E2F1 (Chen et al. 2005; Fogal et al. 2005; Pandolfi et al. 2015). As stated in chapter 3.1 E2F1 knockout ($E2F1^{-/-}$) mice have reduced pancreatic size due to impaired growth and hyperglycaemia due to reduced insulin secretion (Fajas et al. 2004). ASPP2 does not appear to have a role in pancreatic development and homeostasis. As iASPP is expressed in the β-cells of the pancreas, and the $E2F1/E2F2^{-/-}$ mouse has chronic pancreatitis and frank diabetes that is potentiated by p53, it would be logical that iASPP may function in as a regulator of pancreas or β-cell homeostasis. Similar to chapter 3.1, I analysed adult murine pancreas deficient for iASPP to determine if an overt phenotype is present.

Adult $iASPP^{\Delta 8/\Delta 8}$ B6 mice survive up to 6 months and are usually found dead due to suspected acute cardiac dysfunction. Therefore, $iASPP^{\Delta 8/\Delta 8}$ mice were analysed at 6 months, when they were found to have histologically normal acinar and islet structure (n=3) (Figure 5.2A). Pancreatic-specific iASPP deficiency was achieved by crossing B6 $iASPP^{LoxP/LoxP}$ and B6 Pdx1 Cre-recombinase expressing mouse to produce the $iASPP^{-/-}$ mouse. Similar to the $ASPP2^{-/-}$ mice, $iASPP^{-/-}$ mice all survived over 1 year with no overt acinar nor islet phenotype (n=3) (Figure 5.2B). Absence of spontaneous metaplasia and tissue loss is suggestive that iASPP does not function to maintain tissue homeostasis in the absence of cellular stresses. However, a β-cell specific role for iASPP cannot be excluded in the $iASPP^{-/-}$ mouse.

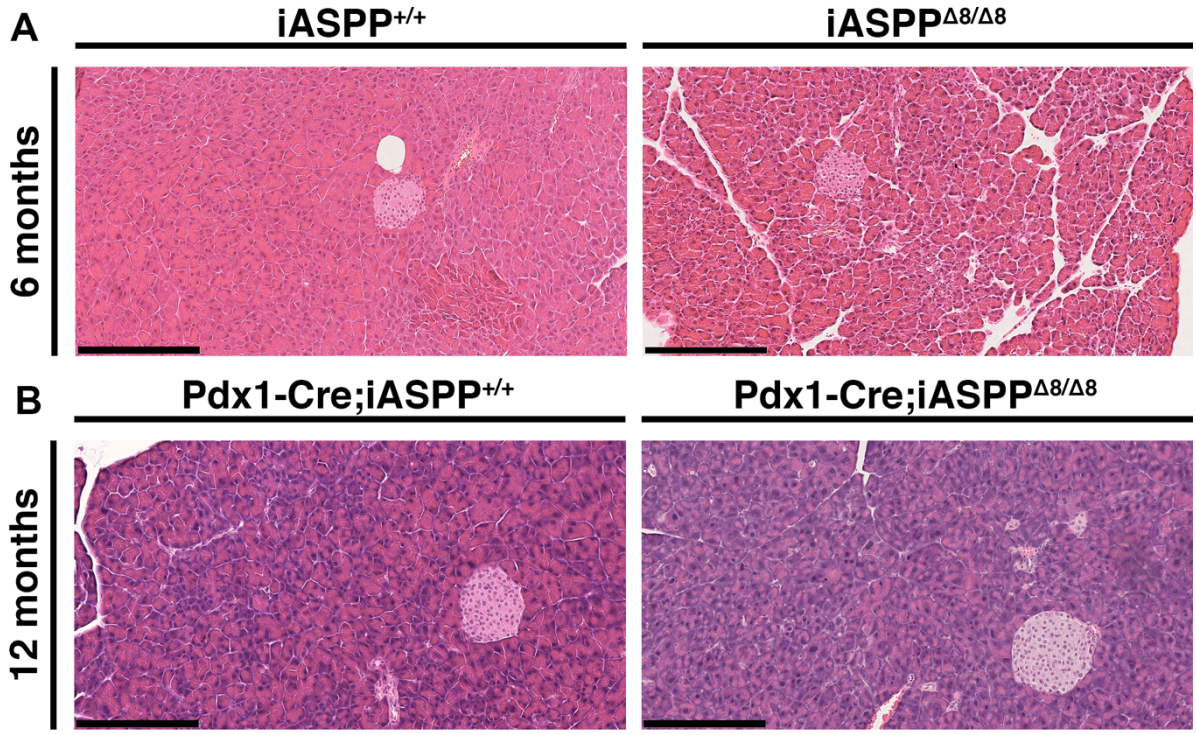

Figure 5.2 iASPP-deficiency does not cause a pancreatic developmental or homeostatic phenotype

A Representative pancreas H&E sections of 6-month old constitutive iASPP knockout littermate mice on a B6 background. iASPP wild-type (left) and iASPP$^{-/-}$ (right). Scale bar 250 μm.

B Representative pancreas H&E sections of 12-month old pancreatic-specific (Pdx1-Cre) mice on B6 background. iASPP wild-type (left) and iASPP$^{-/-}$ (right). Scale bar 250 μm.

5.3 β-cell specific iASPP-deficient mice have normal islets and glucose tolerance

The β-cell specific expression of iASPP was an unexpected finding. However, iASPP, as a transcriptional target of E2F1, may function to inhibit the p53 mediated effects of inflammation and impaired glucose tolerance previously described. To directly test this hypothesis, I created a β-cell specific iASPP-deficient mouse by crossing the B6 LSL-iASPP$^{\Delta 8/\Delta 8}$ mouse with a RIP-Cre expressing mouse (Cre-recombinase linked to the insulin promoter).

Histological examination of the iASPP$^{\Delta 8/\Delta 8}$; RIP-Cre mouse at 32-weeks alongside littermate controls demonstrated no overt islet phenotype, with normal size, cellularity and lack of immune infiltration (Figure 5.3A). Intraperitoneal glucose tolerance testing on littermates on various occasions did not demonstrate either a hypo- or hyperglycaemic response (Figure 5.3B). In summary, although a β-cell specific role for iASPP has not been excluded, there is no clear phenotype in the islet that would preclude the use of a Pdx1-Cre specific iASPP-deficient mice to study inflammation. Pdx1+ cells specify both the exocrine and endocrine cell population and so I cannot exclude a β-cell phenotype in the iASPP$^{-/-}$ cohort.

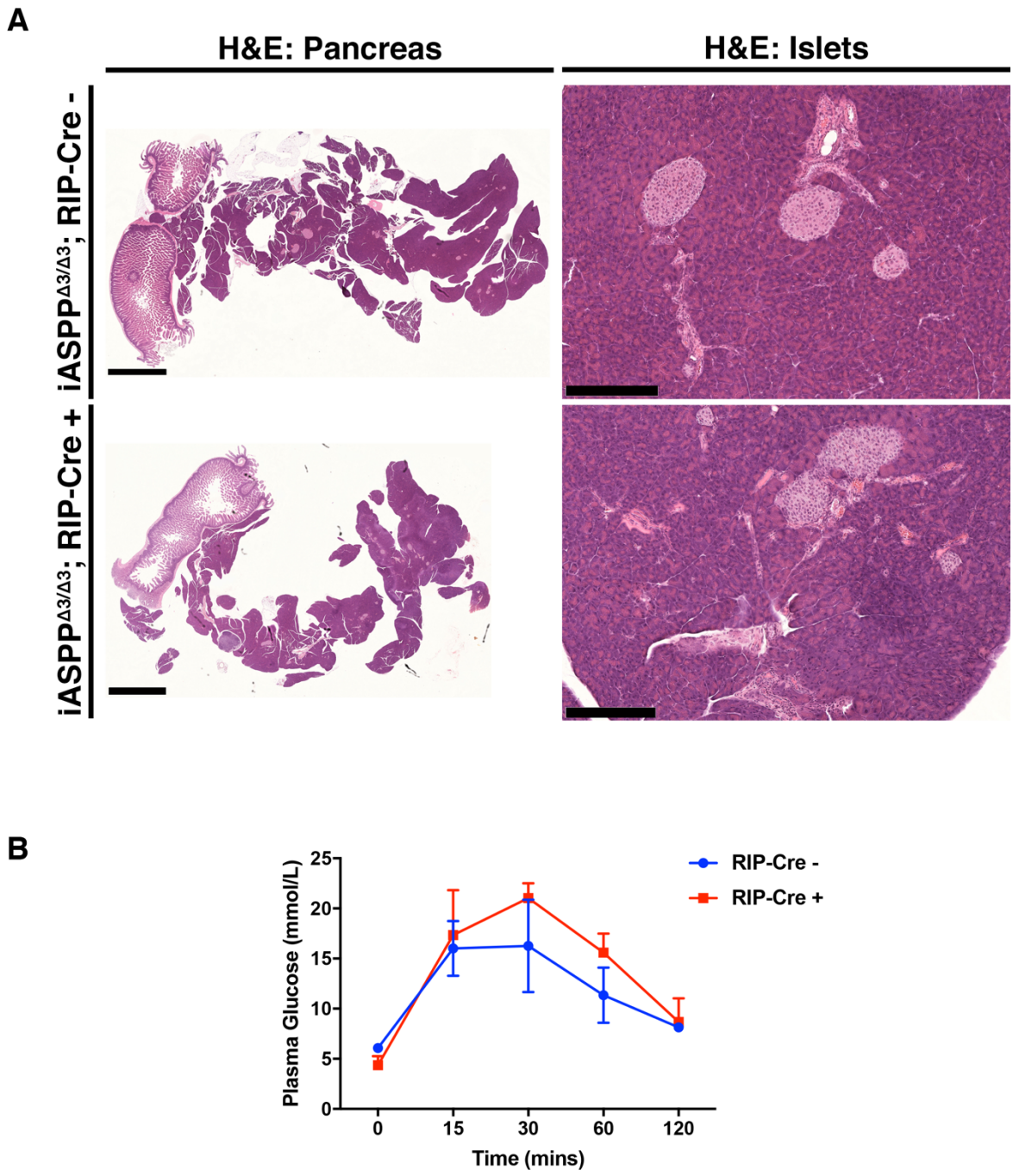

Figure 5.3 β-cell specific iASPP$^{\Delta8/\Delta8}$ have normal islets and glucose tolerance test

A 32-week old whole H&E pancreas and representative section from littermate iASPP$^{\Delta8/\Delta8}$; RIP-Cre- and iASPP$^{\Delta8/\Delta8}$; RIP-Cre+ mice.

B Intraperitoneal glucose tolerance testing comparing iASPP$^{\Delta8/\Delta8}$; RIP-Cre- and iASPP$^{\Delta8/\Delta8}$; RIP-Cre+ mice (n=3).

5.4 Acute pancreatitis in iASPP-deficient mice results in ADM and failure to recover

Upregulation of iASPP occurs as part of the acute pancreatitis response (Figure 3.3B). The constitutive iASPP$^{\Delta 8/\Delta 8}$ mouse on the B6 genetic background has eyes opened at birth, cardiac defects and a microscopically normal pancreas. Therefore, I speculated that iASPP-deficient mice may have increased cell death via apoptosis or more severe inflammation in response to a mild-to-moderate inflammatory stimulus.

To study this, caerulein-induced pancreatitis was induced (16 intraperitoneal injections over 2 days) in 6-month old iASPP$^{\Delta 8/\Delta 8}$ siblings with analysis planned at day 14. At day 12, the iASPP$^{\Delta 8/\Delta 8}$ mouse became thin, hypoactive and demonstrated piloerection and a decision was made to cull the experimental mice (Figure 5.4A). Histologically, the iASPP$^{+/+}$ day 12 pancreas is almost histologically normal. There is reconstitution of eosinophilic content of acinar cells, normal nuclei, and very occasional immune cell infiltration. The iASPP$^{\Delta 8/+}$ pancreas is almost normal in terms of eosinophilic acinar cell content and normal nuclei. However, there are occasional small areas of duct-like structures (Figure 5.4B, centre panels). The iASPP$^{\Delta 8/\Delta 8}$ pancreas was macroscopically much smaller than iASPP$^{\Delta 8/+}$ and iASPP$^{+/+}$ pancreases. Furthermore, eosinophilic acinar cells account for less than 20% of pancreatic mass. Most the iASPP$^{\Delta 8/\Delta 8}$ tissue consists of duct-like structures with numerous infiltrating cells associated (Figure 5.4B, right panels). Immunohistochemical analysis of ductal marker cytokeratin 19 demonstrates the iASPP$^{\Delta 8/\Delta 8}$ structures express the key marker of pancreatic

ductal identity (Figure 5.4C). All ADM structures express key mediators of dedifferentiation and pancreatic development, Pdx1 and Sox9.

In summary, iASPP deficiency results in a profound altered response to pancreatitis. Following the moderate insult of 2 days caerulein followed by recovery, there is widespread acinar-to-ductal metaplasia without recovery. The phenotype is consistent with iASPP deficient cells being more susceptible to transdifferentiation i.e. more plastic, having a reduced tolerance of stress stimuli, or an altered inflammatory response. As the experiment used a constitutive iASPP knockout, it is unknown whether this an acinar intrinsic effect, or related to abnormal immune response from the iASPP-deficient inflammatory cells. Furthermore, it raises the questions whether iASPP protects cells from ADM, the initial step in PDAC tumorigenesis, which could only be tested in a pancreas specific iASPP-deficient mouse.

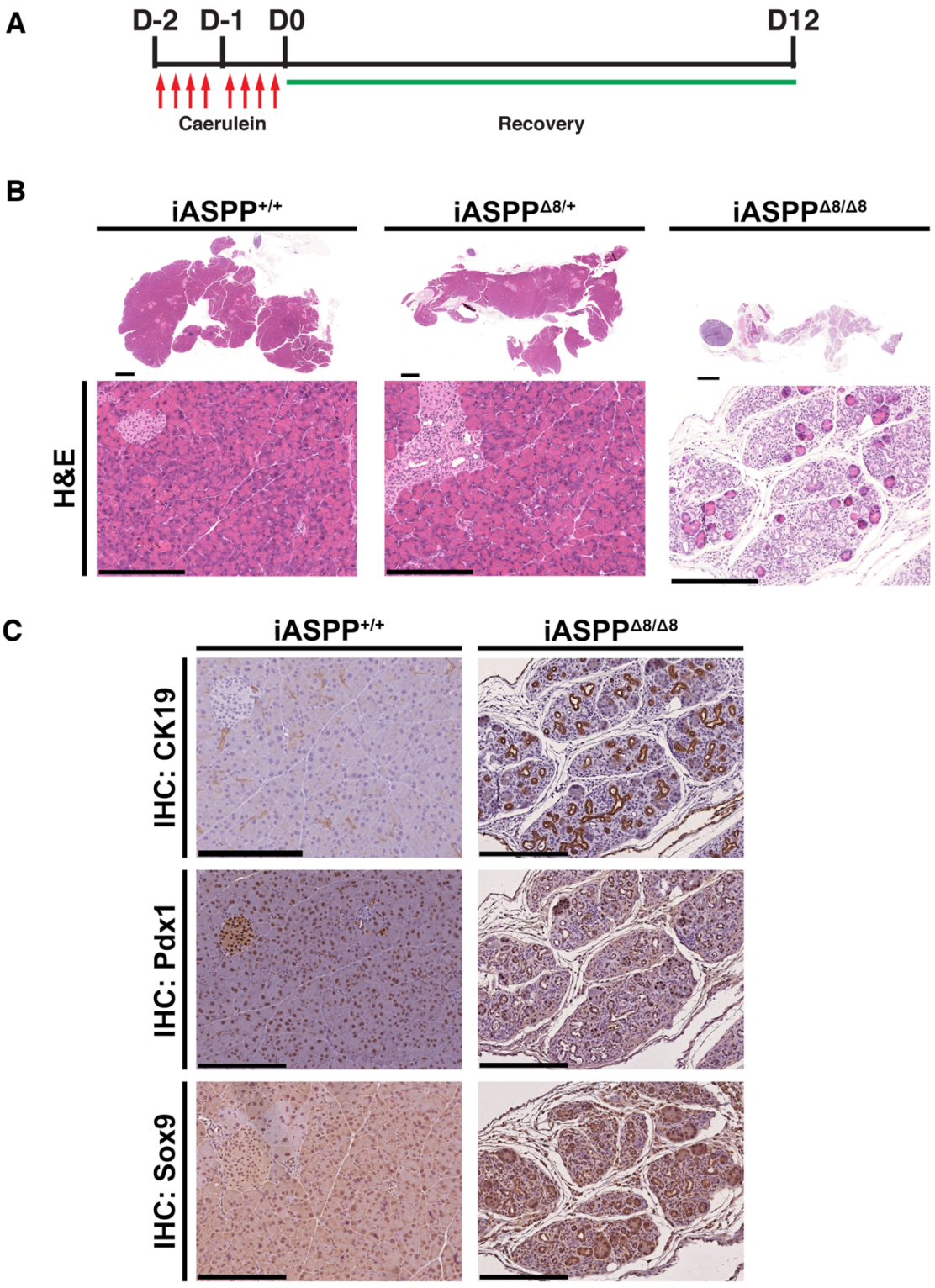

Figure 5.4 Acute pancreatitis in iASPP-deficient mice results in ADM and failure to recover

A Injection schedule. 8 hourly injections on days -2 and -1 of caerulein with 12-day recovery from final injection.

B Histology of day 12 pancreases from iASPP$^{+/+}$, iASPP$^{\Delta 8/+}$ and iASPP$^{\Delta 8/\Delta 8}$ littermates. Upper panels are whole scanned H&E pancreases (scale bar 1 mm). Lower panels representative H&E sections. Scale bar 250 μm.

C Immunohistological comparison of markers of ductal morphology (CK19) and dedifferentiation Pdx1 and Sox9. Scale bar 250 μm.

5.5 Acute pancreatitis in pancreatic-specific iASPP-deficient mice does not result in metaplasia

Constitutive deficiency of iASPP results in profound metaplasia following acute pancreatitis. Inflammation is the driver of the metaplastic phenotype as iASPP$^{\Delta 8/\Delta 8}$ mice without inflammation have no evidence of spontaneous ductal metaplasia. However, the cell type that mediates the acinar metaplasia is potentially the acini cells, the immune cells, the stromal cells or a combination. To test whether acinar iASPP-deficiency modulates the metaplastic phenotype, a pancreatic cell specific iASPP-deficient mouse was created. The LSL-iASPP$^{\Delta 8/\Delta 8}$ mouse was crossed with a Pdx1-Cre expressing mouse in the pure B6 background to create LSL-iASPP$^{\Delta 8/\Delta 8}$; Pdx1-Cre (termed iASPP$^{-/-}$).

Using the same injection protocol as for the constitutive iASPP-deficient mouse, I induced acute pancreatitis in wildtype iASPP (iASPP$^{+/+}$) and iASPP$^{-/-}$ mice with caerulein or PBS (16 IP injections over two consecutive days) (Figure 5.5A). Histological characterisation determined that the iASPP$^{-/-}$ mice do not produce a metaplastic phenotype (Figure 5.5B). Similarly, acute pancreatitis and expression analysis of p53 and MAPK-pathway activation was analysed after 48-hours recovery (Figure 5.5C). No difference in MDM2 downregulation, or p53 levels was observed (Figure 5.5D). Activation of MAPK, as assessed through phosphorylated ERK and was equivalent in both iASPP$^{+/+}$ and iASPP$^{-/-}$.

Analysis of inflammation effects at the 48-hours and 14-day time points following cessation of caerulein injection does not demonstrate a phenotypic difference between wildtype iASPP and iASPP-deficient mice. These data support either a

non-pancreatic cell mediated metaplasia effect, or a combined effect in which iASPP regulates both acinar and immune cell response to inflammation. Analysis of iASPP expression in human pancreatic disease is required to delineate cell-type in which iASPP is altered in pancreatic disease.

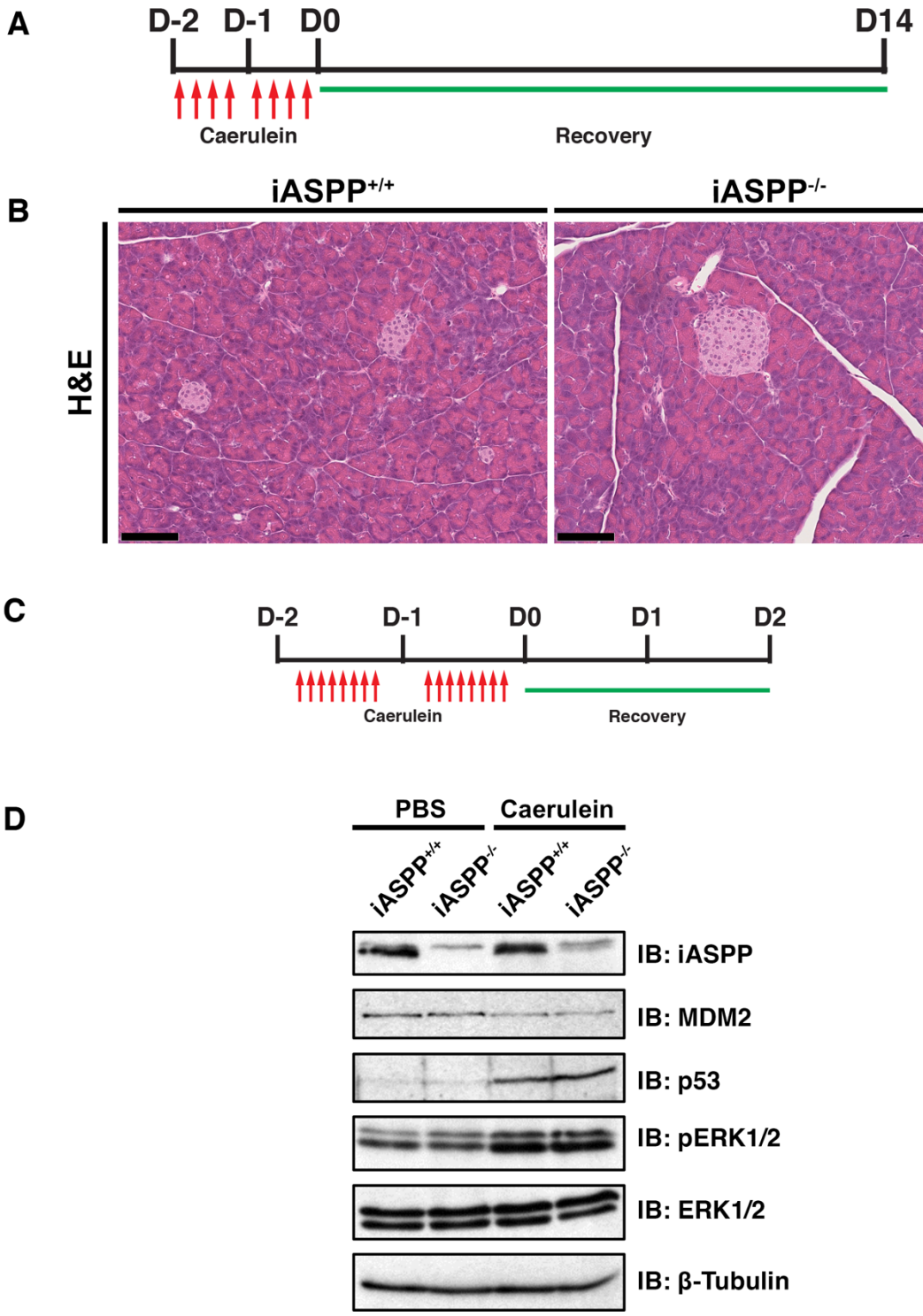

Figure 5.5 Pancreatic-specific iASPP-deficiency does not result in metaplasia

A Injection schedule for 2-days acute pancreatitis and 14-days recovery.
B Representative H&E images of day 14 pancreas in iASPP wild-type and iASPP$^{-/-}$. Scale bar 100 μm.
C Injection schedule for 2-days caerulein or PBS and 2-days recovery.
D Western blot after 48-hours recovery from a 2-day caerulein or PBS injections.

5.6 iASPP is upregulated in human pancreatic disease

Initial evidence from the iASPP-deficient mouse supports a potential proinflammatory, proapoptotic or regeneration-incompetency role for iASPP in a mouse model of pancreatic inflammation. However, the cell of origin for the phenotypic effect of iASPP-deficiency was unclear. I speculated that iASPP expression in human tissue with various pathological conditions would indicate the cell-type that regulates iASPP function. Immunohistochemical staining for iASPP has been used in a number of studies to correlate staining strength and patient outcome. Nine samples of human pancreatic disease were obtained from Professor Robert Goldin (Imperial College, University of London).

Normal pancreas is difficult to obtain as pancreas would not be taken from a non-diseased pancreas due to significant co-morbidity associated with a resection or biopsy procedure. A normal pancreas section was defined from a resected insulinoma case in which no insulinoma cancer cells were present (Figure 5.6A). Analysis determined that iASPP is expressed throughout the acinar cells at a low level with individual strongly staining cells within the pancreatic islets. The pattern is similar to the mouse pancreas. Chronic pancreatitis, found in isolation or in samples with PanIN is characterised by desmoplasia and areas of ADM. In a case of chronic pancreatitis, morphologically normal acini have relatively increased IHC staining for iASPP (Figure 5.6B). Stroma is generally negative for iASPP expression, with ADM and PanIN positive.

Serous cystadenoma is a benign tumour of the pancreas, which differs from IPMN which have more malignant potential. The cystic neoplasms appear to have low levels of iASPP expression equivalent to normal acinar staining intensity (Figure 5.6C). In a case of poorly differentiated PDAC, iASPP is expressed in the PDAC cells. In particular areas that maintain a ductal morphology, iASPP expression is particularly high (Figure 5.6D). A moderately differentiated PDAC example has high iASPP expression in the tumour cells and within isolated cells of the stroma (Figure 5.6E). Nuclear iASPP is present in the PDAC cases.

In summary, iASPP is expressed in acinar cells of the human pancreas with increased expression in inflammatory conditions of chronic pancreatitis and PDAC. Consistent with the mouse induction of iASPP following inflammation, iASPP may function as a mediator of cellular response to inflammation or oncogenic stress.

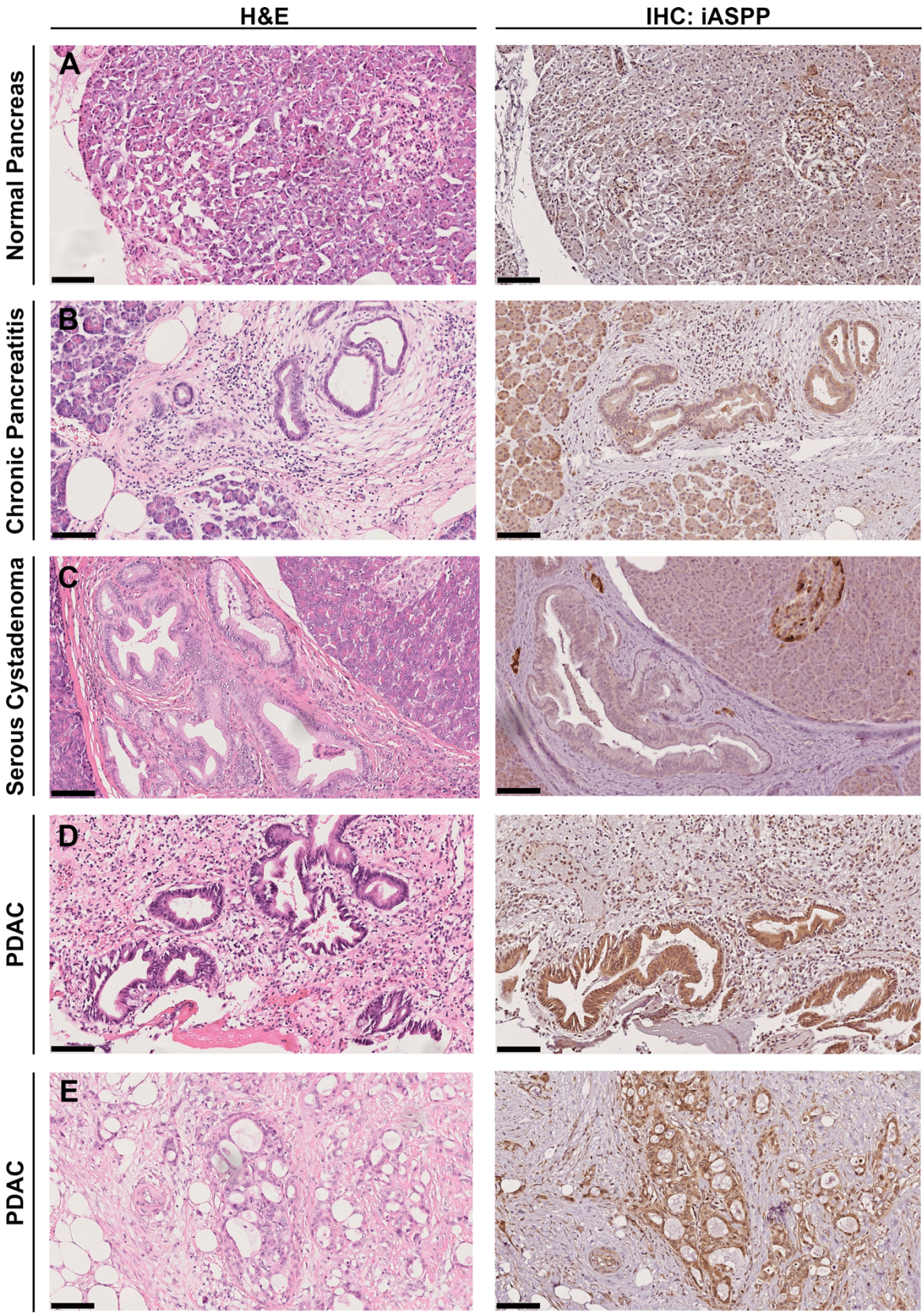

Figure 5.6 iASPP expression is upregulated in pancreatic inflammation and cancer relative to normal pancreas

A Normal pancreas H&E and iASPP IHC sections from case of insulinoma, with no malignant cells present, including normal acini and Islets of Langerhans. including normal acini and an islet. Scale bar 100 µm.

B Chronic pancreatitis H&E and iASPP IHC sections including morphologically normal acini, desmoplasia and PanIN. Scale bar 100 µm.
C Serous cystadenoma H&E and iASPP IHC section including cystic area and normal acini. Scale bar 100 µm.
D Poorly differentiated PDAC H&E and iASPP IHC section with dense stroma and high-grade PDAC. Scale bar 100 µm.
E Moderately differentiated PDAC H&E and iASPP IHC section with stoma and PDAC cells. Scale bar 100 µm.

5.7 iASPP expression correlates with p53 from normal acini to PDAC

The results obtained from the screening of a panel of human pancreatic disease is suggestive of iASPP upregulation in inflammatory, metaplastic, and neoplastic conditions of the pancreas. However, it is not clear whether the areas with high iASPP are under stress. p53 is stabilized under stressed conditions or when mutated. p53 is usually undetectable immunohistologically under non-stressed conditions. If iASPP expression correlates with p53 stabilization this would suggest iASPP is upregulated in stressed cells, and may be inhibiting p53-mediated apoptosis.

I performed direct comparison of immunohistological expression of iASPP and p53 *in vivo* using human PDAC samples containing histologically normal acini, tumour adjacent and PDAC cells (Figure 5.7A and B). In morphologically normal acini, p53 immunostaining is absent, whilst present in the nuclei of tumour adjacent acini and metaplastic acini (Figure 5.7C). Nuclear p53 expression in PDAC is contrasted to the p53 negative stroma with the absence of intense staining favouring a wild-type p53 expression pattern. Lowest iASPP expression occurs in morphologically normal acini and is increased with cytoplasmic and nuclear expression in tumour adjacent acini and ADM cells (Figure 5.7D). In PDAC, especially areas with abnormal ductal morphology, iASPP is strongly expressed in both the cytoplasm and many nuclei.

These data from human pancreatic disease tissue suggests a functional role for iASPP in pancreatic disease in responding to microenvironment inflammation or

stress. Our understanding of iASPP as an inhibitor of p53-mediated apoptosis would imply that iASPP functions as a suppressor of apoptosis in pancreatic disease, and is consistent with an oncogenic role. However, if iASPP responds to inflammatory stresses to impair metaplasia, as demonstrated in the iASPP$^{\Delta 8/\Delta 8}$ mouse (Chapter 5.5), then iASPP may suppress the early initiation events of PDAC.

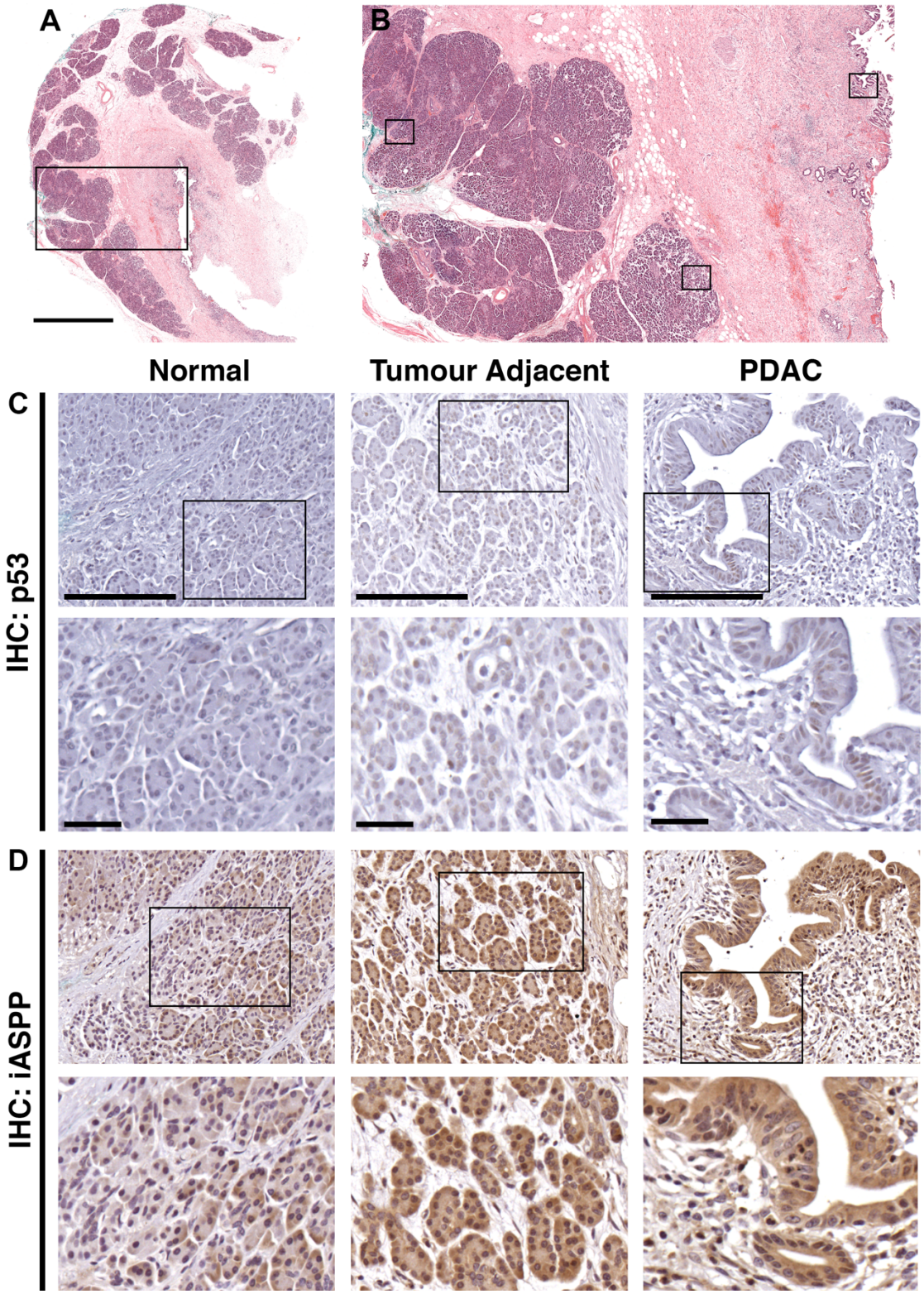

Figure 5.7 iASPP correlates with p53 in human pancreatic disease

A Whole slide scanned H&E section of human PDAC case with an area of histological normal pancreas. Scale bar 1 cm.

B Enlarged section of pancreas with normal (left), tumour adjacent (middle), and PDAC (right) used in C+D IHC analysis.

C IHC for p53 (DO1) with upper row equivalent areas to 5.8B boxes, lower row is boxed area from upper row. Upper row scale bar 250 µm; lower row scale bar 50 µm.

D IHC for iASPP (LX49.3) with upper row equivalent areas to 5.8B boxes, lower row is boxed area from upper row. Upper row scale bar 250 µm; lower row scale bar 50 µm.

5.8 iASPP is infrequently mutated in PDAC and iASPP amplification associates with AKT2 amplification

Four pancreatic ductal adenocarcinoma sequencing studies can be accessed using cBioportal for mutation and copy-number alterations with a total of 777 samples. Analysis of this information demonstrates that in total, two cases had iASPP deep/homodeleted and two cases mutated (Figure 5.8A). Amplification of PPP1R13L was identified in up to 15% case in one study (Witkiewicz et al. 2015). The TCGA study found a 0.5% incidence of iASPP mutation (1/186) with an amino acid change at V629M (Figure 5.8B). Amplification of PPP1R13L was found in 3% cases (6/184), with 83% (5/6) having co-amplification of AKT2 which is amplified in a total of 7% of cases (13/184) (Figure 5.8C). QCMG found a single mutation at K378T (1/109) (Figure 5.8B). UTSW found PPP1R13L amplification occurred in 15% of cases (16/109) with AKT2 co-amplified in 73% cases (11/15) which is amplified in 16% (17/109) of cases overall (Figure 5.8D) (Witkiewicz et al. 2015). AKT2, a putative oncogene, is located at 19q13, along with PPP1R13L, and is associated with poor prognosis in many cancers (Ruggeri et al. 1998).

I assessed survival using the TCGA study with mRNA data (RNA Seq V2) for 178 patients based on PPP1R13L amplification, mRNA upregulation or mutation. Upregulation of mRNA expression was defined with a z-score threshold of +2.0. Overall median survival with (n=20) or without (n=158) PPP1R13L alteration was 19.8 and 20.6 months respectively ($p = 0.854$) (Figure 5.8E). Disease-free median survival with (n=18) or without (n=121) PPP1R13L alteration was 12.4 and 17.1 months respectively ($p = 0.183$) (Figure 5.8F).

In summary, PPP1R13L is rarely mutated in human PDAC across four large studies including 777 patient samples. Amplification is likely to represent amplification of the 19q13 region which is recognised to associate with poor prognosis and AKT2 amplification. Therefore, the investigation of the role of iASPP in PDAC should focus on how iASPP alters the key dysregulated pathways in PDAC tumorigenesis.

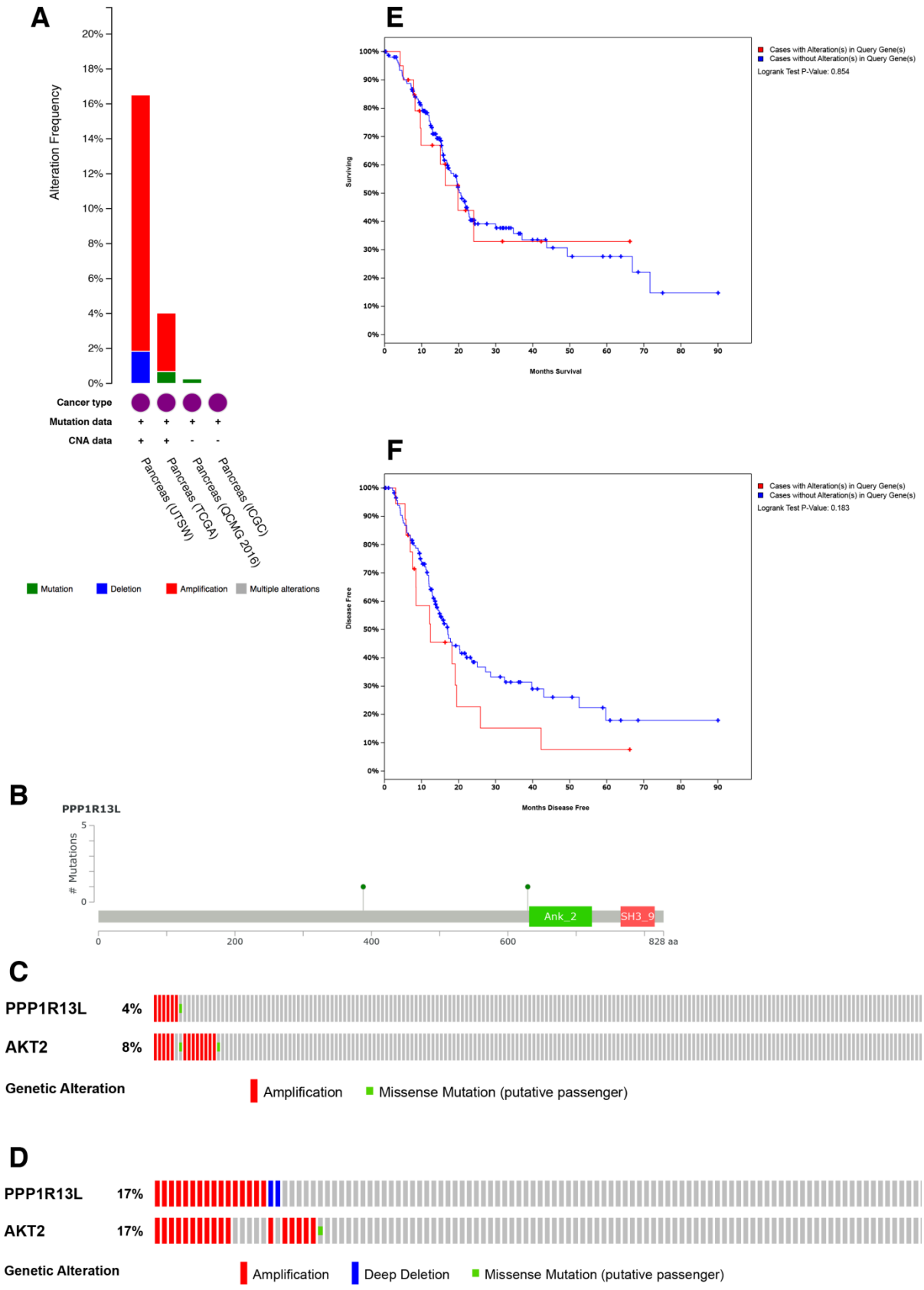

Figure 5.8 iASPP is infrequently mutated in PDAC and associates with AKT2 amplification at 19q13

A Alteration frequency of PPP1R13L in four PDAC sequencing efforts (from cBioportal).
B Mutation location and frequencies of PPP1R13L in 777 sequenced cases.
C PPP1R13L and AKT2 alteration frequency from the TCGA database (184 cases).
D PPP1R13L and AKT2 alteration frequency from the UTSW study (109 cases).
E Kaplan-Meier estimate of overall survival with or without PPP1R13L alteration (amplification/mutation/mRNA upregulation).
F Kaplan-Meier estimate of disease free survival with or without PPP1R13L alteration (amplification/mutation/mRNA upregulation).

5.9 Summary

iASPP expression associates with poor prognosis in various cancers, and is often attributed to the ability of iASPP to inhibit the apoptotic function of p53. In this chapter, I performed an initial characterisation of the role of iASPP in human pancreatic cancer and modelled the effect of iASPP deficiency in a murine model of inflammation. Expression of iASPP in the β-cells in the islets of Langerhans in the mouse and human was unexpected. The iASPP$^{\Delta 8/\Delta 8}$;RIP-Cre mouse found no islet size nor intra-peritoneal glucose tolerance test abnormality. Further characterisation of β-cell and islet function may yield a functional role for iASPP expression. However, it is outside the scope of this thesis to pursue an islet specific role for iASPP.

Similarly to ASPP2, iASPP is upregulated following an acute episode of pancreatitis. Elevated levels correlate with p53 stabilisation and would be consistent with a functional role in inhibiting p53, to prevent apoptosis when cell survival or regeneration would be preferable. Assessing the response at 14-days following final injection in iASPP$^{\Delta 8/\Delta 8}$ demonstrated a profound ductal pro-metaplastic phenotype. Lack of a pro-metaplastic phenotype in the iASPP$^{-/-}$ mouse suggests that loss iASPP in acini is insufficient to alter the tissue response to AP alone, and is it fully or partially mediated by another cell type such as inflammatory cells.

Expression of iASPP in human chronic pancreatitis and PDAC suggests iASPP may also be upregulated in human disease. Correlation of iASPP with p53 is

congruent with iASPP being an inhibitor of p53 mediated apoptosis. In inflammation stress conditions the presence of iASPP may favour resolution and regeneration of tissue, whilst in absence of iASPP it may favour tissue death which would be disadvantageous to the organism. Conversely, iASPP may favour survival and failure of apoptosis in PDAC resulting in tumorigenesis.

Chapter 6: iASPP functions as a tumour suppressor in pancreatic tumorigenesis

Expression of iASPP is consistently linked to prognosis in a plethora of cancers. High iASPP or nuclear expression associates with poor prognosis across multiple tumour types. In chapter five, initial evidence that iASPP$^{\Delta 8/\Delta 8}$ mice were more susceptible to ADM than iASPP$^{+/+}$ was presented. However, iASPP$^{-/-}$ mice (pancreas-specific iASPP$^{\Delta 8/\Delta 8}$) did not replicate those findings suggesting that the pro-ADM phenotype may be mediated by another cell type, such as the immune cells or stroma cells. Human IHC staining for iASPP specifically identified increased iASPP expression in PDAC cells, with lower expression in normal acinar cells away from the tumour. In PDAC, iASPP may inhibit apoptosis and may alter the p53 response in preneoplastic lesions and chronic pancreatitis. To investigate this hypothesis, I created a pancreas-specific iASPP-deficient Kras^{G12D} heterozygous mouse model was created (KC;iASPP$^{-/-}$), with the aim to discover whether iASPP functions as an oncogene *in vivo* and whether iASPP-deficiency results in a pro-ADM phenotype in the context of PDAC initiation.

6.1 KC;iASPP$^{-/-}$ mice have reduced survival and accelerated primary PDAC

To investigate the role of iASPP in regulating the initiation of the earliest lesions in PDAC, I crossed LSL-iASPP$^{\Delta 8/\Delta 8}$ mice with the LSL-Kras$^{G12D/+}$ Pdx1-Cre (KC) model. The resulting mice were termed KC;iASPP$^{-/-}$ (LSL-Kras$^{G12D/+}$ Pdx1-Cre iASPP$^{\Delta 8/\Delta 8}$) and were maintained in parallel to a KC cohort. The mice were kept under University of Oxford standards and in accordance with the Home Office animal licence of Professor Xin Lu. As with KC and KC;ASPP2$^{-/-}$ mice, KC;iASPP$^{-/-}$ mice developed facial and anal papillomas and keratoacanthomas that would result in Schedule 1 culling if persistently bleeding or causing the mouse distress. The lesions did not exhibit an earlier onset, frequency or aggressiveness compared to KC or KC;ASPP2$^{-/-}$ cohorts. KC and KC;iASPP$^{-/-}$ mice were culled with signs and symptoms suggestive of advanced malignancy. A swollen or tense abdomen, cachexia, rapid breathing, hypomobility and hunched stance that did not improve with monitoring were indications for culling. No KC;iASPP$^{-/-}$ were found dead. The earliest mouse requiring culling was 4.5 weeks old and was hunched with cachexia. Macroscopically the pancreas had a tumour at the tail of the pancreas. A swollen abdomen could be indicative of PDAC following inflammation or hepatomegaly related to multiple liver metastases.

Overall median survival for KC and KC;iASPP$^{-/-}$ mice was 267 and 165 days respectively, whilst KPC median survival was 117 days (Figure 6.1A). The majority of mice were electively culled in KC, KPC, and KC;iASPP$^{-/-}$ cohorts. Approximately 60% of KC and KC;iASPP$^{-/-}$ were culled due to being unwell (thin, hunched, rapid

breathing, hypomobility, or ascites). KC;iASPP$^{-/-}$ mice had significantly reduced overall survival compared to KC mice (P = 0.0002), but not as reduced as KPC (P = 0.0019) (Figure 6.1B).

Primary tumour was diagnosed as either macroscopic tumour at death or culling, or subsequent PDAC diagnosis following histological evaluation. Median primary tumour-free survival was significantly different at 358 and 211 days for KC and KC;iASPP$^{-/-}$ mice respectively (P = 0.0013) (Figure 6.1C). Earlier death in KC;iASPP$^{-/-}$ with primary disease supports iASPP suppressing tumour onset. Similarly, the KC;iASPP$^{-/-}$ survived significantly longer than KPC mice with primary PDAC tumour at 211 and 123 days respectively (P = 0.0015) (Figure 6.1D).

A

Mouse Genotype	N =	Median Survival (Days)	Mouse Fate			Cause of Death		
			Elective Cull	Found Dead	Alive	Unwell	Lesion/Mass	Unknown
KC	40	267	35 (88%)	4 (10%)	1 (2%)	23 (59%)	12 (31%)	4 (10%)
KC;iASPP$^{-/-}$	34	165	34 (100%)	0 (0%)	0 (0%)	20 (59%)	14 (41%)	0 (0%)
KPC	23	117	20 (87%)	3 (13%)	0 (0%)	4 (18%)	16 (73%)	2 (9%)

B

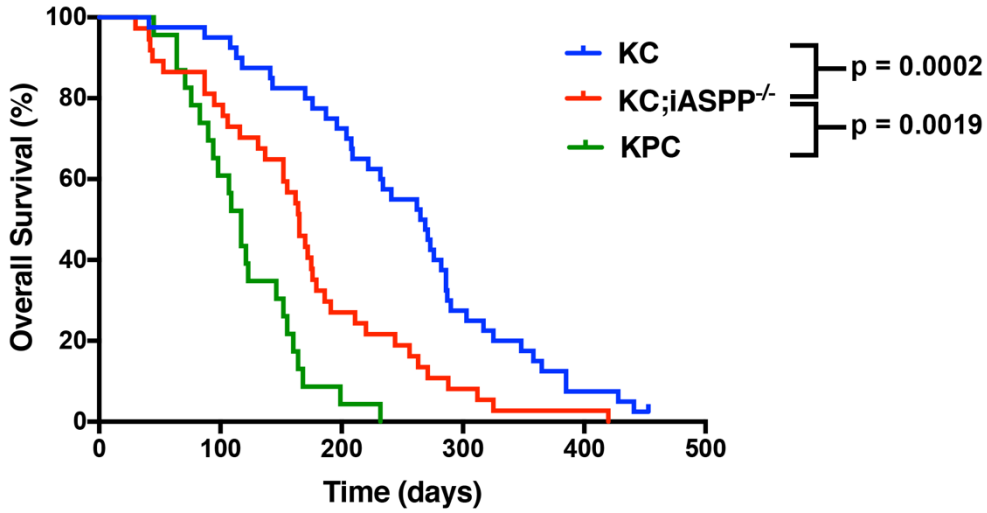

C

Mouse Genotype	Primary Tumor Incidence		Median Survival (Days)
	Primary Tumour	No Primary Tumour	
KC	13 (41%)	19 (59%)	358
KC;iASPP$^{-/-}$	16 (47%)	18 (53%)	211
KPC	10 (56%)	8 (44%)	123

D

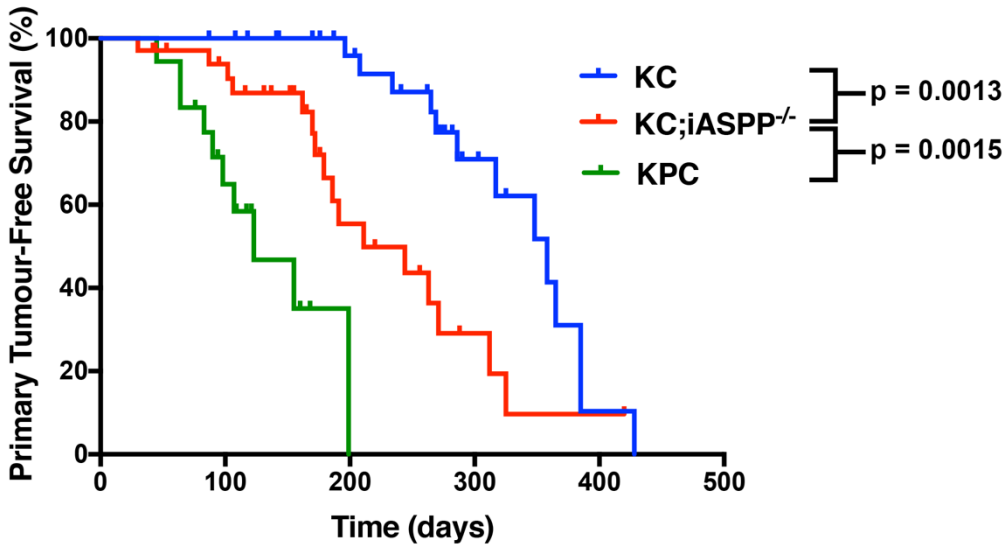

Figure 6.1 Reduced survival in KC;iASPP$^{-/-}$ relative to KC with accelerated primary PDAC

A Median overall survival of KC, KC;iASPP$^{-/-}$, and KPC mice, number of mice counted, mouse fate (culled/found dead/alive) and cause of death.

B Kaplan-Meier analysis of KC (n=40), KC;iASPP$^{-/-}$ (n=34), and KPC (n=23).

C Primary tumour incidence on the basis of macroscopic or histological diagnosis, with median primary tumour-free survival.

D Kaplan-Meier analysis of primary tumour-free survival in KC (n=13), KC;iASPP$^{-/-}$ (n=16), and KPC (n=10) mice.

6.2 KC;iASPP$^{-/-}$ mice have accelerated metastasis *in vivo*

KC;iASPP$^{-/-}$ mice had a reduced median survival and earlier incidence of primary PDAC relative to KC mice. As discussed earlier in chapter 4.5, in human PDAC 70% of deaths occur with widespread metastatic disease. To evaluate whether KC;iASPP$^{-/-}$ also have a significant burden of metastatic disease, I evaluated the occurrence of metastases at necropsy in the KC, KC;iASPP$^{-/-}$ and KPC cohorts. KC;iASPP$^{-/-}$ had a lower incidence than KC of metastatic PDAC at 35% and 50% respectively (Figure 6.2A). However, median survival of mice with metastases at death was lower in KC;iASPP$^{-/-}$ than KC mice at 271 and 317 days respectively, although not significantly different. Metastases were found in a greater proportion in the lung rather than liver in the KC;iASPP$^{-/-}$ cohort relative to the KC cohort. Metastasis-free survival was could not be determined for the KPC cohort due to the low incidence of metastasis identified at post-mortem (Figure 6.2B).

The KC;iASPP$^{-/-}$ cohort were bred with a EYFP (YFP) marker enabling the confirmation that metastases were of Pdx1-expressing cell origin. In an example of a 6-week old mouse with early metastases there was no evidence of primary PDAC, only a few small areas of high-grade PanIN (Figure 6.2C). Pancreas IHC YFP staining confirmed lesions with IHC-negative surrounding stroma. In the lung, a large cystic area of metastatic disease took up most of right lung. Lung IHC YFP staining confirmed widespread positivity with negative areas representing stromal reaction.

iASPP-deficiency in the KC mouse model of PDAC accelerates the onset of primary PDAC and metastatic disease with a reduced median survival compared to the KC cohort. KPC has significantly lower median survival than KC;iASPP$^{-/-}$ suggesting homozygous loss of iASPP does not equate to as severe phenotype as the heterozygous p53 point mutation at R172H. This phenotype would be consistent with iASPP suppressing at least one process in the ADM-PanIN-PDAC progression.

A

Mouse Genotype	Metastasis Status		Metastatic Median Survival (Days)	Metastasis Location		
	Metastasis	No Metastasis		Lung	Liver	Other
KC	16 (50%)	16 (50%)	317	5/16	12/16	1/16
KC;iASPP$^{-/-}$	12 (35%)	22 (65%)	271	8/12	4/12	1/12
KPC	4 (22%)	14 (78%)	Undefined	3/4	1/4	0/4

B

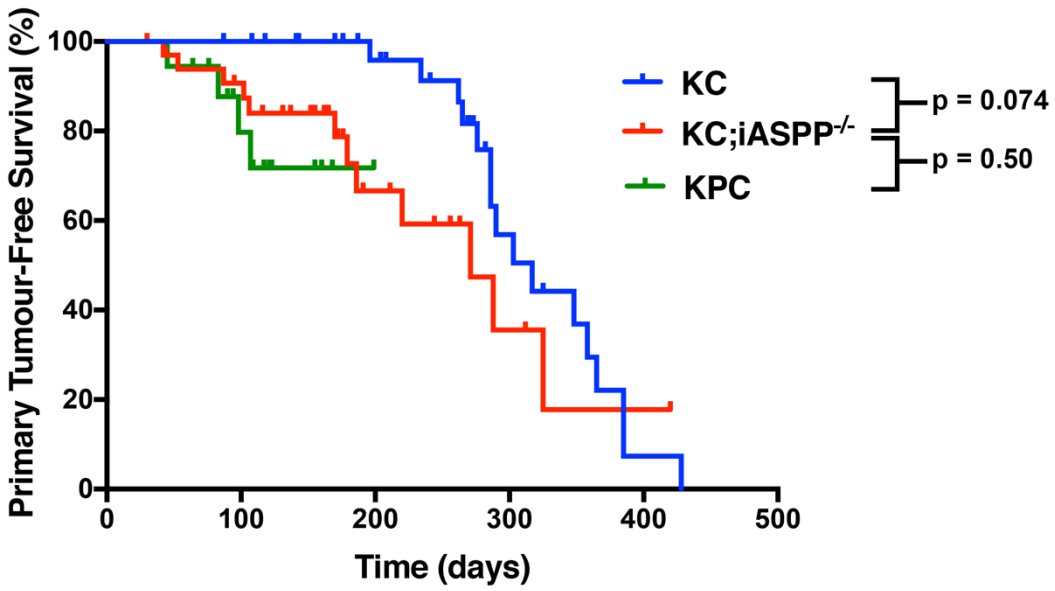

C

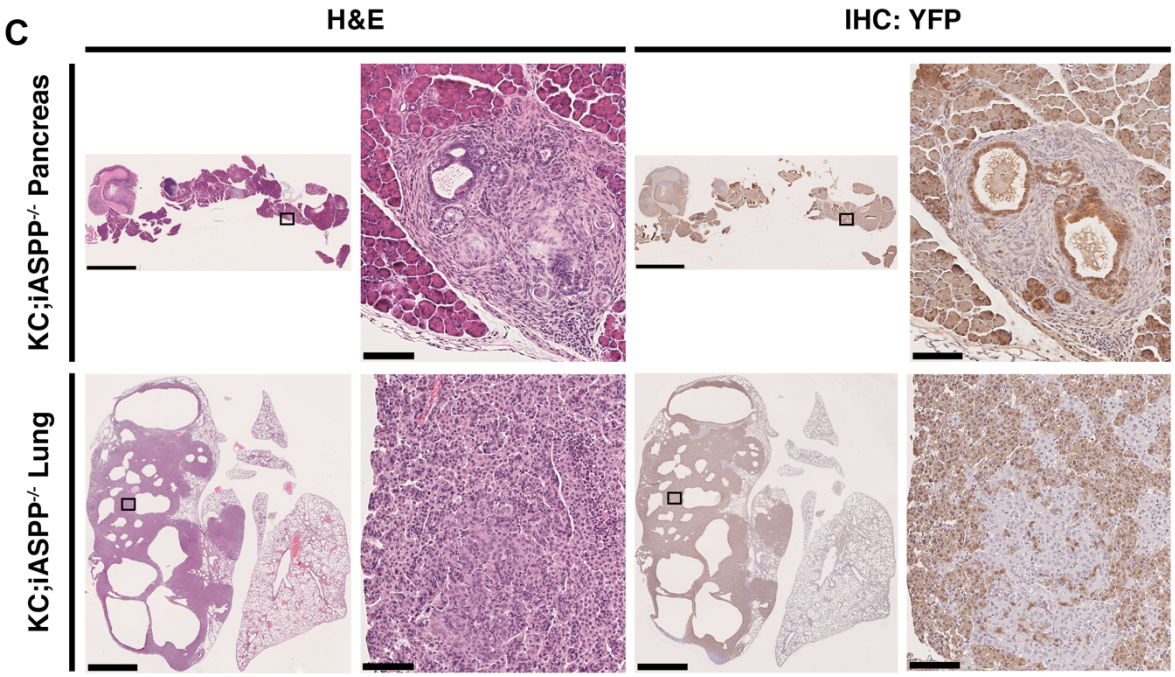

Figure 6.2 KC;iASPP$^{-/-}$ mice have accelerated metastasis relative to KC

A Metastasis status of KC, KC;iASPP$^{-/-}$ and KPC mice, median survival with metastatic disease and metastasis location.

B Kaplan-Meier analysis of KC (n=16), KC;iASPP$^{-/-}$ (n=12) and KPC (n=4) cohorts with confirmed metastatic disease at death.

C Representative pancreas and lung sections of 6-week old KC;iASPP$^{-/-}$ (EYFP/EYFP) mouse culled with rapid breathing and poor growth. Whole

organ H&E and IHC for YFP in pancreas and lung sections. Scale bar 2.5 mm. Inset sections of high-grade pancreas (upper) and metastatic tumour (lower). Scale bar 100 μm.

6.3 iASPP-deficient acini have reduced ADM efficiency driven by oncogenic Kras and TGFα

Evidence from the KC mouse model that loss of iASPP accelerates both primary and metastatic PDAC suggests iASPP suppresses PDAC tumorigenesis. Early onset of KC;iASPP$^{-/-}$ PDAC, seen as soon as 6 weeks, suggests the suppression occurs at either the level of ADM or early PanIN stages. To investigate if loss of iASPP makes ADM more efficient in response to either TGFα or oncogenic Kras, I utilized the *ex vivo* acinar-to-ductal metaplasia assay as in Chapter 4.6 (Figure 6.3A). In the wild-type (Pdx1-Cre+) and iASPP$^{-/-}$ mice there is a less than 10% efficiency of ADM (Figure 6.3A). However, the iASPP$^{-/-}$ acini stimulated with TGFα have a lower average ADM efficiency and greater range of metaplasia (Figure 6.3A). KC acini, either with or without TGFα, achieve expected ADM efficiency (83 and 84% respectively) within the 70 to 90% rates reported in the literature (Shi et al. 2013). However, KC;iASPP$^{-/-}$, with or without TGFα, had reduced ADM efficiency (38 and 39% respectively) (Figure 6.3B).

Loss of iASPP suppressing ADM would be inconsistent with an accelerated PDAC phenotype. ADM is stimulated by similar factors that promote PanINs and progression of PDAC, such as TGFα, EGF, and IL-1α. Central to ADM is activation of the MAPK/ERK pathway, with evidence from ADM from oncogenic Kras possessing mice, that is blocked by either EGFR or ADAMTS17 knockout or stimulated by overexpression of TGFα (Ardito et al. 2012; Means et al. 2005). However, the phenotype is consistent with the developmental iASPP phenotype that links the wa1, wa2, wa3 and woe mouse phenotypes seen in mice. Wa-3

phenocopies wa1 and wa2, TGFα and EGFR mutants, that share an eyes open at birth phenotype. Therefore, the iASPP *ex vivo* phenotype is consistent with an oncogenic role for iASPP. However, iASPP-deficiency in the KC mouse significantly accelerates PDAC and metastases *in vivo* suggesting a non-cell autonomous mechanism in accelerating PDAC.

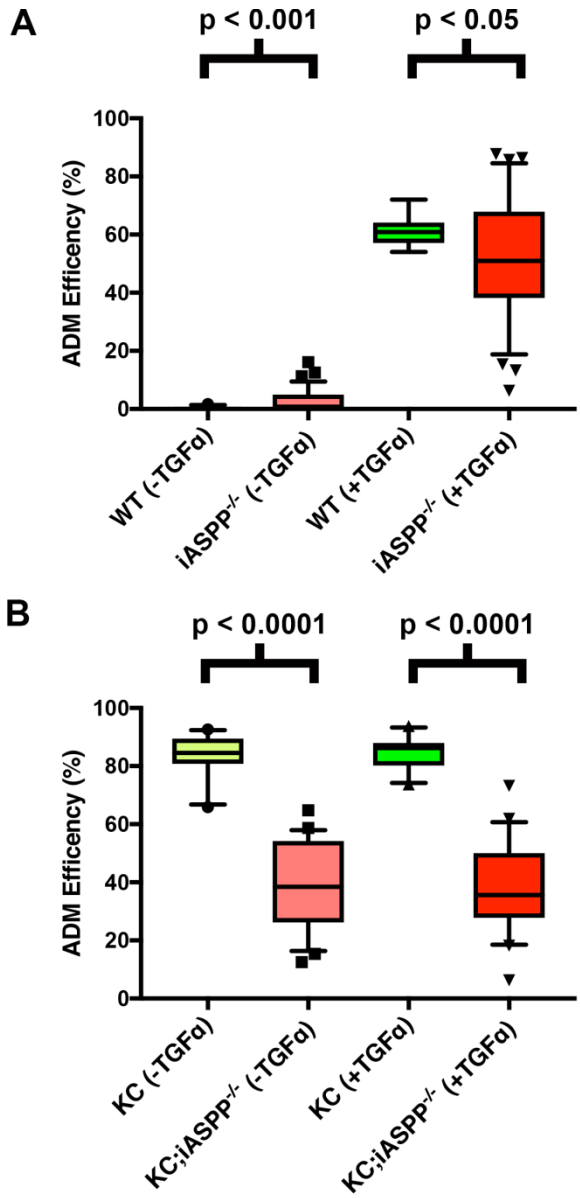

Figure 6.3 iASPP is required for efficient acinar-to-ductal metaplasia

A Plot of ADM efficiency with and without TGFα stimulation in acini obtained from iASPP; Pdx1-Cre. Symbols represent data points outside the plotted 10-90% error bars.

B Plot of ADM efficiency with and without TGFα stimulation in acini obtained from KC and KC;iASPP$^{-/-}$. Symbols represent data points outside the plotted 10-90% error bars.

6.4 iASPP suppresses ADM driven by inflammation and oncogenic Kras

In vivo loss of iASPP accelerates the onset of mPDAC and reduces median survival of KC;iASPP$^{-/-}$ mice relative to KC mice. However, *ex vivo* both TGFα stimulated iASPP-deficient acini (iASPP$^{-/-}$) and KC;iASPP$^{-/-}$ acini are less efficient at ADM than wild-type iASPP expressing controls. Previous papers utilizing the *in vivo* and *ex vivo* models to demonstrate an effect of genetic deletion of a protein usually have congruous results, such as Sox9 and EGFR/ADAMTS17 (Ardito et al. 2012; Kopp et al. 2012). The ADM assay results are consistent with the iASPP$^{\Delta 8/\Delta 8}$ developmental phenotype of eyelids open at birth that suggests a hypoactivated EGFR/ TGFα-MAPK/ERK pathway. The iASPP$^{\Delta 8/\Delta 8}$ mouse demonstrated profound ADM following a short course of mild-moderate inflammation with recovery. Therefore, I hypothesized that regulation of inflammation, such as caerulein-induced pancreatitis, is the mechanism by which iASPP suppresses ADM and PanIN development that progresses to PDAC.

I exposed the KC and KC;iASPP$^{-/-}$ mice to weekly single injections of caerulein (250 μg/Kg) over four weeks in order to assess the effect of a mild-moderate inflammatory stimuli on oncogenic Kras mediated ADM (Figure 6.4A). The KC mouse had a small number of ADM foci post-caerulein, with the majority of pancreatic tissue normal acini (Figure 6.4B). In contrast, the KC;iASPP$^{-/-}$ post-caerulein mouse pancreas demonstrates almost complete loss of normal acini, replaced with areas of ADM and mPanIN. Furthermore, the KC;iASPP$^{-/-}$ pancreas has widespread infiltration of immune cells and fibrosis. Immunohistochemical staining for cytokeratin 19 demonstrates the extensive nature of the KC;iASPP$^{-/-}$

ADM. At planned culling date, a lung metastasis was noted at necropsy, confirmed by multiple cysts and diffuse YFP and CK19 positive staining (Figure 6.4C).

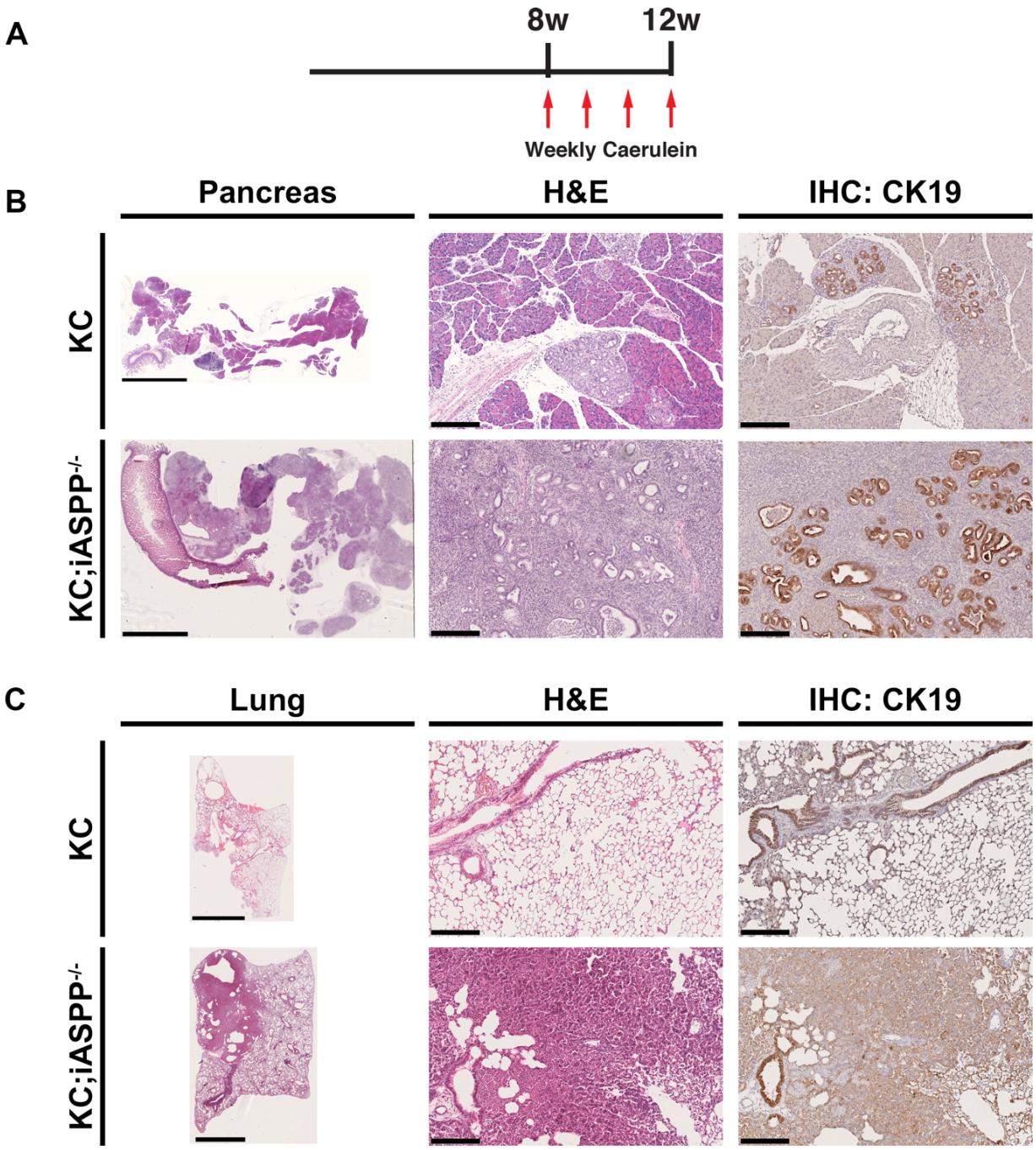

Figure 6.4 iASPP suppresses inflammation-driven ADM and PanINs

A Injection schedule. KC and KC;iASPP$^{-/-}$ mice were injected with weekly single dose caerulein for 4 weeks.

B Representative H&E whole pancreas section (scale bar 2.5 mm), H&E section, middle panel (scale bar 250 μm), and immunohistochemical staining for cytokeratin 19, right panel (scale bar 250 μm) for 12-week old KC and KC;iASPP$^{-/-}$ mice.

C Representative H&E lung lobe sections (scale bar 2.5 mm), H&E section, middle panel (scale bar 250 μm), and immunohistochemical staining for cytokeratin 19 right panel (scale bar 250 μm) for 12-week old KC and KC;iASPP$^{-/-}$ mice.

6.5 iASPP suppression of inflammation-driven ADM and PanIN formation is not due to aberrant regeneration

Inflammation is the critical mediator of accelerated ADM in the iASPP-deficient oncogenic Kras mice. Absence of an *ex vivo* TGFα-stimulated phenotype is against a cell-autonomous mechanism for ADM. I hypothesized that the iASPP-deficient mice are hypersensitive to inflammation-driven ADM, due to intrinsically greater plasticity compared to iASPP wild-type tissue or are maintained in a more dedifferentiated state. However, an alternative theory would be the indirect hyperactivation of the immune system and microenvironment by the iASPP-deficient cells, a state not appreciable in an *ex vivo* system.

Accelerated primary and metastatic PDAC with the loss of iASPP does not appear to be at the level of ADM resulting from increased activation of the MAPK by either oncogenic Kras or TGFα. Experimentally, oncogenic Kras progression to PDAC is accelerated *in vivo* by inflammatory stress. As previously shown, the iASPP$^{\Delta 8/\Delta 8}$ mouse exhibit almost complete loss of normal acini and conversion to a ductal morphology following acute inflammation. Therefore, I investigated the role of chronic, low level inflammatory stress, induced by weekly injections of caerulein on the phenotype of KC and KC;iASPP$^{-/-}$ mice.

Six single weekly injections of 250 μg/Kg caerulein were performed on mice from 6-weeks of age, performed in parallel with littermates from the KC and KC;iASPP$^{-/-}$ colonies. Three- and ten-week time points after the last injection were used to allow for acute inflammatory effects to resolve and to analyse the phenotypic

changes in the tissue (Figure 6.5A). At 10-weeks following last injection there is phenotypically no difference between Pdx1-Cre only and iASPP$^{-/-}$ tissue. No ADM was evident and no vacuoles nor necrosis were present (Figure 6.5B).

After 3-weeks recovery KC;iASPP$^{-/-}$ have significantly more areas of ADM with numerous PanINs present. Prominent dense stroma accompanies areas of metaplasia and there is considerable immune cell infiltration. After 10-weeks recovery KC mice have large areas of normal acinar morphology, interspersed with small collections of ADM and PanINs with one area of high-grade PanIN. At 10-weeks recovery, KC;iASPP$^{-/-}$ mice have almost complete loss of normal acini. The bulk of the pancreas is stromal tissue and immune cell infiltrates and there are multiple areas of high-grade lesions (Figure 6.5C).

Consistent with the role in the iASPP$^{\Delta 8/\Delta 8}$ mouse, inflammation in the KC;iASPP$^{-/-}$ model accelerates ADM and PanIN formation. The sparse ADM and PanIN cellularity relative to the stroma and immune cell infiltrates suggest that iASPP-deficiency facilitates an exaggerated inflammatory response to caerulein mediated inflammation, even after a short intermittent injecting schedule.

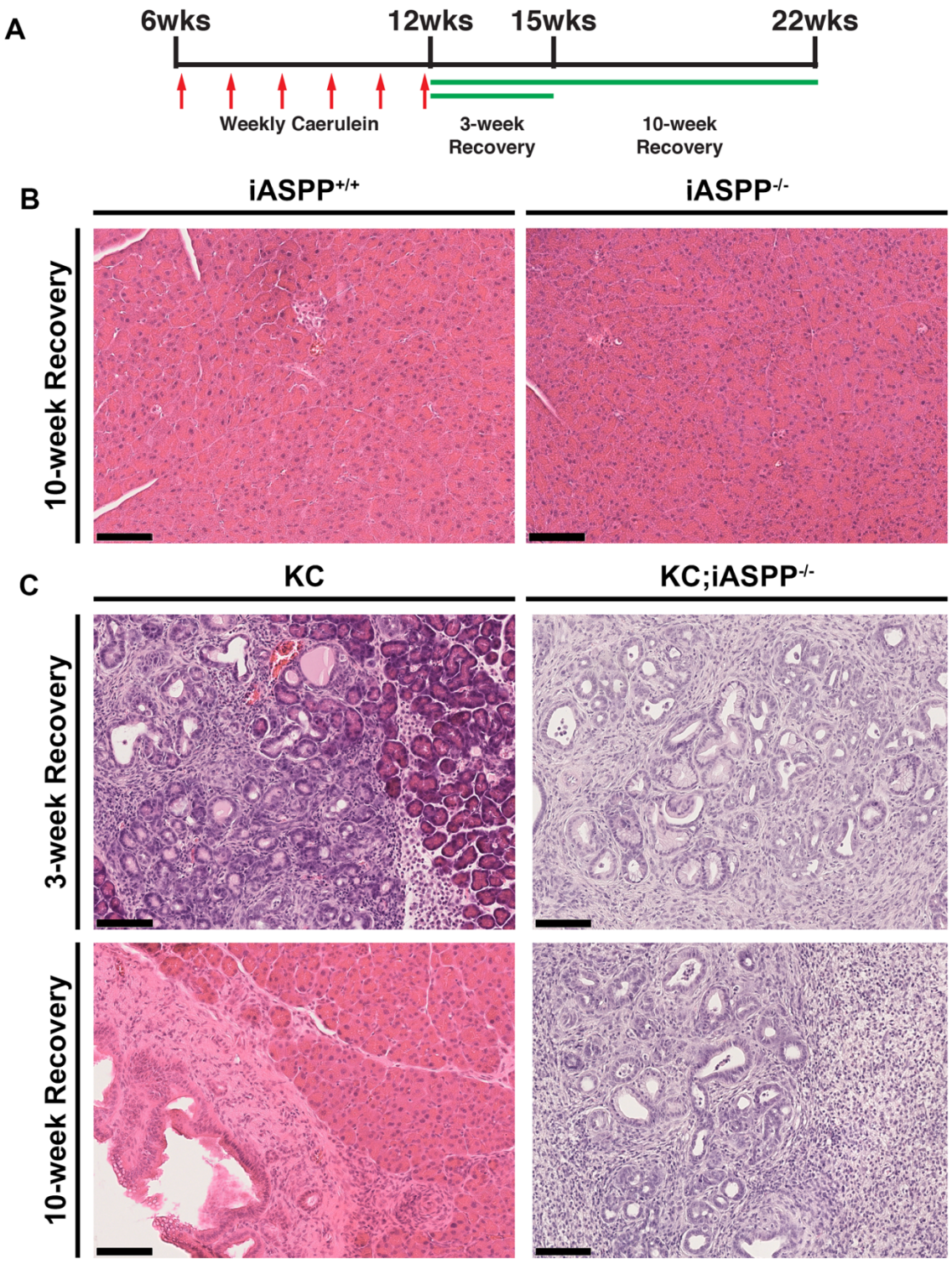

Figure 6.5 iASPP suppresses oncogenic Kras ADM in response to inflammation

A Injection and recovery schedule. Weekly injection of caerulein 250μg/Kg between 6- and 12-weeks of age.

B Representative H&E sections of Pdx1-Cre only and iASPP$^{-/-}$ pancreas following 6 weekly caerulein injections and 10-weeks recovery. Scale bar 100 μm.

C Representative H&E sections of KC and KC;iASPP$^{-/-}$ pancreas following 6-weekly caerulein injections after 3- and 10-weeks recovery. Scale bar 100 μm.

6.6 KC and KC;iASPP$^{-/-}$ ADM and mPanINs do not significantly differ in senescence, apoptosis and proliferation

Accelerated ADM and PanINs in KC;iASPP$^{-/-}$ following inflammation suggested that the acini, ADM or PanINs may respond to inflammatory stress differently in iASPP-deficient tissue in terms of dedifferentiation (to facilitate metaplasia), bypassing of senescence, apoptosis and proliferation. Pdx1 is required embryonically in pancreatic development is upregulated in PDAC. Overexpression of Pdx1 can promote ADM. Pdx1 is upregulated in the dedifferentiation of acini to facilitate the reprogramming and metaplasia to a ductal morphology. I first established that Pdx1 is ubiquitously expressed in the metaplastic ducts KC and KC;iASPP$^{-/-}$ mice following inflammation (Figure 6.6A). To evaluate senescent cells, a barrier to progression to PDAC, p21 staining was used. Few cells were positive for p21 in either KC or KC;iASPP$^{-/-}$ tissue (Figure 6.6B). Following inflammation p53 is positive in the majority of ADM and PanIN cells (Figure 6.6C). As iASPP is an inhibitor of p53-mediated apoptosis, staining for cleaved-caspase 3 an effector of apoptosis was performed. Cleaved-caspase 3 positivity was noted in ADM and PanINs without a clear increase in KC;iASPP$^{-/-}$ (Figure 6.6D). Finally, proliferation was assessed with Ki67 expression, and no difference in ADM or PanIN positivity was found (Figure 6.6E). In conclusion, there is no clear difference in the differentiation state, senescence, proliferation, and apoptosis.

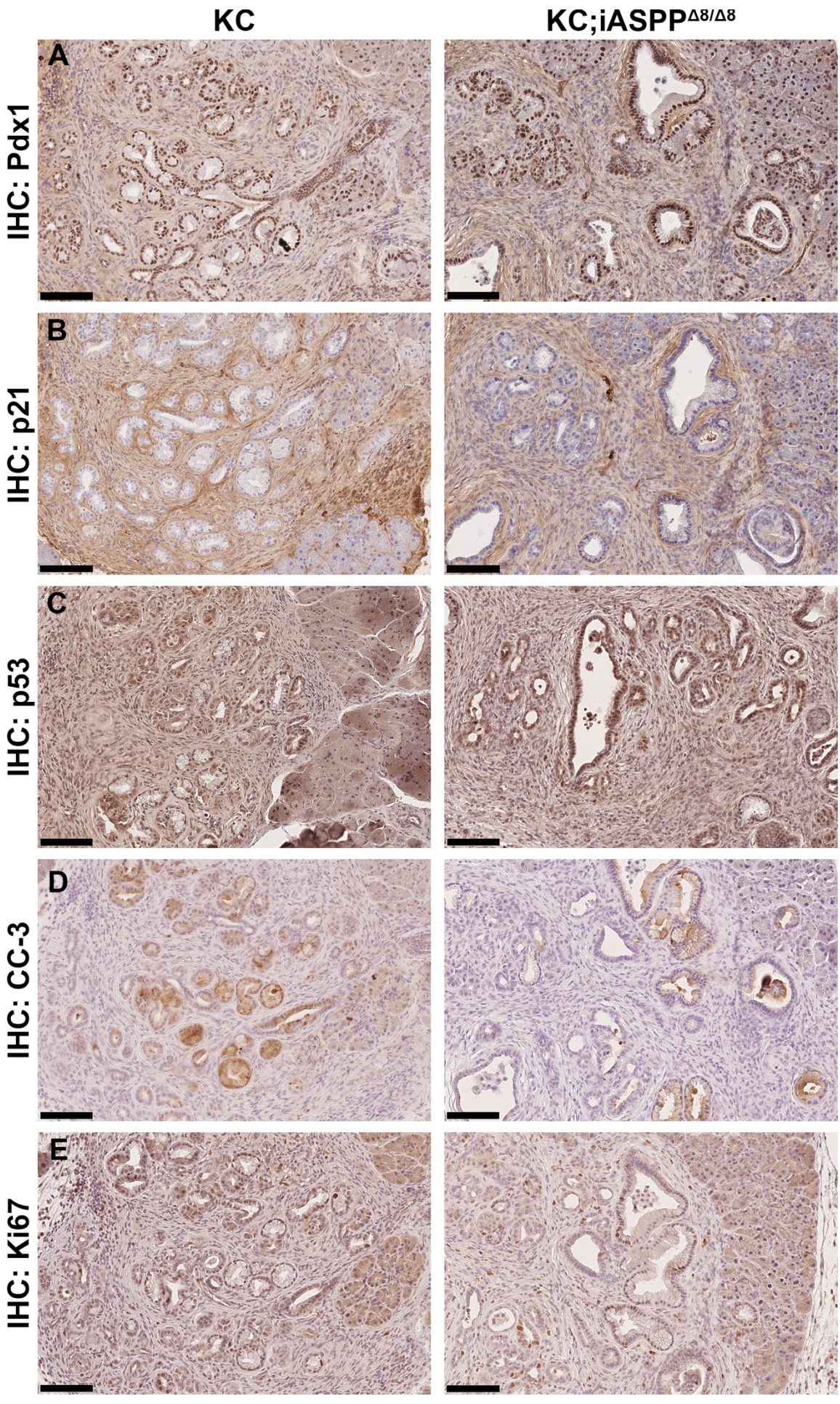
KC
KC;iASPP$^{\Delta 8/\Delta 8}$
A
IHC: Pdx1
B
IHC: p21
C
IHC: p53
D
IHC: CC-3
E
IHC: Ki67

Figure 6.6 iASPP metaplasia and PanIN lesions do not have a senescence, apoptotic or proliferation phenotype

A IHC for Pdx1, marker of acinar dedifferentiation, in a representative tissue sample (n=3). Scale bar 100 μm.
B IHC for p21, marker of cellular senescence, in a representative tissue sample (n=3). Scale bar 100 μm.
C IHC for p53, regulator of senescence and apoptosis, in a representative tissue sample (n=3). Scale bar 100 μm.
D IHC for cleaved-caspase 3, a marker of apoptosis, in a representative tissue sample (n=3). Scale bar 100 μm.
E IHC for Ki67, marker of proliferation, in a representative tissue sample (n=3). Scale bar 100 μm.

6.7 iASPP mRNA expression correlates with NF-κB, cytokeratin-19 and TGFα, markers of poor prognosis

iASPP is rarely mutated in human cancer, but iASPP expression is frequently correlated with poor prognosis. Invariably, high iASPP associates with poorer prognosis than low iASPP expression, typically assessed by immunohistochemical intensity scoring. Large-scale human cancer sequencing projects are publicly accessible and some report mRNA expression levels alongside genetic changes such as mutations, deletions and amplifications. Interrogating these databases enables the association of specific gene expression or pathway alterations. To establish whether iASPP expression associates with key proteins involved in inflammation and metaplasia in human PDAC, the 185 patient TCGA pancreatic adenocarcinoma RNA-Seq database was interrogated via cBioportal. 2764 genes had a correlation greater than 0.3 or less than -0.3 for both Pearson's and Spearman's correlation. 1099 genes were positively correlated and 1665 were negatively correlated.

High expression of p65 is associated poor prognosis as are higher levels of NF-κB gene target transcription (Weichert et al. 2007). I found that the mRNA levels of NF-κB family members *RELA* and *RELB*, encoding p65 and RelB respectively, correlate with iASPP mRNA (Spearman's correlation 0.6 and 0.42 respectively) (Figure 6.7A and B). *TGFA*, encoding TGFα, also positively correlates with iASPP expression (Spearman's correlation 0.54) (Figure 6.7C). TGFα is a soluble factor that binds the EGF receptor, potentiates oncogenic Kras MAPK/ERK pathway activation. Overexpression of TGFα in transgenic mice induces hyperplasia in the

intestine and liver, metaplasia of acinar cells to ductal morphology and carcinoma of the breast (Sandgren et al. 1990). In human pancreatic cancer, TGFα expression associates with poor prognosis. Interestingly, waved-1 (wa1) mice contain a mutation in TGFα and share the same waved hair phenotype of the waved-3 (wa3) containing an iASPP mutation. iASPP-deficient acini are less efficient at undergoing ADM in response to TGFα than iASPP-wild-type acini. Cytokeratin 19, encoded by *KRT19*, expression defines the ductal component of the pancreas and is expressed in cells that have undergone ADM and is expressed PanINs and PDAC. Cytokeratin 19 expression in human PDAC associates with poor prognosis (Yao et al. 2017). iASPP mRNA expression is correlated with cytokeratin 19 mRNA (Spearman's correlation 0.75) (Figure 6.7D).

SMAD4 is a transcription factor that regulates the expression of genes related to proliferation and differentiation, functioning as an effector of TGFβ signalling. SMAD4 is frequently truncated and mutated in PDAC with an incidence over 20% cases and SMAD4 expression is associated with good prognosis (Bailey et al. 2016; Shugang et al. 2016). iASPP expression is negatively correlated with SMAD4 expression (Spearman's correlation -0.6) (Figure 6.7E). *BCL2*, encoding Bcl-2, is a transcriptional target of NF-κB and functions as an inhibitor of apoptosis, as is iASPP. In contrast to the antiapoptotic, and therefore proto-oncogenic function, Bcl-2 expression, associated with favourable prognosis in PDAC (Smith et al. 2011), is negatively correlated with iASPP mRNA expression (Spearman's correlation -0.5) (Figure 6.7F).

iASPP expression correlates with other proteins associated with poor prognosis, while being negatively correlated with markers of good prognosis. Theoretically, iASPP may be marker of a poor prognostic cancer and functions to suppress the deregulated mechanisms that result in increased tumourgenicity.

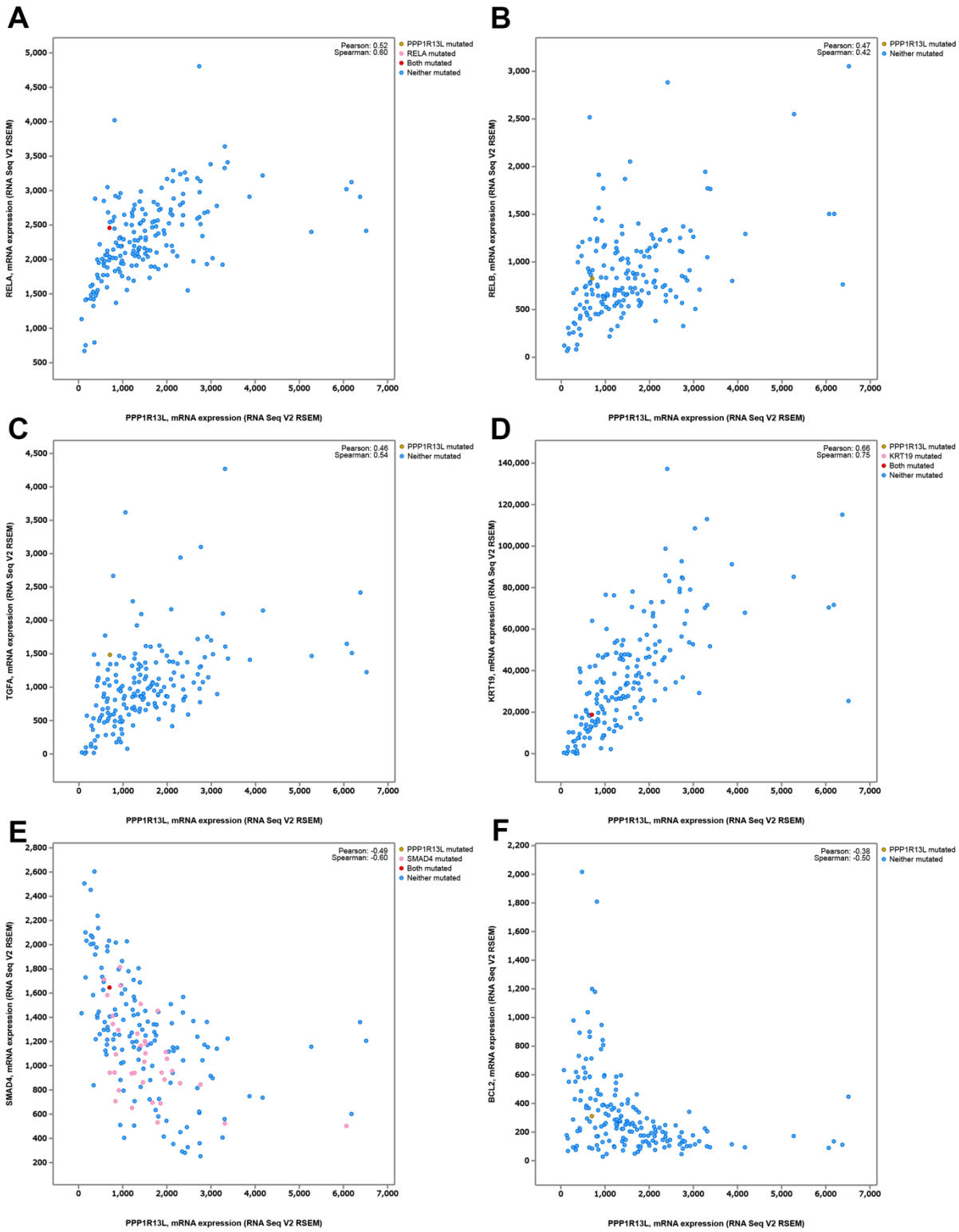

Figure 6.7 iASPP mRNA expression correlates with poor prognosis markers RELA, TGFα and Cytokeratin 19 in human PDAC

A RELA mRNA levels correlated to iASPP mRNA levels.
B RELB mRNA levels correlated to iASPP mRNA levels.
C TGFα mRNA levels correlated to iASPP mRNA levels.
D KRT19 mRNA levels correlated to iASPP mRNA levels.
E SMAD4 mRNA levels correlated to iASPP mRNA levels.
F BCL2 mRNA levels correlated to iASPP mRNA levels.

6.8 iASPP expression associates with altered inflammatory mediator expression

Correlating iASPP mRNA expression to markers of poor prognosis suggests iASPP responds to a pro-tumorigenic or poor prognostic cancer state. The KC;iASPP$^{-/-}$ mouse demonstrates accelerated tumorigenesis, that is potentiated by inflammation. Consequently, I further interrogated the TCGA pancreatic adenocarcinoma RNA-Seq database in order to characterise whether iASPP expression correlates with markers of inflammation.

Inflammation mediated by IL-1 signalling is central to inflammatory disorders and cancers, including pancreatic cancer. It is proposed that Kras^{G12D} activates AP-1 and induces IL-1α to activate NF-κB and its target gene IL-1α (Ling et al. 2012). IL-1α can be amplified by this feedforward mechanism, potentially explaining the progressive NF-κB dysregulation that occurs with PanIN to PDAC progression. IL-1α overexpression correlates with NF-κB activity and poor prognosis. IL-1 Receptor Antagonist (IL-1RA), encoded by the *IL-1RN* gene, inhibits NF-κB activation (Zhuang et al. 2016). I found that iASPP expression correlates with IL1RN expression (Spearman's correlation 0.5) (Figure 6.8A). Conversely, *IL1R1*, encoding IL-1 Receptor 1, is negatively correlated with iASPP mRNA (Spearman's correlation -0.39) (Figure 6.8B). IL-1R1 is required for the activation of NF-κB and expression of pro-inflammatory genes in response to IL-1α and IL-1β binding. Taken together high iASPP expression correlates with mechanisms that would reduce flux through the IL-1 pathway.

IL-6 cytokine signalling is required for the maintenance and progression of PanINs, while IL-6 ablation prevents cancer progression (Zhang et al. 2013). Oncogenic Kras mice with IL-6$^{-/-}$ have accelerated acinar cell recovery and proliferation following inflammation. IL-6 is a proinflammatory cytokine that upon binding IL-6 receptor (IL-6R) forms the IL-6/IL-6R complex that recruits glycoprotein 130 (gp130) classically. *IL6ST* encodes gp130, which forms a hexameric complex with two IL-6, two IL-6R, and two gp130 subunits. IL-6R may also exist in a soluble form, sIL-6R, which can elicit trans-signalling when bound to IL-6 though ubiquitous expression of gp130 (Yao et al. 2014). IL-6 signalling activates JAK-STAT, MAPK and PI3K-AKT, all pathways crucial for PDAC development. I found that iASPP is negatively correlated with IL6R and IL6ST mRNA expression (Spearman's correlation -0.46 and -0.45 respectively) (Figure 6.8C and D).

CXCL12, predominantly expressed by stromal cells, can bind CXCR4 expressed on PanINs and PDAC to activate both the PI3K-Akt and MAPK pathway. Active Akt and ERK result in the phosphorylation and destabilization of IκBα to promote nuclear NF-κB accumulation and transactivation of downstream targets genes such as sonic hedgehog (Singh et al. 2012). I found that iASPP is negatively correlated with CXCL12 mRNA expression (Spearman's correlation -0.46) (Figure 6.8E). IL-33 belongs to the IL-1 cytokine family and is expressed in response to IL-1β and IFN-γ. IL-33, acting in synergy with IL-1, results in intracellular signalling cascades including NF-κB activation and subsequent IL-6 upregulation (Schmieder et al. 2012). iASPP mRNA is negatively correlated with IL-33 mRNA expression (Spearman's correlation -0.51) (Figure 6.8F).

In summary, the TCGA PDAC RNA-Seq database suggests iASPP mRNA expression in human PDAC correlates with a pro-inflammatory state. Higher mRNA expression of RELA and RELB, possibly a marker of a chronically NF-κB dysregulated state, correlates with iASPP mRNA. A negative correlation with proinflammatory interleukin signalling mechanisms for IL1 (↑IL-1RN, ↓IL-1R1, and ↓IL33) and IL-6 (↓IL6R and ↓IL6ST) may suggest higher iASPP mRNA exists in a cytokine abundant state. For comparison, no equivalent correlates exist for ASPP2 or p53 using the same database (data not shown). Relative high iASPP mRNA expression may represent a response to a proinflammatory pancreatic cancer subtype.

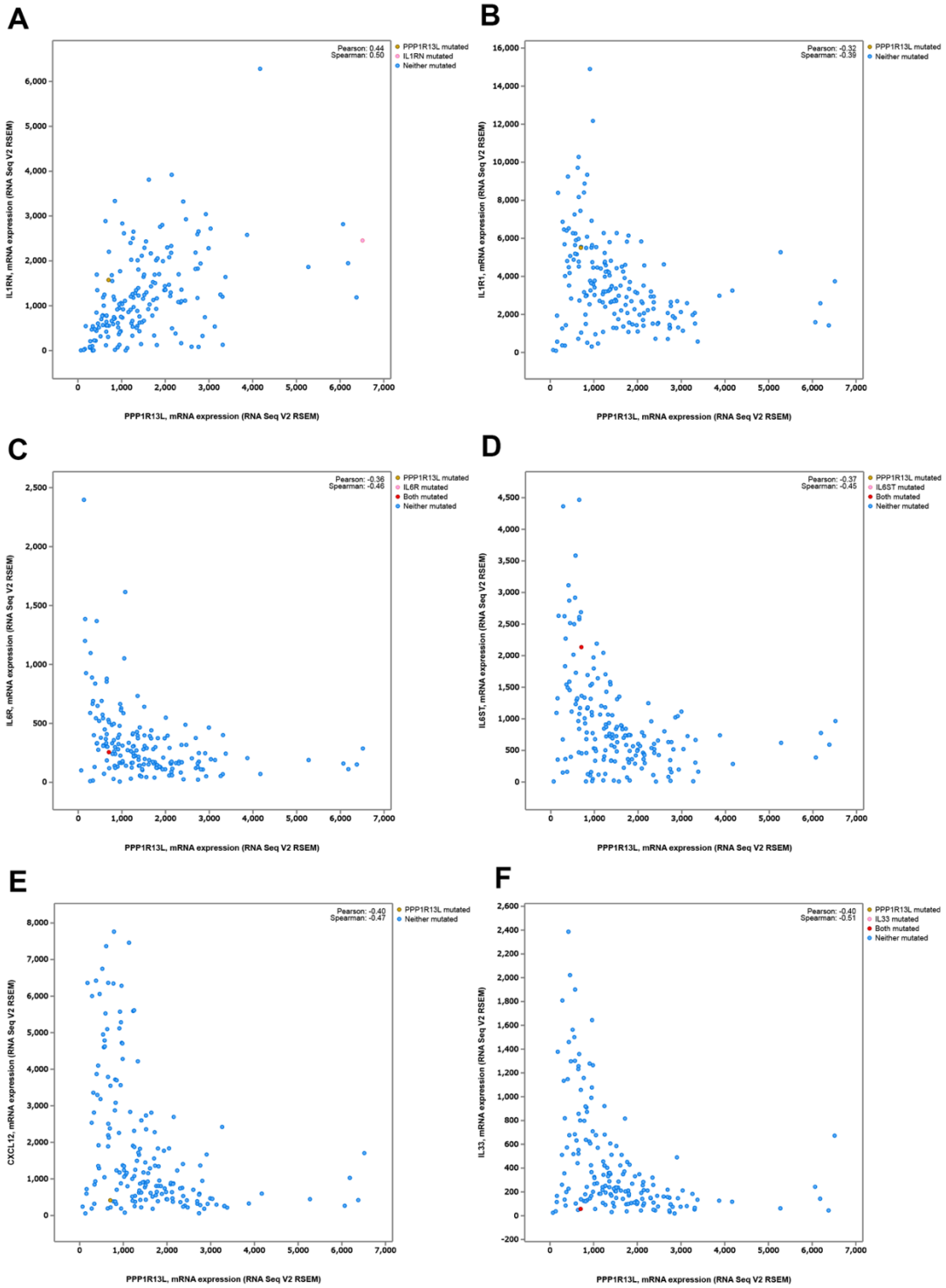

Figure 6.8 Comparison of iASPP mRNA levels with interleukin and cytokine signalling mediators of inflammation

A IL1RN mRNA levels correlated to iASPP mRNA levels.
B IL1R1 mRNA levels correlated to iASPP mRNA levels.
C IL6R mRNA levels correlated to iASPP mRNA levels.
D IL6ST mRNA levels correlated to iASPP mRNA levels.
E CXCL12 mRNA levels correlated to iASPP mRNA levels.
F IL33 mRNA levels correlated to iASPP mRNA levels.

6.9 KC;iASPP$^{-/-}$ mice following inflammation have upregulated p53, RelA p65 and GSDME

A proinflammatory iASPP-deficient mechanism that is potentiated by pancreatitis to accelerate KC;iASPP$^{-/-}$ tumorigenesis is consistent with the *in vivo* and *ex vivo* findings presented. Therefore, I speculated that p53, RelA/p65 and markers of inflammatory cell death may be altered in KC;iASPP$^{-/-}$ post-inflammation. To investigate this, weekly caerulein injected KC and KC;iASPP$^{-/-}$ mice were examined 48-hours after final caerulein injection (Figure 6.9A).

As expected, higher levels of p53 were present in the KC;iASPP$^{-/-}$ tissue (Figure 6.9B). Higher RelA p65 staining intensity was demonstrated in the KC;iASPP$^{-/-}$ pancreas, along with nuclear localisation (Figure 6.9C). RelA p65 is capable of regulating the transcription of a myriad inflammatory signalling effectors on nuclear translocation. Finally, regulator of inflammatory cell death (pyroptosis) gasdermin (DFNA5 or GSDME) is specifically upregulated in the metaplastic and PanIN lesions (Figure 6.9D). Interestingly, GSDME is cleaved by caspase-3 to mediate progression of pyroptotic cell death (Rogers et al. 2017). Pyroptosis is a cellular death process characterized by release of pro-inflammatory cytokines such as IL-1 and IL18. The inflammasome and pyroptosis has been linked to mediating cell death following pancreatitis (Hoque et al. 2011). I speculated that iASPP is a barrier to inflammatory cell death, which would explain both reduced ADM efficiency *ex vivo* and the pro-ADM and tumorigenesis phenotypes demonstrated *in vivo*.

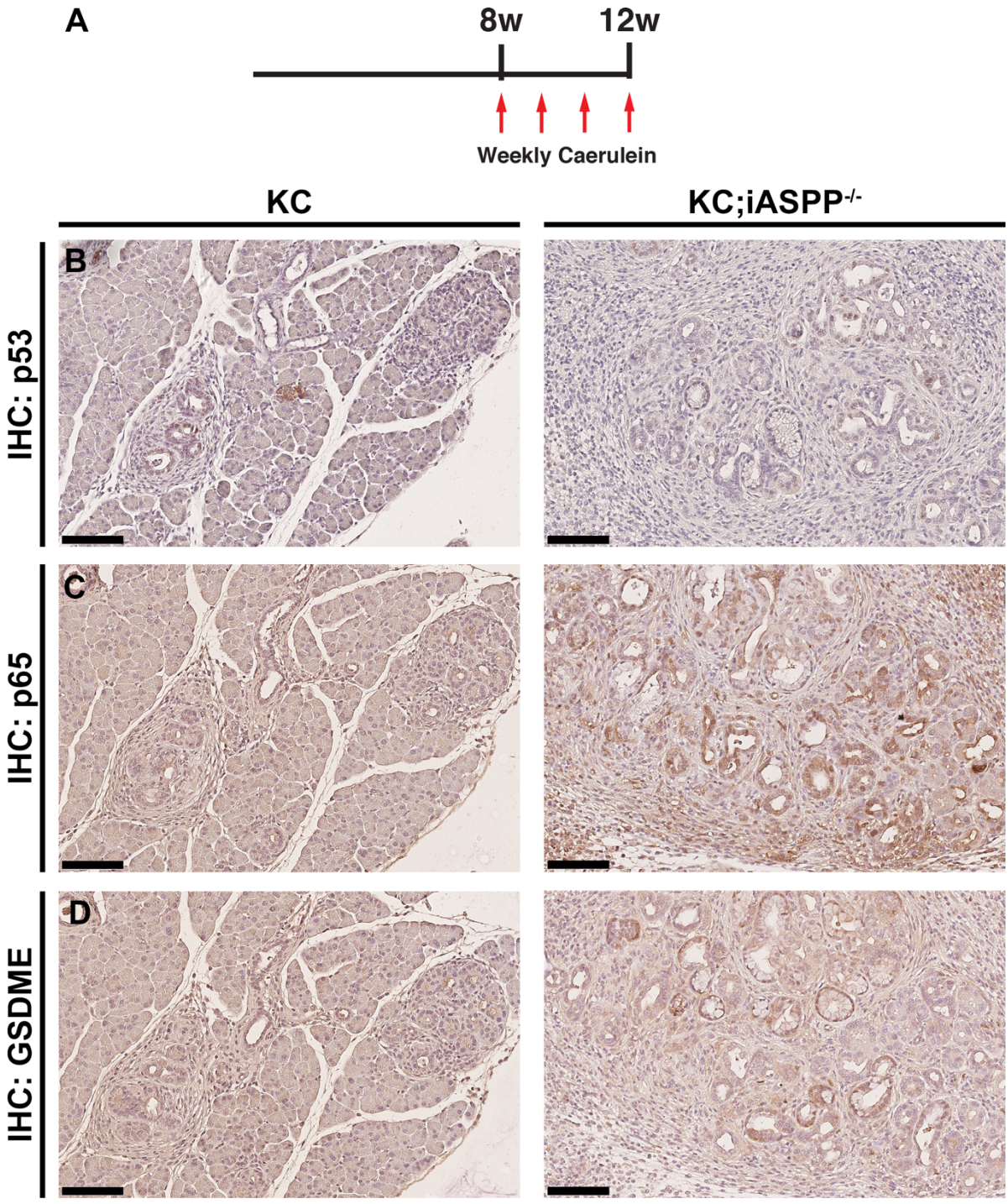

Figure 6.9 KC;iASPP$^{-/-}$ mice following inflammation have upregulated p53, RelA p65 and GSDME

A Injection schedule. KC and KC;iASPP$^{-/-}$ mice were injected with weekly single dose caerulein for 4 weeks.

B IHC for p53 in representative sections of KC and KC;iASPP$^{-/-}$ following inflammation. Scale bar 100 μm.

C IHC for p65 in representative sections of KC and KC;iASPP$^{-/-}$ following inflammation. Scale bar 100 μm.

D IHC for gasdermin (GSDME) in representative sections of KC and KC;iASPP$^{-/-}$ following inflammation. Scale bar 100 μm.

6.10 Cytokine profiling does not reveal a difference in microenvironment between KC and KC;iASPP$^{-/-}$ mice at 12-weeks

Human PDAC RNA-Seq data suggests high iASPP mRNA correlates with poor prognosis markers and an inflammatory phenotype. However, in the KC;iASPP$^{-/-}$ mouse model, there is accelerated tumorigenesis, which would be consistent with increased inflammatory stress or inflammatory cell death. Reduced efficiency of ductal metaplasia in an *ex vivo* model favours a non-cell autonomous mechanism that promotes tumorigenesis in KC;iASPP$^{-/-}$ mice. Various extrinsic inflammatory mediators, such as cytokines and chemokines, are hypothesized to promote oncogenic Kras mediated PDAC. Cytokine profiling in the early stages of ADM and PanIN development may indicate that inflammatory mediators that are differentially expressed between KC and KC;iASPP$^{-/-}$ mice.

12-week old KC (n=2) and KC;iASPP$^{-/-}$ (n=2) mice were electively culled with no evidence of primary PDAC (palpable pancreatic masses or cysts) nor metastases. Histological analysis of the head of pancreas tissue determined that KC;iASPP$^{-/-}$ mice had a relatively minor increase in ADM and PanIN relative to the age-match KC mice (Figure 6.10A). Using whole tissue lysates from the snap frozen pancreatic tails, there was a minor difference in the dot intensities of a murine cytokine array (Figure 6.10B). Quantification and averaging of means dot intensity found minor differences in cytokine levels, with slight increases in IL-1RA and IL-1β levels in the KC;iASPP$^{-/-}$ mice (Figure 6.10C).

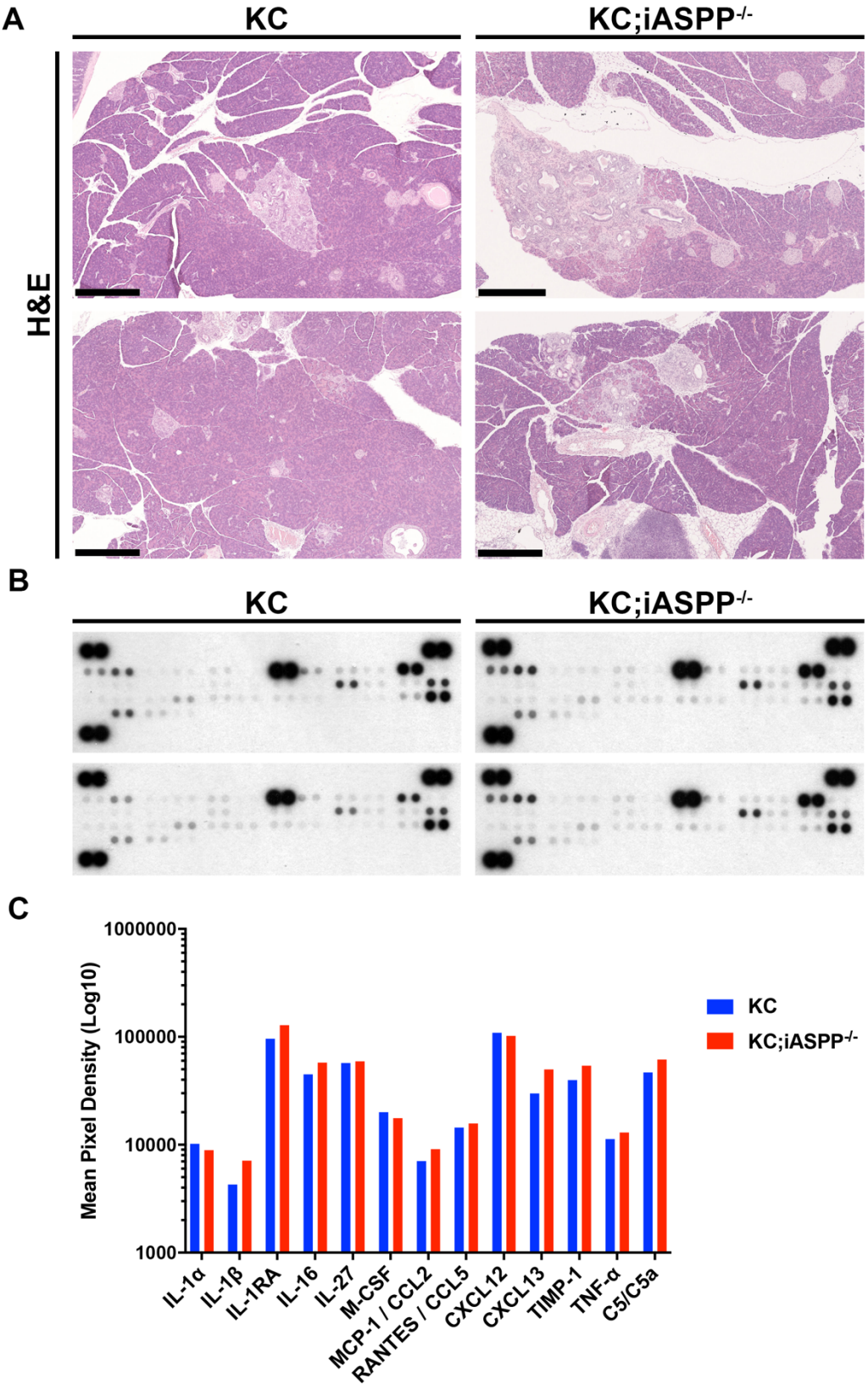

Figure 6.10 Cytokine profiling of KC and KC;iASPP$^{-/-}$ pancreas

A Representative sections of H&E stained 12-week old KC and KC;iASPP$^{-/-}$ pancreases used in cytokine profiling.

B Scanned blots from 12-week old KC and KC;iASPP$^{-/-}$ pancreas.

C Plot of mean pixel density (log10) of selected cytokines.

6.11 iASPP suppresses the pro-inflammatory cytokine response following inflammation

The absence of a clear pro-inflammatory cytokine phenotype when analysing whole mouse tissue lysates may be due to the insensitivity of whole tissue analysis. To potentiate the difference in KC and KC;iASPP$^{-/-}$ I investigated whether caerulein-induced inflammation is required. Using tissue obtained 48-hours after 4 single weekly injections of caerulein I analysed the cytokine profile in Pdx1-Cre only, iASPP$^{-/-}$, KC and KC;iASPP$^{-/-}$ tissue (Figure 6.11A).

Histologically there is no difference between Pdx1-Cre only and iASPP$^{-/-}$ mouse pancreas following inflammation (data not shown). There is a profound difference between the KC and KC;iASPP$^{-/-}$ pancreas with almost no normal acini in KC;iASPP$^{-/-}$ mice and abundant stroma and inflammatory infiltrates (Figure 6.11B). A murine cytokine array demonstrated little difference between Pdx1-Cre only, iASPP$^{-/-}$, and KC whole tissue lysates (Figure 6.11C). However, the KC;iASPP$^{-/-}$ lysate had increased levels of multiple cytokines. Mean pixel density was calculated and demonstrated KC;iASPP$^{-/-}$ had specific upregulation of IL-1α, IL-1β and IL-1RA. Other cytokines identified were mediators of immune cell function and activation such as CCL2, CCL5, CCL12, CXCL12, TREM-1 and GM-CSF (Figure 6.11D).

Given the immune systems of KC and KC;iASPP$^{-/-}$ mice are equivalent, and oncogenic Kras pancreatic tissue with iASPP-deficiency is the only difference in tissue it may suggest that the iASPP suppresses the pro-metaplastic and

tumorigenic microenvironment. A potential mechanism for regulating the immune microenvironment is via controlling pro-inflammatory cytokines. Suppressing an IL-1 family response would be consistent with human PDAC mRNA data in which high iASPP mRNA correlates with pro-inflammatory regulators and IL-1RA.

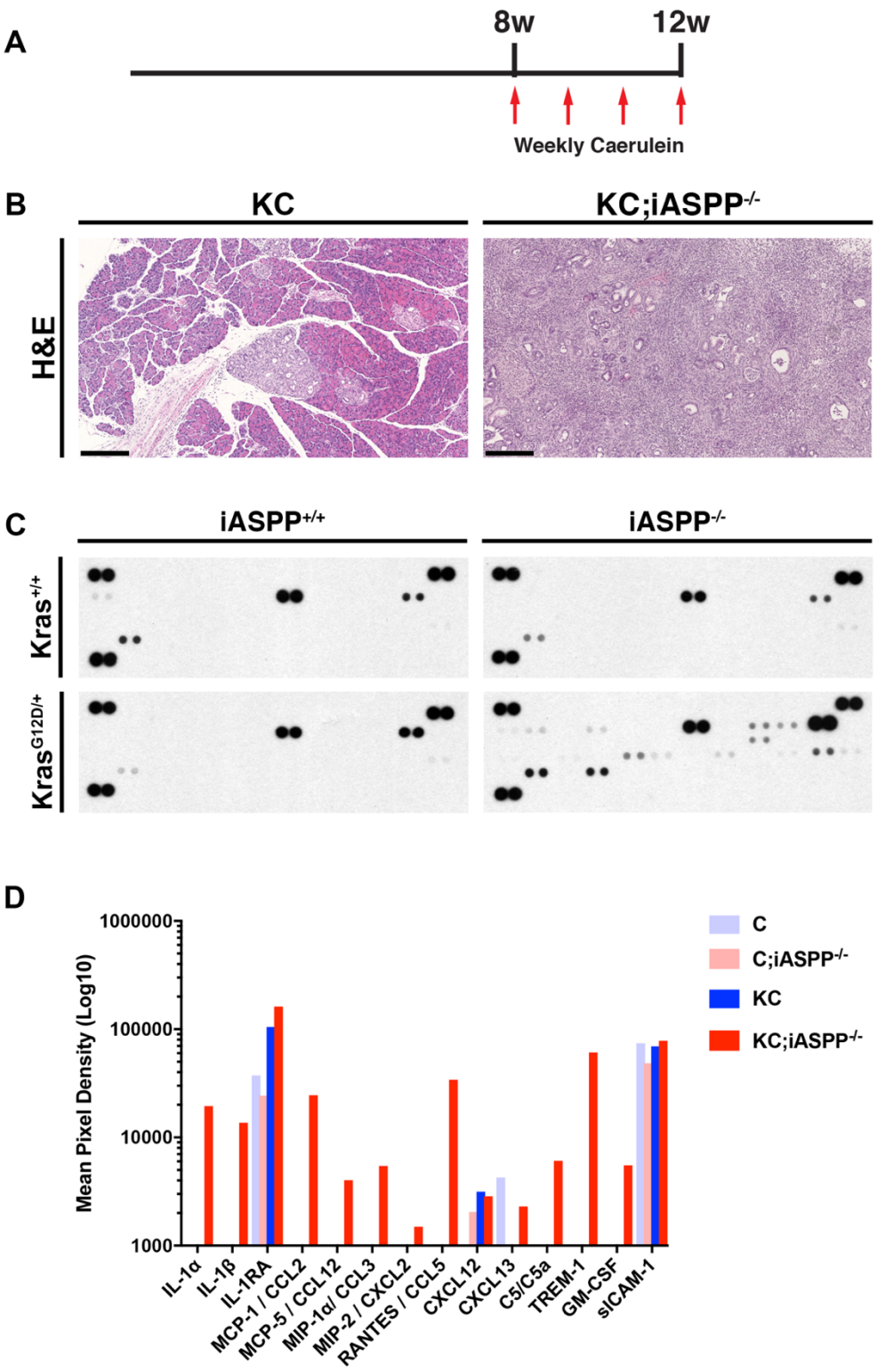

Figure 6.11 iASPP suppresses the pro-inflammatory cytokine response following inflammation

A Injection schedule. Pdx1-Cre+, iASPP$^{-/-}$, KC and KC;iASPP$^{-/-}$ mice were injected with weekly single dose caerulein for 4 weeks.

B Representative H&E images of KC and KC;iASPP$^{-/-}$ following inflammation. Scale bar 250 μm.

C Scanned dot-plots for whole tissue lysates.

D Plot of mean pixel density (log10) of selected cytokines

6.12 Summary

Central to the published literature on iASPP is that iASPP is an oncogene. However, to date, no *in vivo* model has demonstrated a tumour suppressive effect of iASPP-deficiency. In this chapter I have described the first murine model of cancer with iASPP-deficiency. Importantly, rather than having a tumour suppressive effect, KC;iASPP$^{-/-}$ mice have accelerated PDAC and metastatic disease. The phenotype is potentiated by the intermittent administration of caerulein to cause a mild-to-moderate pancreatitis. The failure of the acinar explant *ex vivo* study to demonstrate a concordant iASPP-deficiency phenotype suggested rather than cell-autonomous hyperactivation of the MAPK/ERK pathway with iASPP-deficiency, a more complex mechanism existed. Reduced ADM efficiency may be a consequence of cell death, senescence or increased inflammatory stress. Using human PDAC RNA-Seq data, I found iASPP mRNA correlates with other markers of poor prognosis and correlates with pro-inflammatory markers. To conclude, my evidence suggests iASPP is a regulator of the inflammatory response to acute and chronic pancreatitis and may be the basis for a model to study inflammatory pancreatic cancer.

Chapter 7: Discussion

Pancreatic cancer has an abysmal prognosis with approximately 3% patients surviving to 5-years following diagnosis. Central to PDAC development is oncogenic Kras, present in over 90% of cases (Bailey et al. 2016). However, oncogenic Kras mutation in adult mice is insufficient for tumorigenesis and requires long latency or inflammatory stress to potentiate neoplasia (Guerra et al. 2007; Hingorani et al. 2003). Understanding the mechanisms by which metaplastic and early neoplastic lesions are prevented from progressing to PDAC is important in developing prevention and treatment strategies. Furthermore, PDAC is inherently difficult to treat once diagnosed, as there are no effective radiotherapy or chemotherapy options. Transcriptional profiling based on RNA-sequencing has provided insights into the core deregulated pathways in PDAC. Studies of human pancreatic cancer and mouse models of PDAC have consistently demonstrated the important role of the immune system, inflammation and the tumour microenvironment as key determinants of tumour progression and response to therapy. In this thesis I sought to understand how normal acini, preneoplastic cells and cancer cells respond to inflammation and tumour suppression by focusing on the ASPP family members ASPP2 and iASPP, known regulators of the NF-κB and p53 families.

Investigating the function of specific genes can be approached in numerous ways. Transgenic mice, in which a gene of interest is knocked out or overexpressed in a tissue specific manner, provides a powerful tool that enables function to be deduced by evaluating alterations in development, homeostasis, signalling

pathways and response to stress. PDAC is an ideal model for studying the interaction of an oncogenic-driver mutation, inflammation and the tumour microenvironment. NF-κB family dysregulation, but not mutation, is characteristic of PDAC resulting in a prosurvival and immunosuppressive tumour microenvironment. However, p53 is frequently mutated or deleted in PDAC, with loss of wild-type tumour suppressor, especially apoptosis and senescence induction, or the acquisition of novel oncogenic functions through mutant p53. Furthermore, *TP53BP2*, encoding ASPP2, is one of 32 significantly mutated genes in PDAC but the functional significance to tumour development or prognosis is unclear (Bailey et al. 2016). Similarly, little is known about iASPP, although this has been identified as a putative oncogene based on the association of high iASPP expression associating with poor prognosis, and on the ability of iASPP to bind and inhibit the apoptotic function of p53. No cancer mouse model has yet been developed to study whether iASPP functions as an oncogene *in vivo*.

The squamous PDAC subtype is characterized by activation of gene networks similar to the C2-squamous-like class of breast, bladder, lung and head and neck cancers (Hoadley et al. 2014; Bailey et al. 2016). Both the C2-squamous-like class and squamous PDAC subtypes have TP63 activation with increased expression of ΔNp63 in particular. The RNA-seq defined squamous subtype and the histological adenosquamous phenotype associates with poor prognosis in PDAC (Bailey et al. 2016; Imaoka et al. 2014). Pure histological squamous pancreatic cancer is a rare event, suggesting the importance of ΔNp63 is by regulating the transcriptional environment in cancer (Al-Shehri et al. 2008). I hypothesized ASPP2 may function to suppress the squamous PDAC subtype through IκB binding, therefore favouring

p65 translocation to the nucleus, where it represses expression of the ΔNp63 isoform (Tordella et al. 2013). To test that hypothesis I first sequentially demonstrated ASPP2-deficiency does not result in a developmental nor homeostasis defect in the mouse. Subsequently, I observed that ASPP2-deficiency in the context of pancreas specific oncogenic Kras (KC;ASPP2$^{-/-}$) resulted in reduced overall survival of the cohort relative to the oncogenic Kras alone. ASPP2 does not regulate the efficiency of acinar-to-ductal metaplasia in acinar explants (chapter 4.6) nor *in vivo* either spontaneously (chapter 4.1) or when potentiated by inflammation (chapter 4.8). Also, I concluded ASPP2 does not alter the progression of PanINs to PDAC as median survival in cases of primary PDAC unaltered by ASPP2 status. However, analysis of metastatic disease survival demonstrated a significantly reduced median survival for KC;ASPP2$^{-/-}$ mice. These results have led me to conclude that ASPP2 regulates a mechanism that suppresses early metastasis.

The occurrence of a phenotypic squamous pancreatic cancer has not been described in a mouse model of pancreatic cancer to my knowledge (chapter 4.9). However, since this was a single occurrence in my analysed cohorts, it is unclear whether this represents an actual consequence of ASPP2 deficiency. The histological analysis presented in the thesis did not assess for adenosquamous versus adenocarcinoma incidence in these mice, which should be performed by blinded assessors. However, IHC staining did reveal a subset of KC;ASPP2$^{-/-}$ tumours and metastases that express p63 with and without squamous morphology (chapter 4.9). ASPP2 is upregulated in response to inflammation and oncogenic Kras, so can compete with p65 in binding IκB to favour p65 nuclear translocation. I

therefore speculate that p63 isoform expression may be limited in spontaneous KC;ASPP2$^{-/-}$ high-grade mPanINs and mPDAC as p65 may be adequately translocating to the nucleus to repress p63. However, in inflammation stimulated KC;ASPP2$^{-/-}$ mice, p63 expression may be promoted as IκB favours p65 binding in absence of competition from ASPP2 (chapter 4.10) (Figure 7.1).

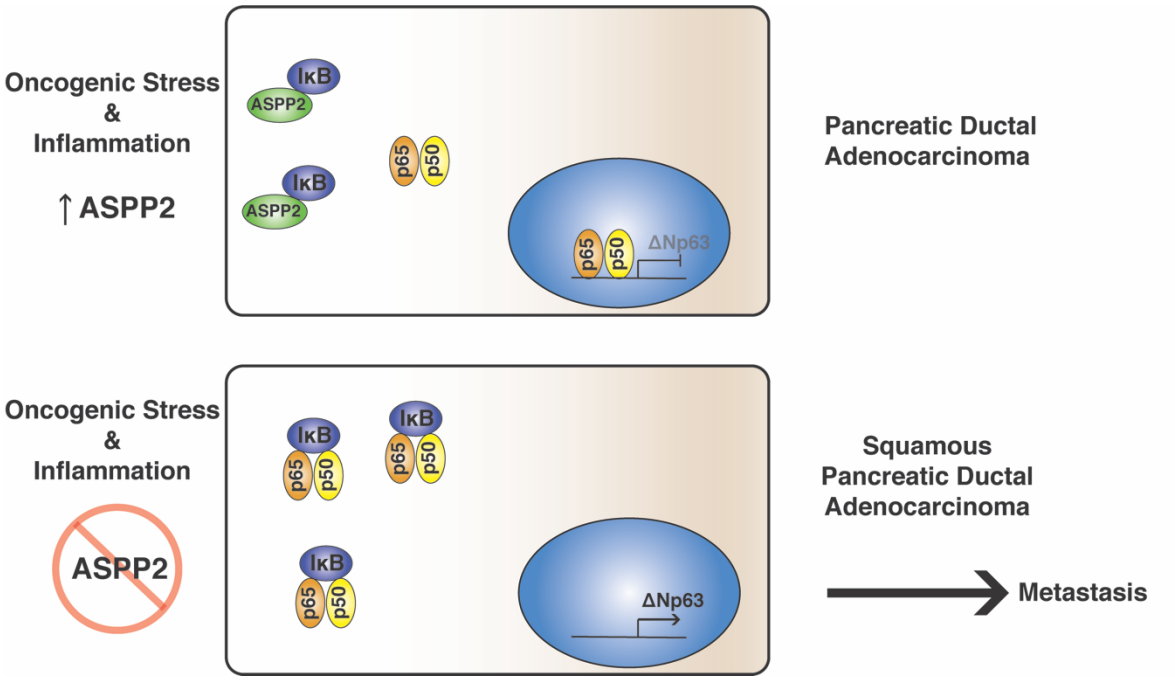

Figure 7.1 Proposed mechanism for ASPP2 as a suppressor of squamous subtype of PDAC

KPC mice, heterozygous for the p53 R172H point mutation, have increased metastatic burden compared to heterozygous p53-null mice (Hingorani et al. 2005). Consequently, I expected that the KPC;ASPP2$^{-/-}$ mouse would have a shorter median survival than KPC mice. However, I observed no differences in overall survival, primary PDAC-free survival, and metastasis-free survival in between KPC and KPC;ASPP2$^{-/-}$ mice, with a non-significant trend towards increased median survival in KPC;ASPP2$^{-/-}$ (chapter 4.4). A greater number of

KPC;ASPP2$^{-/-}$ metastases were diagnosed without reduced survival, and no examples of pure squamous morphology were identified (chapter 4.5). Review of mouse cohorts found some older KPC mice were used in studies involving KC;iASPP$^{-/-}$ mice. However, all KPC;ASPP2$^{-/-}$ mice were used for survival purposes and included in the survival analyses. Therefore, our KPC survival data is likely to underestimate median survival, especially as the literature reports KPC median survival to be 5.5 months (Hingorani et al. 2005).

In this thesis I provide initial evidence that the previously reported mechanism for ASPP2 suppression of spontaneous SCC via potentiating p65 translocation to the nucleus via competitive IκB binding to repress ΔNp63 may function in PDAC to regulate a squamous subtype of PDAC (Figure 7.1). The consequence of ASPP2 deficiency, either by mutation or downregulation, may be upregulation of ΔNp63, a p63 isoform that can be oncogenic and promote stem cell properties (Memmi et al. 2015; Melino 2011). Metastatic disease is present at death in 70% human PDAC cases and the squamous PDAC subtype has the worst prognosis for transcriptionally defined PDAC subtypes (Bailey et al. 2016). Therefore, confirmatory work is required to determine whether KC;ASPP2$^{-/-}$ or KPC;ASPP2$^{-/-}$, as either primary or metastatic PDAC, have specifically increased ΔNp63. Furthermore, RNA-Seq of ASPP2-deficient mPDAC is required to understand whether these cohorts represent a squamous PDAC model. This will be achieved by RNA-seq of primary KC;ASPP2$^{-/-}$ tumours, and by deriving KC, KPC, KC;ASPP2$^{-/-,}$ or KPC;ASPP2$^{-/-}$ primary mPDAC cell lines to analyse expression. Motility and invasion assays and injection into nude mice of derived cell lines would be able to confirm a pro-metastatic or pro-EMT phenotype for ASPP2-

deficient PDAC. Inflammation may also be a determining factor and rescuing the phenotype either by interfering with NF-κB components or over expressing ASPP2 to confirm the hypothesized mechanism.

The KC;iASPP$^{-/-}$ mouse is the first iASPP-deficient murine model of cancer to my knowledge. In contrast to the proposed oncogenic role of iASPP in suppressing p53-mediated apoptosis, I have found accelerated primary and metastatic PDAC (chapter 6.1 and 6.2). Histological primary mPDAC occurred as early as 9-weeks, with metastatic disease present as early as 4.5-weeks. Interestingly, although the germline iASPP-deficient mouse had no developmental or homeostasis pancreatic phenotype at 6-months, a short episode of acute pancreatitis resulted in profound metaplasia and inflammation (chapter 5.5). This phenotype contrasted with the normal inflammatory response of iASPP$^{-/-}$ (pancreas-specific iASPP-deficient) mice following recovery and the reduced ADM efficiency seen in explant acini culture *ex vivo* (chapter 5.5 and 6.3).

KC;iASPP$^{-/-}$ mice exhibited a proinflammatory response with extensive ADM and PanIN formation, immune cell infiltration, and stromal activation was greatly potentiated by intermittent caerulein (chapter 6.4). Cytokine profiling of primary mouse tissue demonstrated numerous altered cytokines and chemokines with known associations with proinflammatory roles (chapter 6.11). Linking expression of iASPP in human PDAC to known mediators of inflammation and survival highlighted the association of iASPP to markers of poor prognosis (chapter 6.7). I hypothesised that iASPP is upregulated in inflammatory cancers as iASPP appeared to be upregulated in response to oncogenic or tumour microenvironment

related stress (chapter 5.4). If iASPP is upregulated in inflammatory cancers, then it will likely associate with poor prognosis. Furthermore, if iASPP functions to suppress the inflammatory response, either by binding known regulators of the inflammatory response such as NF-κB or p53, then iASPP may actually be a tumour suppressor *in vivo*. iASPP as a suppressor of inflammation is consistent with the evidence from a human family with an iASPP nonsense mutation potentially via p65 suppression (Falik-Zaccai et al. 2017). A cytokeratin-14 iASPP-deficient mouse model had increased immune cell infiltration and larger papilloma following TPA administration (K Chung, unpublished). FACS analysis of the KC, KPC and KC;iASPP$^{-/-}$ mice demonstrate a proinflammatory phenotype, not present in the KPC mouse that have a poorer prognosis (E Akama-Garren, unpublished).

Characterisation of iASPP as a suppressor of the progression to PDAC is required to fully assess the mechanism. iASPP may suppress NF-κB by direct binding, regulating a proinflammatory pathway such as through the IL-1 family or could indirectly be related to an immune cell response to ADM or PanIN initiation. To investigate this further, I would need to perform a RNA-seq experiment comparing KC, KPC and KC;iASPP$^{-/-}$ samples to assess for proinflammatory transcription profiles. Further investigation of the role of inflammatory cell death, such as pyroptosis, would account for the effects of IL-1 family members, and potentially support an oncogenic *in vitro* and *ex vivo* role and tumour suppressor *in vivo* role for iASPP.

Bibliography

Aguirre, A.J. et al., 2003. Activated Kras and Ink4a/Arf deficiency cooperate to produce metastatic pancreatic ductal adenocarcinoma. *Genes & development*, 17(24), pp.3112–26.

Al-Shehri, A., Silverman, S. & King, K.M., 2008. Squamous cell carcinoma of the pancreas. *Current oncology (Toronto, Ont.)*, 15(6), pp.293–7.

Algül, H. et al., 2007. Pancreas-specific RelA/p65 truncation increases susceptibility of acini to inflammation-associated cell death following cerulein pancreatitis. *The Journal of clinical investigation*, 117(6), pp.1490–501.

Ardito, C.M. et al., 2012. EGF receptor is required for KRAS-induced pancreatic tumorigenesis. *Cancer cell*, 22(3), pp.304–17.

Bailey, P. et al., 2016. Genomic analyses identify molecular subtypes of pancreatic cancer. *Nature*, 531(7592), pp.47–52.

Bardeesy, N. et al., 2006. Smad4 is dispensable for normal pancreas development yet critical in progression and tumor biology of pancreas cancer. *Genes & Development*, 20(22), pp.3130–3146.

Basturk, O. et al., 2005. DeltaNp63 expression in pancreas and pancreatic neoplasia. *Modern Pathology*, 18(9), pp.1193–1198.

Bayne, L.J. et al., 2012. Tumor-derived granulocyte-macrophage colony-stimulating factor regulates myeloid inflammation and T cell immunity in pancreatic cancer. *Cancer cell*, 21(6), pp.822–35.

Benoit, V. et al., 2006. Transcriptional activation of cyclooxygenase-2 by tumor suppressor p53 requires nuclear factor-kappaB. *Oncogene*, 25(42), pp.5708–5718.

Bergamaschi, D. et al., 2004. ASPP1 and ASPP2: common activators of p53 family members. *Molecular and cellular biology*, 24(3), pp.1341–50.

Bergamaschi, D. et al., 2003. iASPP oncoprotein is a key inhibitor of p53 conserved from worm to human. *Nature genetics*, 33(2), pp.162–7.

Bergamaschi, D. et al., 2006. iASPP preferentially binds p53 proline-rich region and modulates apoptotic function of codon 72–polymorphic p53. *Nature Genetics*, 38(10), pp.1133–1141.

Brody, J.R. et al., 2009. Adenosquamous carcinoma of the pancreas harbors KRAS2, DPC4 and TP53 molecular alterations similar to pancreatic ductal adenocarcinoma. *Modern Pathology*, 22(5), pp.651–659.

Brooks, C.L. & Gu, W., 2006. p53 Ubiquitination: Mdm2 and Beyond. *Molecular Cell*, 21(3), pp.307–315.

Buti, L. et al., 2011. Helicobacter pylori cytotoxin-associated gene A (CagA) subverts the apoptosis-stimulating protein of p53 (ASPP2) tumor suppressor pathway of the host. *Proceedings of the National Academy of Sciences of the United States of America*, 108(22), pp.9238–43.

Cai, J. et al., 2010. The Hippo signaling pathway restricts the oncogenic potential of an intestinal regeneration program. *Genes & development*, 24(21), pp.2383–8.

Cai, Y. et al., 2012. iASPP inhibits p53-independent apoptosis by inhibiting transcriptional activity of p63/p73 on promoters of proapoptotic genes. *Apoptosis : an international journal on programmed cell death*, 17(8), pp.777–83.

Carrière, C. et al., 2009. *Acute pancreatitis markedly accelerates pancreatic*

cancer progression in mice expressing oncogenic Kras,
Chen, D. et al., 2005. Apoptosis-stimulating protein of p53-2 (ASPP2/53BP2L) is an E2F target gene. *Cell Death and Differentiation*, 12(4), pp.358–368.
Chen, R. et al., 2016. Downregulation of ASPP2 improves hepatocellular carcinoma cells survival via promoting BECN1-dependent autophagy initiation. *Cell Death and Disease*, 7(12), p.e2512.
Chien, Y. et al., 2011. Control of the senescence-associated secretory phenotype by NF-κB promotes senescence and enhances chemosensitivity. *Genes & development*, 25(20), pp.2125–36.
Clark, C.E. et al., 2007. Dynamics of the Immune Reaction to Pancreatic Cancer from Inception to Invasion. *Cancer Research*, 67(19).
Collins, M.A. et al., 2012. Oncogenic Kras is required for both the initiation and maintenance of pancreatic cancer in mice. *Journal of Clinical Investigation*, 122(2), pp.639–653.
Coppé, J.-P. et al., 2008. Senescence-Associated Secretory Phenotypes Reveal Cell-Nonautonomous Functions of Oncogenic RAS and the p53 Tumor Suppressor J. Downward, ed. *PLoS Biology*, 6(12), p.e301.
Corcoran, R.B. et al., 2011. STAT3 Plays a Critical Role in KRAS-Induced Pancreatic Tumorigenesis. *Cancer Research*, 71(14).
Coussens, L.M., Zitvogel, L. & Palucka, A.K., 2013. Neutralizing tumor-promoting chronic inflammation: a magic bullet? *Science (New York, N.Y.)*, 339(6117), pp.286–91.
Daniluk, J. et al., 2012. An NF-κB pathway-mediated positive feedback loop amplifies Ras activity to pathological levels in mice. *The Journal of clinical investigation*, 122(4), pp.1519–28.
Duan, R.D. et al., 1995. Activation of MAP kinase kinase (MEK) and Ras by cholecystokinin in rat pancreatic acini. *The American journal of physiology*, 268(6 Pt 1), pp.G1060-5.
Engelmann, D. & Pützer, B.M., 2014. Emerging from the shade of p53 mutants: N-terminally truncated variants of the p53 family in EMT signaling and cancer progression. *Science Signaling*, 7(345).
Espanel, X. & Sudol, M., 2001. Yes-associated protein and p53-binding protein-2 interact through their WW and SH3 domains. *The Journal of biological chemistry*, 276(17), pp.14514–23.
Fajas, L. et al., 2004. Impaired pancreatic growth, beta cell mass, and beta cell function in E2F1 (-/-)mice. *The Journal of clinical investigation*, 113(9), pp.1288–95.
Falik-Zaccai, T.C. et al., 2017. Sequence variation in PPP1R13L results in a novel form of cardio-cutaneous syndrome. *EMBO molecular medicine*, 9(3), pp.319–336.
Field, S.J. et al., 1996. E2F-1 functions in mice to promote apoptosis and suppress proliferation. *Cell*, 85(4), pp.549–61.
Fogal, V. et al., 2005. ASPP1 and ASPP2 are new transcriptional targets of E2F. *Cell Death and Differentiation*, 12(4), pp.369–376.
Freund, A. et al., 2010. Inflammatory networks during cellular senescence: causes and consequences. *Trends in Molecular Medicine*, 16(5), pp.238–246.
Gan, W. et al., 2017. CDK1 interacts with iASPP to regulate colorectal cancer cell proliferation through p53 pathway. *Oncotarget*, 5(0).
Gao, K. et al., 2015. The E3 ubiquitin ligase Itch and Yap1 have antagonistic roles in the regulation of ASPP2 protein stability. *FEBS Letters*, 589(1), pp.94–101.

Gen, Y. et al., 2017. ASPP2 suppresses invasion and TGF-β1-induced epithelial–mesenchymal transition by inhibiting Smad7 degradation mediated by E3 ubiquitin ligase ITCH in gastric cancer. *Cancer Letters*, 398, pp.52–61.
Grivennikov, S.I., Greten, F.R. & Karin, M., 2010. Immunity, inflammation, and cancer. *Cell*, 140(6), pp.883–99.
Gudkov, A. V, Gurova, K. V & Komarova, E.A., 2011. Inflammation and p53: A Tale of Two Stresses. *Genes & cancer*, 2(4), pp.503–16.
Guerra, C. et al., 2007. Chronic pancreatitis is essential for induction of pancreatic ductal adenocarcinoma by K-Ras oncogenes in adult mice. *Cancer cell*, 11(3), pp.291–302.
Guerra, C. et al., 2011. Pancreatitis-induced inflammation contributes to pancreatic cancer by inhibiting oncogene-induced senescence. *Cancer cell*, 19(6), pp.728–39.
Guevara, N. V. et al., 1999. The absence of p53 accelerates atherosclerosis by increasing cell proliferation in vivo. *Nature Medicine*, 5(3), pp.335–339.
Gukovsky, I. et al., 1998. Early NF-kappa B activation is associated with hormone-induced pancreatitis. *Am J Physiol Gastrointest Liver Physiol*, 275(6), pp.G1402-1414.
Hassemer, E.L. et al., 2010. The waved with open eyelids (woe) locus is a hypomorphic mouse mutation in Adam17. *Genetics*, 185(1), pp.245–55.
Hayden, M.S., West, A.P. & Ghosh, S., 2006. NF-κB and the immune response. *Oncogene*, 25(51), pp.6758–6780.
Helps, N.R. et al., 1995. Protein phosphatase 1 interacts with p53BP2, a protein which binds to the tumour suppressor p53. *FEBS letters*, 377(3), pp.295–300.
Herron, B.J. et al., 2005. A mutation in NFkB interacting protein 1 results in cardiomyopathy and abnormal skin development in wa3 mice. *Human molecular genetics*, 14(5), pp.667–77.
Hingorani, S.R. et al., 2005. Trp53R172H and KrasG12D cooperate to promote chromosomal instability and widely metastatic pancreatic ductal adenocarcinoma in mice. *Cancer Cell*, 7(5), pp.469–483.
Hingorani, S.R.S.R. et al., 2003. Preinvasive and invasive ductal pancreatic cancer and its early detection in the mouse. *Cancer cell*, 4(6), pp.437–50.
Hiraoka, N. et al., 2006. Prevalence of FOXP3+ Regulatory T Cells Increases During the Progression of Pancreatic Ductal Adenocarcinoma and Its Premalignant Lesions. *Clinical Cancer Research*, 12(18).
Hoadley, K.A. et al., 2014. Multiplatform Analysis of 12 Cancer Types Reveals Molecular Classification within and across Tissues of Origin. *Cell*, 158(4), pp.929–944.
Hoque, R. et al., 2011. TLR9 and the NLRP3 inflammasome link acinar cell death with inflammation in acute pancreatitis. *Gastroenterology*, 141(1), pp.358–69.
Hruban, R.H. et al., 2006. Pathology of Genetically Engineered Mouse Models of Pancreatic Exocrine Cancer: Consensus Report and Recommendations. *Cancer Research*, 66(1).
Hu, Y. et al., 2015. Caspase cleavage of iASPP potentiates its ability to inhibit p53 and NF-κB. *Oncotarget*, 6(40), pp.42478–42490.
Huang, H. et al., 2013. Activation of nuclear factor-κB in acinar cells increases the severity of pancreatitis in mice. *Gastroenterology*, 144(1), pp.202–10.
Iacobuzio-Donahue, C.A. et al., 2009. DPC4 gene status of the primary carcinoma correlates with patterns of failure in patients with pancreatic cancer. *Journal of clinical oncology : official journal of the American Society of Clinical Oncology*,

27(11), pp.1806–13.
Iglesias-Ara, A. et al., 2015. E2F1 and E2F2 prevent replicative stress and subsequent p53-dependent organ involution. *Cell Death and Differentiation*, 22(10), pp.1577–1589.
Iglesias, A. et al., 2004. Diabetes and exocrine pancreatic insufficiency in E2F1/E2F2 double-mutant mice. *The Journal of clinical investigation*, 113(10), pp.1398–407.
Imaoka, H. et al., 2014. Clinical Characteristics of Adenosquamous Carcinoma of the Pancreas. *Pancreas*, 43(2), pp.287–290.
Ino, Y. et al., 2013. Immune cell infiltration as an indicator of the immune microenvironment of pancreatic cancer. *British Journal of Cancer*, 108(4), pp.914–923.
Iwabuchi, K. et al., 1994. Two cellular proteins that bind to wild-type but not mutant p53. *Proceedings of the National Academy of Sciences of the United States of America*, 91(13), pp.6098–102.
Ji, B. et al., 2009. Ras activity levels control the development of pancreatic diseases. *Gastroenterology*, 137(3), pp.1072–82, 1082–6.
Jiang, L. et al., 2011. iASPP and chemoresistance in ovarian cancers: effects on paclitaxel-mediated mitotic catastrophe. *Clinical cancer research : an official journal of the American Association for Cancer Research*, 17(21), pp.6924–33.
Kampa, K.M. et al., 2009. Apoptosis-stimulating protein of p53 (ASPP2) heterozygous mice are tumor-prone and have attenuated cellular damage-response thresholds. *Proceedings of the National Academy of Sciences of the United States of America*, 106(11), pp.4390–5.
Karin, M. & Clevers, H., 2016. Reparative inflammation takes charge of tissue regeneration. *Nature*, 529(7586), pp.307–15.
Kopp, J.L. et al., 2012. Identification of Sox9-dependent acinar-to-ductal reprogramming as the principal mechanism for initiation of pancreatic ductal adenocarcinoma. *Cancer cell*, 22(6), pp.737–50.
Krebs, A.M. et al., 2017. The EMT-activator Zeb1 is a key factor for cell plasticity and promotes metastasis in pancreatic cancer. *Nature Cell Biology*, 19(5), pp.518–529.
van Laethem, J.L., 1999. Ki-ras oncogene mutations in chronic pancreatitis: which discriminating ability for malignant potential? *Annals of the New York Academy of Sciences*, 880, pp.210–8.
Lampel, M. & Kern, H.F., 1977. Acute interstitial pancreatitis in the rat induced by excessive doses of a pancreatic secretagogue. *Virchows Archiv. A, Pathological anatomy and histology*, 373(2), pp.97–117.
Lesina, M. et al., 2016. RelA regulates CXCL1/CXCR2-dependent oncogene-induced senescence in murine Kras-driven pancreatic carcinogenesis. *The Journal of clinical investigation*, 126(8), pp.2919–32.
Levine, A.J. & Oren, M., 2009. The first 30 years of p53: growing ever more complex. *Nature Reviews Cancer*, 9(10), pp.749–758.
Lin, B.L. et al., 2011. Down-regulation of iASPP in human hepatocellular carcinoma cells inhibits cell proliferation and tumor growth. *Neoplasma*, 58(3), pp.205–10.
Ling, J. et al., 2012. KrasG12D-induced IKK2/β/NF-κB activation by IL-1α and p62 feedforward loops is required for development of pancreatic ductal adenocarcinoma. *Cancer cell*, 21(1), pp.105–20.

Liou, G.-Y. et al., 2013. Macrophage-secreted cytokines drive pancreatic acinar-to-ductal metaplasia through NF-κB and MMPs. *The Journal of cell biology*, 202(3), pp.563–77.
Liou, G.-Y. et al., 2015. Mutant KRAS-induced expression of ICAM-1 in pancreatic acinar cells causes attraction of macrophages to expedite the formation of precancerous lesions. *Cancer discovery*, 5(1), pp.52–63.
Liu, C.-Y. et al., 2011. PP1 cooperates with ASPP2 to dephosphorylate and activate TAZ. *The Journal of biological chemistry*, 286(7), pp.5558–66.
Liu, X. et al., 2015. Overexpression of iASPP-SV in glioma is associated with poor prognosis by promoting cell viability and antagonizing apoptosis. *Tumour biology : the journal of the International Society for Oncodevelopmental Biology and Medicine*.
Liu, Z.-J. et al., 2005. Downregulated mRNA expression of ASPP and the hypermethylation of the 5′-untranslated region in cancer cell lines retaining wild-type p53. *FEBS Letters*, 579(7), pp.1587–1590.
Llanos, S. et al., 2011. Inhibitory member of the apoptosis-stimulating proteins of the p53 family (iASPP) interacts with protein phosphatase 1 via a noncanonical binding motif. *The Journal of biological chemistry*, 286(50), pp.43039–44.
Löhr, M. et al., 2005. Frequency of K-ras mutations in pancreatic intraductal neoplasias associated with pancreatic ductal adenocarcinoma and chronic pancreatitis: a meta-analysis. *Neoplasia (New York, N.Y.)*, 7(1), pp.17–23.
Lopez, C.D. et al., 2000. Proapoptotic p53-interacting protein 53BP2 is induced by UV irradiation but suppressed by p53. *Molecular and cellular biology*, 20(21), pp.8018–25.
Lossos, I.S. et al., 2002. Apoptosis stimulating protein of p53 (ASPP2) expression differs in diffuse large B-cell and follicular center lymphoma: correlation with clinical outcome. *Leukemia & lymphoma*, 43(12), pp.2309–2317.
Lowe, J.M. et al., 2014. p53 and NF-κB coregulate proinflammatory gene responses in human macrophages. *Cancer research*, 74(8), pp.2182–92.
Lowenfels, A.B. et al., 1997. Hereditary pancreatitis and the risk of pancreatic cancer. International Hereditary Pancreatitis Study Group. *Journal of the National Cancer Institute*, 89(6), pp.442–6.
Lowenfels, A.B. et al., 1993. Pancreatitis and the Risk of Pancreatic Cancer. *New England Journal of Medicine*, 328(20), pp.1433–1437.
Lu, B. et al., 2010. Increased expression of iASPP, regulated by hepatitis B virus X protein-mediated NF-κB activation, in hepatocellular carcinoma. *Gastroenterology*, 139(6), p.2183–2194.e5.
Lu, M. et al., 2013. Restoring p53 function in human melanoma cells by inhibiting MDM2 and cyclin B1/CDK1-phosphorylated nuclear iASPP. *Cancer cell*, 23(5), pp.618–33.
Lu, M., Miller, P. & Lu, X., 2014. Restoring the tumour suppressive function of p53 as a parallel strategy in melanoma therapy. *FEBS Letters*, 588(16), pp.2616–21.
Luetteke, N.C. et al., 1993. TGFα deficiency results in hair follicle and eye abnormalities in targeted and waved-1 mice. *Cell*, 73(2), pp.263–278.
Luetteke, N.C. et al., 1994. The mouse waved-2 phenotype results from a point mutation in the EGF receptor tyrosine kinase. *Genes and Development*, 8(4), pp.399–413.
Lüttges, J. et al., 2000. Ductal lesions in patients with chronic pancreatitis show K-

ras mutations in a frequency similar to that in the normal pancreas and lack nuclear immunoreactivity for p53. *Cancer*, 88(11), pp.2495–504.
Maier, H.J. et al., 2013. Requirement of NEMO/IKKγ for effective expansion of KRAS-induced precancerous lesions in the pancreas. *Oncogene*, 32(21), pp.2690–2695.
Malka, D. et al., 2002. Risk of pancreatic adenocarcinoma in chronic pancreatitis. *Gut*, 51(6), pp.849–52.
Means, A.L. et al., 2005. Pancreatic epithelial plasticity mediated by acinar cell transdifferentiation and generation of nestin-positive intermediates. *Development (Cambridge, England)*, 132(16), pp.3767–76.
Medzhitov, R., 2008. Origin and physiological roles of inflammation. *Nature*, 454(7203), pp.428–435.
Melino, G., 2011. p63 is a suppressor of tumorigenesis and metastasis interacting with mutant p53. *Cell death and differentiation*, 18(9), pp.1487–99.
Memmi, E.M. et al., 2015. p63 Sustains self-renewal of mammary cancer stem cells through regulation of Sonic Hedgehog signaling. *Proceedings of the National Academy of Sciences of the United States of America*, 112(11), pp.3499–504.
Mitchem, J.B. et al., 2013. Targeting tumor-infiltrating macrophages decreases tumor-initiating cells, relieves immunosuppression, and improves chemotherapeutic responses. *Cancer research*, 73(3), pp.1128–41.
Miyatsuka, T. et al., 2006. Persistent expression of PDX-1 in the pancreas causes acinar-to-ductal metaplasia through Stat3 activation. *Genes & development*, 20(11), pp.1435–40.
Mori, T. et al., 2000. Aberrant overexpression of 53BP2 mRNA in lung cancer cell lines. *FEBS Letters*, 465(2–3), pp.124–128.
Morris, E. V et al., 2014. Nuclear iASPP may facilitate prostate cancer progression. *Cell death & disease*, 5, p.e1492.
Morton, J.P. et al., 2010. Mutant p53 drives metastasis and overcomes growth arrest/senescence in pancreatic cancer. *Proceedings of the National Academy of Sciences of the United States of America*, 107(1), pp.246–51.
Nakagawa, H. et al., 2000. APCL, a central nervous system-specific homologue of adenomatous polyposis coli tumor suppressor, binds to p53-binding protein 2 and translocates it to the perinucleus. *Cancer research*, 60(1), pp.101–5.
Naumovski, L. & Cleary, M.L., 1996. The p53-binding protein 53BP2 also interacts with Bc12 and impedes cell cycle progression at G2/M. *Molecular and cellular biology*, 16(7), pp.3884–92.
Nielsen, S.R. et al., 2016. Macrophage-secreted granulin supports pancreatic cancer metastasis by inducing liver fibrosis. *Nature Cell Biology*, 18(5), pp.549–560.
Nieto, M.A. et al., 2016. EMT: 2016. *Cell*, 166(1), pp.21–45.
Niu, J. et al., 2004. Identification of an autoregulatory feedback pathway involving interleukin-1alpha in induction of constitutive NF-kappaB activation in pancreatic cancer cells. *The Journal of biological chemistry*, 279(16), pp.16452–62.
Notari, M. et al., 2015. iASPP, a previously unidentified regulator of desmosomes, prevents arrhythmogenic right ventricular cardiomyopathy (ARVC)-induced sudden death. *Proceedings of the National Academy of Sciences of the United States of America*, 112(9), pp.E973-81.
Notari, M. et al., 2011. Inhibitor of apoptosis-stimulating protein of p53 (iASPP)

prevents senescence and is required for epithelial stratification. *Proceedings of the National Academy of Sciences of the United States of America*, 108(40), pp.16645–50.
O'Prey, J. et al., 2010. p53-mediated induction of Noxa and p53AIP1 requires NFκB. *Cell Cycle*, 9(5), pp.947–952.
Okuda, Y., Okuda, M. & Bernard, C.C.A., 2003. Regulatory role of p53 in experimental autoimmune encephalomyelitis. *Journal of neuroimmunology*, 135(1–2), pp.29–37.
Olive, K.P. et al., 2009. Inhibition of Hedgehog Signaling Enhances Delivery of Chemotherapy in a Mouse Model of Pancreatic Cancer. *Science*, 324(5933), pp.1457–1461.
Ozdemir, B.C. et al., 2014. Depletion of carcinoma-associated fibroblasts and fibrosis induces immunosuppression and accelerates pancreas cancer with reduced survival. *Cancer cell*, 25(6), pp.719–34.
Pandolfi, S. et al., 2015. HEDGEHOG/GLI-E2F1 axis modulates iASPP expression and function and regulates melanoma cell growth. *Cell Death and Differentiation*, 22(12), pp.2006–2019.
Pylayeva-Gupta, Y. et al., 2012. Oncogenic Kras-induced GM-CSF production promotes the development of pancreatic neoplasia. *Cancer cell*, 21(6), pp.836–47.
Quail, D.F. & Joyce, J.A., 2013. Microenvironmental regulation of tumor progression and metastasis. *Nature Medicine*, 19(11), pp.1423–1437.
Rahib, L. et al., 2014. Projecting Cancer Incidence and Deaths to 2030: The Unexpected Burden of Thyroid, Liver, and Pancreas Cancers in the United States. *Cancer Research*, 74(11).
Rakonczay, Z. et al., 2008. The role of NF- B activation in the pathogenesis of acute pancreatitis. *Gut*, 57(2), pp.259–267.
Rhim, A.D. et al., 2014. Stromal elements act to restrain, rather than support, pancreatic ductal adenocarcinoma. *Cancer cell*, 25(6), pp.735–47.
Rogers, C. et al., 2017. Cleavage of DFNA5 by caspase-3 during apoptosis mediates progression to secondary necrotic/pyroptotic cell death. *Nature Communications*, 8, p.14128.
Rosenfeldt, M.T. et al., 2013. p53 status determines the role of autophagy in pancreatic tumour development. *Nature*, 504(7479), pp.296–300.
Rothwell, P.M. et al., 2011. Effect of daily aspirin on long-term risk of death due to cancer: analysis of individual patient data from randomised trials. *The Lancet*, 377(9759), pp.31–41.
Royer, C. et al., 2014. ASPP2 Links the Apical Lateral Polarity Complex to the Regulation of YAP Activity in Epithelial Cells H. Wanjin, ed. *PLoS ONE*, 9(10), p.e111384.
Ruggeri, B.A. et al., 1998. Amplification and overexpression of theAKT2 oncogene in a subset of human pancreatic ductal adenocarcinomas. *Molecular Carcinogenesis*, 21(2), pp.81–86.
Ryan, K.M. et al., 2000. Role of NF-κB in p53-mediated programmed cell death. *Nature*, 404(6780), pp.892–897.
Samuels-Lev, Y. et al., 2001. ASPP Proteins Specifically Stimulate the Apoptotic Function of p53. *Molecular Cell*, 8(4), pp.781–794.
Sandgren, E.P. et al., 1990. Overexpression of TGFα in transgenic mice: Induction of epithelial hyperplasia, pancreatic metaplasia, and carcinoma of the breast. *Cell*, 61(6), pp.1121–1135.

Schittenhelm, M.M. et al., 2013. Attenuated expression of apoptosis stimulating protein of p53-2 (ASPP2) in human acute leukemia is associated with therapy failure. K. Roemer, ed. *PloS one*, 8(11), p.e80193.
Schmieder, A., Multhoff, G. & Radons, J., 2012. Interleukin-33 acts as a pro-inflammatory cytokine and modulates its receptor gene expression in highly metastatic human pancreatic carcinoma cells. *Cytokine*, 60(2), pp.514–521.
Sgroi, D.C. et al., 1999. In Vivo Gene Expression Profile Analysis of Human Breast Cancer Progression. *Cancer Research*, 59(22).
Shatz, M., Menendez, D. & Resnick, M.A., 2012. The Human TLR Innate Immune Gene Family Is Differentially Influenced by DNA Stress and p53 Status in Cancer Cells. *Cancer Research*, 72(16), pp.3948–3957.
Shi, G. et al., 2013. Maintenance of acinar cell organization is critical to preventing Kras-induced acinar-ductal metaplasia. *Oncogene*, 32(15), pp.1950–8.
Shugang, X. et al., 2016. Prognostic Value of SMAD4 in Pancreatic Cancer: A Meta-Analysis. *Translational oncology*, 9(1), pp.1–7.
Simpson, M.A. et al., 2009. A mutation in *NFκB interacting protein 1* causes cardiomyopathy and woolly haircoat syndrome of Poll Hereford cattle. *Animal Genetics*, 40(1), pp.42–46.
Singh, A.P. et al., 2012. CXCL12/CXCR4 protein signaling axis induces sonic hedgehog expression in pancreatic cancer cells via extracellular regulated kinase- and Akt kinase-mediated activation of nuclear factor κB: implications for bidirectional tumor-stromal interactions. *The Journal of biological chemistry*, 287(46), pp.39115–24.
Siveke, J.T. et al., 2007. Concomitant pancreatic activation of Kras(G12D) and Tgfa results in cystic papillary neoplasms reminiscent of human IPMN. *Cancer cell*, 12(3), pp.266–79.
Smith, R.A. et al., 2011. Meta-analysis of immunohistochemical prognostic markers in resected pancreatic cancer. *British Journal of Cancer*, 104(9), pp.1440–1451.
Song, B. et al., 2015. Downregulation of ASPP2 in pancreatic cancer cells contributes to increased resistance to gemcitabine through autophagy activation. *Molecular Cancer*, 14(1), p.177.
Sottocornola, R. et al., 2010. ASPP2 binds Par-3 and controls the polarity and proliferation of neural progenitors during CNS development. *Developmental cell*, 19(1), pp.126–37.
Staib, F., 2005. The p53 Tumor Suppressor Network Is a Key Responder to Microenvironmental Components of Chronic Inflammatory Stress. *Cancer Research*, 65(22), pp.10255–10264.
Takada, N. et al., 2002. RelA-associated inhibitor blocks transcription of human immunodeficiency virus type 1 by inhibiting NF-kappaB and Sp1 actions. *Journal of virology*, 76(16), pp.8019–30.
Toonen, J., Liang, L. & Sidjanin, D.J., 2012. Waved with open eyelids 2 (woe2) is a novel spontaneous mouse mutation in the protein phosphatase 1, regulatory (inhibitor) subunit 13 like (Ppp1r13l) gene. *BMC Genetics*, 13.
Tordella, L. et al., 2013. ASPP2 suppresses squamous cell carcinoma via RelA/p65-mediated repression of p63. *Proceedings of the National Academy of Sciences of the United States of America*, 110(44), pp.17969–74.
Turnquist, C. et al., 2014. STAT1-induced ASPP2 transcription identifies a link between neuroinflammation, cell polarity, and tumor suppression. *Proceedings of the National Academy of Sciences of the United States of*

America, 111(27), pp.9834–9.
Vives, V. et al., 2006. ASPP2 is a haploinsufficient tumor suppressor that cooperates with p53 to suppress tumor growth. *Genes & development*, 20(10), pp.1262–7.
Wang, Y. et al., 2013. ASPP1 and ASPP2 bind active RAS, potentiate RAS signalling and enhance p53 activity in cancer cells. *Cell death and differentiation*, 20(4), pp.525–34.
Wang, Y. et al., 2014. ASPP2 controls epithelial plasticity and inhibits metastasis through β-catenin-dependent regulation of ZEB1. *Nature cell biology*, 16(11), pp.1092–1104.
Weichert, W. et al., 2007. High expression of RelA/p65 is associated with activation of nuclear factor-κB-dependent signaling in pancreatic cancer and marks a patient population with poor prognosis. *British Journal of Cancer*, 97(4), pp.523–530.
Weissmueller, S. et al., 2014. Mutant p53 drives pancreatic cancer metastasis through cell-autonomous PDGF receptor β signaling. *Cell*, 157(2), pp.382–94.
Wilson, A.M. et al., 2014. Inhibitor of Apoptosis-Stimulating Protein of p53 (iASPP) Is Required for Neuronal Survival after Axonal Injury P. Gonzalez, ed. *PLoS ONE*, 9(4), p.e94175.
Witkiewicz, A.K. et al., 2015. Whole-exome sequencing of pancreatic cancer defines genetic diversity and therapeutic targets. *Nature Communications*, 6, p.6744.
Wu, Z. et al., 2017. Inhibitory member of the apoptosis-stimulating protein of p53 is overexpressed in bladder cancer and correlated to its progression. *Medicine*, 96(19), p.e6640.
Xue, W. et al., 2007. Senescence and tumour clearance is triggered by p53 restoration in murine liver carcinomas. *Nature*, 445(7128), pp.656–60.
Yamasaki, L. et al., 1996. Tumor induction and tissue atrophy in mice lacking E2F-1. *Cell*, 85(4), pp.537–48.
Yang, J.-P. et al., 1999. NF-κB subunit p65 binds to 53BP2 and inhibits cell death induced by 53BP2. *Oncogene*, 18(37), pp.5177–5186.
Yang, J.P. et al., 1999. Identification of a novel inhibitor of nuclear factor-kappaB, RelA-associated inhibitor. *The Journal of biological chemistry*, 274(22), pp.15662–70.
Yao, H. et al., 2017. Glypican-3 and KRT19 are markers associating with metastasis and poor prognosis of pancreatic ductal adenocarcinoma. *Cancer Biomarkers*, 17(4), pp.397–404.
Yao, X. et al., 2014. Targeting interleukin-6 in inflammatory autoimmune diseases and cancers. *Pharmacology & Therapeutics*, 141(2), pp.125–139.
Zak, J. et al., 2016. ASPP2 deficiency causes features of 1q41q42 microdeletion syndrome. *Cell Death and Differentiation*, 23(12), pp.1973–1984.
Zhang, Y. et al., 2014. CD4+ T Lymphocyte Ablation Prevents Pancreatic Carcinogenesis in Mice. *Cancer Immunology Research*, 2(5).
Zhang, Y. et al., 2013. Interleukin-6 Is Required for Pancreatic Cancer Progression by Promoting MAPK Signaling Activation and Oxidative Stress Resistance. *Cancer Research*, 73(20), pp.6359–6374.
Zhang, Y. et al., 2017. Myeloid cells are required for PD-1/PD-L1 checkpoint activation and the establishment of an immunosuppressive environment in pancreatic cancer. *Gut*, 66(1), pp.124–136.
Zheng, S.-J. et al., 2005. Tumor suppressor p53 inhibits autoimmune inflammation

and macrophage function. *Diabetes*, 54(5), pp.1423–8.
Zheng, X. et al., 2015. Epithelial-to-mesenchymal transition is dispensable for metastasis but induces chemoresistance in pancreatic cancer. *Nature*, advance on.
Zhu, Z. et al., 2005. Control of ASPP2/(53BP2L) protein levels by proteasomal degradation modulates p53 apoptotic function. *The Journal of biological chemistry*, 280(41), pp.34473–80.
Zhuang, Z. et al., 2016. IL1 Receptor Antagonist Inhibits Pancreatic Cancer Growth by Abrogating NF-κB Activation. *Clinical Cancer Research*, 22(6), pp.1432–1444.